ANALYTICAL BASE TRANSIT TIME MODEL OF A BIPOLAR TRANSISTOR CONSIDERING MAJORITY CARRIER CURRENT IN THE BASE

A Thesis Submitted to the Department of Electrical and Electronic Engineering
in Partial Ful_llment of the Requirement for the Degree of

DOCTOR OF PHILOSOPHY

by

Md. Iqbal Bahar Chowdhury

Department of Electrical and Electronics Engineering
BANGLADESH UNIVERSITY OF ENGINEERING AND TECHNOLOGY

JUNE 2011

The thesis titled "**Analytical Base Transit Time Model of a Bipolar Transistor Considering Majority Carrier Current in the Base**" submitted by Md. Iqbal Bahar Chowdhury, Roll No. P04030603P, Session April 2003 has been accepted as satisfactory in partial ful_llment of the requirements for the degree of **Doctor of Philosophy** on June 01, 2011.

BOARD OF EXAMINERS

1. _____
   Dr. M. M. Shahidul Hassan — Chairman
   Professor, Department of EEE, BUET

2. _____
   Dr. Md. Saifur Rahman — Member
   Professor and Head, Department of EEE, BUET — (Ex-officio)

3. _____
   Dr. Mohammad Ali Choudhury — Member
   Professor, Department of EEE, BUET

4. _____
   Dr. Satya Prasad Majumder — Member
   Professor, Department of EEE, BUET

5. _____
   Dr. Quazi Deen Mohd. Khosru — Member
   Professor, Department of EEE, BUET

6. _____
   Dr. Sharif Mohammad Mominuzzaman — Member
   Professor, Department of EEE, BUET

7. _____
   Dr. Abul N. Khondker — Member
   Associate Professor, Department of ECE, — (External)
   Clarkson University, New York, USA

Declaration

It is hereby declared that this thesis or any part of it has not been submitted elsewhere for the award of any degree or diploma.

Md. Iqbal Bahar Chowdhury
Ph. D. Candidate

To the bereaved soul of my father,
to my mother who possesses endless love for me,
to my wife whose love makes this world heavenly for me
and
of course, to Meehal, Rajeet and Ziyad whom Allah (SWT)
blessed me with.

List of Tables

List of Figures

Table of Contents

List of Symbols

C_{An} Auger coefficient for electrons
C_{Ap} Auger coefficient for holes
D_n Electron diffusivity
$D_{n,eff}$ Effective electron diffusivity considering injection-level dependency
D_p Hole diffusivity
E_C Conduction band edge energy
E_V Valence band edge energy
E_G Band-gap energy
E_n Electric field acting on electrons
$E_{n,eff}$ Effective electric field acting on electrons considering injection-level dependency
E_p Electric field acting on holes
F_e Constant representing the doping dependency of the electron diffusivity
F_h Constant representing the doping dependency of the hole diffusivity
G_e Constant representing the electric field dependency of the electron diffusivity
G_h Constant representing the electric field dependency of the hole diffusivity
J_n Electron current density
J_p Hole current density
J_C Collector current density
J_β Bessel function of the first kind of the order β
$M(x)$ Confluent hypergeometric function
N_A Base doping density
N_C Collector doping density
N_E Emitter doping density
$N_{m,ref}$ Reference doping density for doping-dependent carrier mobility
$N_{n,ref}$ Reference doping density for doping-dependent effective intrinsic carrier concentration

N_{ref}^{0} Reference doping density for doping-dependent carrier lifetime
R_x Inverse life time for minority carriers
T Temperature in degree Kelvin
V_{BC} Base-Collector voltage
V_{BE} Base-Emitter voltage
V_T Thermal voltage
W_B Base width
W_C Collector width
W_E Emitter width
$Y_\beta(x)$ Bessel function of the second kind of the order β

g Generation rate constant for the lateral injection through the base
f_w Constant representing the Webster effect
k Boltzmann's constant
n Electron concentration
n_i Intrinsic carrier concentration
n_{ie} Effective intrinsic carrier concentration considering doping dependency
n_{i0} Effective intrinsic carrier concentration without considering doping dependency
p Hole concentration
q Electronic charge
r_a Ratio between the Auger Coefficients for electrons and holes
r_s Ratio between the hole and electron lifetimes without considering doping dependency
v_{sn} Electron saturation velocity
v_{sp} Hole saturation velocity

β Order of the Bessel function
η Logarithmic slope of the base doping profile
γ_1 Constant exponent indicating doping dependence of electron mobility
γ_2 Constant exponent indicating doping dependence of intrinsic carrier concentration
γ_3 Constant exponent indicating doping dependence of hole mobility
μ_n Electron mobility considering doping and field dependency
μ_{n0} Electron mobility considering only doping dependency
$\mu_n(0)$ Electron mobility without considering doping and field dependency
μ_p Hole mobility considering doping and field dependency
μ_{p0} Hole mobility considering only doping dependency
$\mu_p(0)$ Hole mobility without considering doping and field dependency
τ_n Electron lifetime considering doping dependency

τ_n^0 Electron lifetime without considering doping dependency

τ_p Hole lifetime considering doping dependency

τ_p^0 Hole lifetime without considering doping dependency

τ_B Base transit time

Abstract

In deriving an analytical model for the base transit time τ_B for bipolar junction transistors (BJTs), various non-ideal effects have to be considered. These effects include the bandgap narrowing effects due to heavy doping, the Webster and the Kirk effects due to high injection and the effects due to the position and field dependence of the transport parameters (i.e. carrier mobility and carrier lifetime). The non-uniformity of the doping profile, and the doping levels make the transport parameters to be position and field dependent. The electric field in the base is mainly due to the non-uniformity of the doping profile. However, the field is modulated by the injection levels, the gradient of the transport parameters and the majority carrier current density in the base. For low doping levels, the effects of majority carrier current density are insignificant. When base doping level is heavy ($\geq 10^{18}\ cm^{-3}$), the effects of majority carrier current density are no longer negligible. Moreover, at such high base doping, recombination mechanisms and the lateral base injection become significant, which also enhance the effects of majority carrier current density. However, consideration of J_p as well as all non-ideal effects results in a nonlinear, nonhomogeneous, variable-coefficient differential equation, the solution of which is intractable. In this work, a modified current equation reflecting the injection-level dependency has been derived for the first time in the literature. The electric field term deduced in this equation is able to identify the effects of the band-gap narrowing, the injection level and the majority carrier current density. Concept of perturbation theory is applied to linearize the governing differential equation. An exponential approximation technique is introduced to address the intractability problem and used to convert this differential equation into a solvable form. The results of the developed model shows that J_p has a significant effect on the base transit time. Close match with the numerical simulation results and also with measurement data with two experimental setups justifies the validity of the developed model.

Acknowledgements

Alhamdulillah. First of all, I thank to Allah (SWT) to give me the opportunity to work on a topic for which I have great interest, to enrich me with His continual Rahmat to carry out the rigorous research work and to help complete the research successfully. Throughout the period, only He supported and helped me.

Next I would like to thank Professor M. M. Shahidul Hassan, my supervisor, for his continuous suggestions and constant support for carrying out the research. I am also thankful to Professor Mohammad Ali Choudhury, for his guidance over the last couple of years of chaos and confusion and also, for his valuable suggestions regarding the thesis write-up.

Dr. Abul N. Khondker expressed his interest in my work and borne a lot of pains not only to pin-point my errors but also to rectify my language of thesis keeping my intention as much as possible. I am simply grateful to him.

I am also thankful to the present Head of the Department, Professor Md. Saifur Rahman, for his kind support. I recall the supports provided to me by the Heads of the Department since 2003.

I recall Professor M. Rezwan Khan, Vice Chancellor, United international University and Professor Chowdhury Mofizur Rahman, Pro-Vice Chancellor, United International University for their encouragement.

I am especially grateful to Dr. Fayyaz Khan, Head, EEE, United International University to provide me the opportunities to carry out my research work. My friend Dr. Khawza Iftekher Uddin Ahmed, also made me grateful since without his support and encouragement I, even, would fail to start my research.

The development of an analytical model is a tedious and painful (for brain and mind) job. My special thanks goes to my junior colleague Md. Enayetur Rahman who not only alleviated this

pain but also helped me overcome the frustration. I express gratitude to my colleagues (past and present) who hold my hands during the bad days.

I am thankful and grateful to my spouse for her *support, patience and love* over last four years during which she had to live as an academic widow.
The heavenly company and love of my three musketeers (sons)- Meehal, Rajeet and Ziyaad are invaluable. I am not trying to express anything for them since that is an impossible task, except simply uttering "I love you, all".

Of course, I am grateful to my mother and my family members for their patience and *love*. Without them this work would never have come into existence (literally).

Finally, I wish to thank the followings: Shahriar Ahmed Chowdhury (for his friendship), S. M. Moududul Islam & Raiyan Kabir (for encouragement), Ms. Nargis Jahan (for valuable advices) and specially Walid (for a very uncommon friendship and support during the short stay in Staffordshire, England).

At the end, I gratefully recall the support from my ex-colleague Salman Salem Sinwary, Assistant Professor, Department of BBA, Ahsanulllah University of Science and Technology for his invaluable help by lending his own laptop when I was in deep trouble due to viral-attack of my laptop.

Farmgate, Dhaka Md. Iqbal Bahar Chowdhury

Chapter 1
Introduction

The base transit time is a very important parameter that determines several other performance parameters of bipolar junction transistors. These parameters include the maximum frequency of operation (f_{max}), the cut-off frequency (f_T) and the noise figure, all of which determine the high-frequency characteristics of a bipolar transistor. It is observed that the high-frequency performance dominates over other performances of transistors. This increasing requirement forces researchers to identify the effects that limit the high frequency performance and to devise the technologies to overcome or at least circumvent these limitations. In this context, therefore, the accurate modeling for the base transit time is becoming important as the different technologies are evolving to improve the performance of bipolar junction transistor. The physics underlying the modeling of this transit time is still under rigorous research, as this knowledge can be applicable to the devices that involve p-n junction(s) e.g. the hetero-junction bipolar transistor (HBT), photodiodes, phototransistors etc.

The Base transit time depends on various factors among which the effects of majority carrier current, flowing through the base, has been largely ignored in the literature. In this research work, an analytical model is developed considering this effect that is applicable to all current injection levels. In this chapter, first, the bipolar junction transistor and the base transit time are briefly reviewed. Then the objective and scope of this work is presented. The

organization of the work is also included at the end of this chapter.

1.1 Bipolar Junction Transistor

Rapid advancement of solid state devices has started since the invention of the Bipolar Junction Transistor (BJT) in 1948 by a research team of Bell Telephone Laboratories. Now a days, semiconductor devices encompass almost all the aspects of modern life. Transistors are now key elements in high speed computers, space vehicles, satellite, all modern communication and power systems.

Transistors work on two different principles: bipolar operation and unipolar operation. In the unipolar devices only one carrier, which is of majority, is involved. Field-effect transistors (FET) are of this type. Operation of the other type involves both type of carriers: electron and hole and hence it is called bipolar devices. Unipolar devices, specially metal-oxide-semiconductor FETs find applications in the digital circuits specifically for their excellent switching characteristics. On the other hand bipolar devices have applications mostly in the analog circuits because of their better amplification of switching performances. Therefore the research of modern BJT transistors needs to address the frequency limitations, the high power effects and the switching behaviour.

Figure (1.1) shows the cross sectional view of an npn bipolar junction transistor. Two p-n diodes connected back-to-back with a common n or p type region called the base sandwiched between them operate in a way so that transistor operation becomes possible. The carriers in one p-n diode are injected into the base. They travel through the base and finally reach the other p-n diode. The contact from which carriers are injected is called emitter and the contact where these carriers are reached is called collector. Based on the biasing of these two diodes three modes of operation are possible. Of these modes, one mode called the active forward mode is used for amplification purposes. This mode is obtained

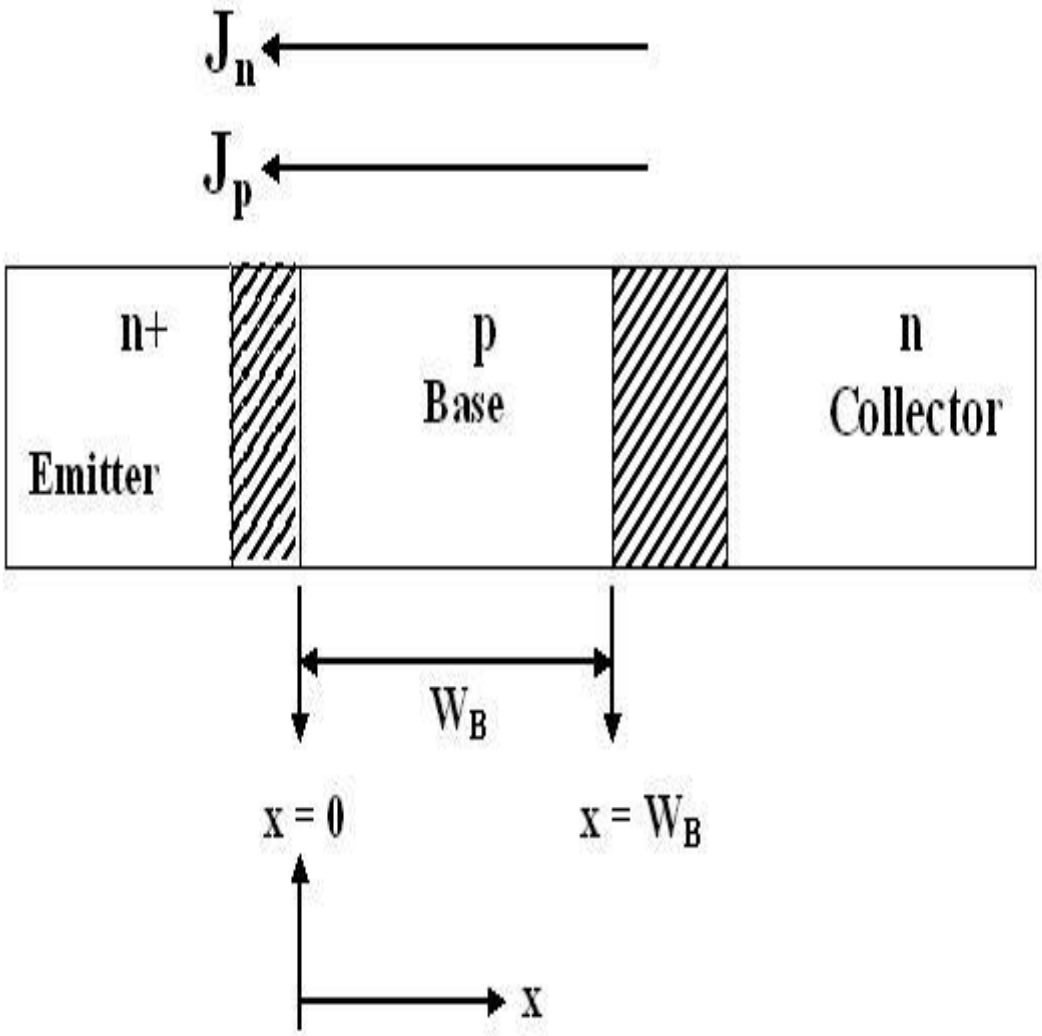

Figure 1.1: The Cross sectional view of a Typical npn Bipolar Junction Transistor showing the Directions of current flow.

when one p-n diode, called base-emitter (B-E) junction, is forward-biased while the other diode, known as base-collector (B-C) junction is reverse-biased. In this mode of operation, majority carriers from the B-E junction are injected into the base region due to diffusion aided by the bias. These carriers increase the concentration of minority carriers of the base significantly. The strong electric field, caused by the reverse-biased B-C junction, is responsible for transporting the increased carriers across the base and to reach the other end of the transistor. Also, involved in the process are the minority carriers in the base that control the current flow of the transistor. Although base region of a transistor is made thinner for practical transistors, there exists several mechanisms and non-ideal effects which influence the storage and speed of minority carriers in the base. As a result, the current gain that determines the emitter efficiency, an important parameter for amplification, and the transit time, which limits the high-frequency performance, are adversely affected.

The complete expressions for currents in bipolar junction transistors can be derived from the following assumptions:

1. Injection level is low,
2. The electric field intensity in the bulk, region outside the depletion regions is so small that the drift current of minority carriers in the bulk is negligible,
3. No recombination and generation takes place in the depletion region,
4. The widths of the emitter and collector regions are greater than the diffusion length of the minority carriers so that the minority carrier densities reach their equilibrium values at the contacts,
5. The collector area is much larger than the emitter area so as to collect all electrons crossing the collector junction,
6. Each of the three bulk regions is uniformly doped and both junctions are considered to be step junctions so that the change in impurity density, from one region to

another, is abrupt,

7. The emitter current is made up entirely on electrons; the emitter injection efficiency is one and
8. The active part of the base and two junctions are of uniform cross sectional area; current flow in the base is essentially one-directional from emitter to collector.

1.2 Base Transit Time

As mentioned in the previous section, the transistor performance analysis is mainly based on emitter efficiency that depends on the current gain and the high frequency models based on transit times. The analysis of emitter efficiency is beyond the scope of this thesis. This research deals with base transit time modeling and identifies the limiting factors of high frequency performance.

The high frequency performance is characterized by various figures of merit, e.g. the maximum frequency of operation (f_{max}), the beta cutoff frequency (f_T) and the alpha-cut off frequency f_α. These parameters are summarized as below:

- Unity-gain Bandwidth frequency, f_T : This is the frequency at which common-emitter short-circuit current gain $\beta = h_{fe} (\equiv \frac{\partial I_C}{\partial I_B})$ is unity.
- Beta Cutoff Frequency, f_β : This is the frequency at which common-emitter short-circuit current gain $\beta = h_{fe} (\equiv \frac{\partial I_C}{\partial I_B})$ becomes 70.7% of the mid-band gain. For practical amplifiers the usable limit for beta cutoff frequency is $0.1 f_T$.
- Alpha Cutoff Frequency, f_α : This is the frequency at which common-base short-circuit current gain $\alpha = h_{fb} (\equiv \frac{\partial I_C}{\partial I_E})$ becomes 70.7% of the mid-band gain. For practical amplifiers, $f_\alpha \approx f_T$.

- Maximum Frequency of Operation, f_{max} : This defines the maximum oscillation frequency. It is the frequency at which unilateral gain becomes unity and can be expressed as [1],

$$f_{max} \approx \frac{1}{2S}\left(\frac{f_T}{2\pi r_0 C_0}\right)^{\frac{1}{2}} \tag{1.1}$$

where S is the emitter stripe width, $r_0 \approx \frac{\rho_B}{W_B}$, ρ_B is the average resistivity of the base layer and C_0 is the collector capacitance per unit areathe other parameters are constant and defined in [1]. The above equation can be rewritten in terms of the base resistance R_B and the collector capacitance C_C as

$$f_{max} \approx \frac{1}{2}\left(\frac{f_T}{2\pi R_B C_C}\right)^{\frac{1}{2}} \tag{1.2}$$

where

$$R_B = r_0 \frac{S}{L} \tag{1.3}$$

$$C_C = C_0 SL \tag{1.4}$$

From the above discussion, it is evident that the main characterizing parameter for high frequency operation is the unity-gain-bandwidth frequency f_T. This cutoff frequency depends on the physical structure of transistor and can be defined through the total transit time τ_{ec} as,

$$f_T = \frac{1}{2\pi\tau_{ec}} \tag{1.5}$$

where the the transit time τ_{ec} is the total time required for injected minority carriers to travel from emitter to collector. This transit time can be divided in five components:

1. Emitter transit time, τ_E

2. Base-emitter depletion layer charging time, τ_{eb}

3. Base transit time, τ_B

4. Base-collector depletion layer charging time, τ_{bc}

5. Collector transit time, τ_C

Therefore,

$$\tau_{ec} = \tau_E + \tau_{eb} + \tau_B + \tau_{bc} + \tau_C \tag{1.6}$$

A rigorous analysis has been made by J. J. H. van der Beisen [2], where he showed that the most influential component is the base transit time, which comprises almost 70% of the total transit time. The next significant contribution comes from emitter transit time. All other transit times are negligible. Of all these transit time components, the most complicated one is the base transit time owing to inclusion of various non-ideal effects. However, a complete analysis that includes all these effects is not available in the literature.

The average time taken by the minority electrons to travel through the base region is called base transit time τ_B. Mathematically, τ_B can be defined as,

$$\tau_B = -q\int_0^{W_B} \frac{n(x)}{J_n(x)}dx \tag{1.7}$$

where W_B is the base width. For the low and high injection regions, the analytical formulation for the base transit time has been derived. For low injection, $n(x) << N_A(x)$ and for high injection region, $n(x) >> N_A(x)$. For uniform base doping, the expressions for base transit time is reduced to [3],

$$\tau_B = \frac{W_B^2}{2D_n} \tag{1.8}$$

$$\tau_B = \frac{W_B^2}{4D_n} \tag{1.9}$$

The base transit time depends on a number of factors such as

1. Type of Doping profile i.e. uniform, exponential, Gaussian etc,
2. Band-gap narrowing effect,
3. Doping, injection level and J_p dependent electric field,
4. Doping and field dependent mobility,
5. Doping and injection level dependent minority carrier lifetime,
6. SRH and Auger Recombination in the base,
7. Webster effect,
8. Velocity saturation at the base-collector (B-C) junction,
9. Base width,
10. Base sheet resistance,
11. Collector current density,
12. Temperature etc.

1.3 Literature Review

In 1985 H. Kroemer [4] generalized the two integral relations deduced by Moll and Ross for the current flowing through the base of a BJT to the case of a hetero structure bipolar transistor with nonuniform energy gap in the base region and developed a base transit model. He showed that the expression for base transit time for low injection region is reduced to equation (8). J. J. H. van der Beisen [2] studied the base transit time as a function of base-emitter bias and divided the total transistor time into five components. For this purpose he used a regional analysis but did not provide any closed form expression. J. S. Yuan [5] investigated the effect of base doping profile on the transit time for all levels of injection. He numerically evaluated the base transit time using a proposed equation for minority carrier profile and boundary conditions and therefore, his work is not concise.

K. Suzuki [6] developed a transit model for uniformly doped bipolar transistor for high level of injection. In this model he considered the velocity saturation effect at the base-collector junction. Later he [7] obtained an expression for base transit time with non-uniformly doped base for high level injection before the onset of the Kirk effect using

perturbation theory. But, the equation form for base transit time is not concise and contains several integrals.

Pingxi *et. el.* [8] proposed a model of transit time that included all of the above-mentioned effects. However, their model is based on iterative techniques. Hence, the obtained expressions in this work are not concise and are inconvenient to understand the device physics. Later, a set of initial conditions was proposed by [9] based on unform doping profile to reduce the computational time needed in the work [8]. This work is also inconvenient since it too is based on the iterative method.

M. Z. R. Khan *et. el.* [10] proposed a model for all injection levels using best curve-fitting technique, where intermediate injection level model was derived from the low and high injection models. Therefore, these models are not accurate. Later Hassan *et. el.* [11] developed the intermediate injection level model by extending the low injection models using perturbation theory. This model also considered both the field and doping dependence of the mobility.

Conventionally, derivation of all analytical models including the works [2, 3, 5-12] for τ_B were made by neglecting majority-carrier current in the quasi-neutral base. Liou *et al.* [13, 14] in their work considered the role of J_p in an npn transistor on τ_B; but their model is based on simulation results of J_p rather than a closed-form analytical expression and it uses position-independent transport parameters and applies iterative approach for solution.

The works in References [15, 16] considered the J_p-dependence in order to develop an analytical model for base transit time. Although these works give a closed-form expression for base transit time and consider all the non-ideal effects discussed in the literature, the models are limited to low injection condition only. Moreover, these models do not include the effects of recombination and the lateral base injection in the quasi-neutral

base region, which must be included to properly investigate the effects of J_p. Including the lateral base injection, Iqbal and Hassan later developed models for nonuniform base doping profile [17] under low-level injection. Later, including recombination mechanisms low-level-injection model [18] and intermediate-level-injection model [19] have been developed by the same authors. Although these models are applicable for non-uniform doping profile, the models neglect J_p-dependency.

1.4 Objective

In an npn transistor, its base Transit time τ_B is a function of minority carrier concentration n(x) and minority carrier current $J_n(x)$. n(x) and $J_n(x)$ depend on various factors among which majority carrier current (J_p) dependence is not considered yet in the literature, as previously mentioned. The main concern of this thesis is to investigate the effect of this J_p, flowing through the base, on τ_B. An analytical model of the base transit time considering this J_p effect is therefore needed. This model must include all the non-ideal effects incorporated so far in the in the literature. This helps understand the significance of J_p-consideration in the analytical modeling of τ_B. Since the recombination mechanism and the lateral injection through the base have effects on J_p, the desired analytical model should include their effects. However, incorporation of all these effects along with J_p leads to a nonlinear, nonhomogeneous and variable-coefficient differential equation. Therefore the governing equation becomes mathematically intractable.

The main objective of this work is to resolve the mathematical intractability of the analytical modeling by applying appropriate techniques and using reasonable approximations. Next the effects of J_p using the developed model are to be analyzed by comparing with a reference model, which neglects the J_p-dependency only. Finally, the validity of the developed model need to be justified against the numerical results and also, with the experimental data.

1.5 Scope of the Work

The analytical modeling presented in this thesis considers majority carrier current in the base. The model includes all the non-ideal effects except plasma-induced band-gap narrowing due to increased injected electrons in the base. The model also neglects the temperature dependance. Therefore, the developed model is applicable for room temperature.

1.6 Organization of the Work

The work described in this thesis is organized as follows. The overview of the basic semiconductor equations as well as the brief description of various non-ideal effects are presented in the Chapter 2. Chapter 3 details the problems and challenges for the development of analytical modeling of base transit time. Chapter 4 describes the appropriate techniques, methods and approximations needed to overcome these problems and challenges. Chapter 5 details both the low injection modeling and the intermediate injection modeling developed. The results and the accompanying discussions are presented in Chapter 6. Future suggestions for the derivation of the analytical modeling as well as concluding remarks are given in the Chapter 7.

Chapter 2
Theory: Equations, Formulations and Models

In order to conceive the physics behind the non-ideal effects on the base transit time of bipolar junction transistors, the basics of semiconductor theory need to be understood clearly. Although the fundamental concept of semiconductors requires knowledge of complicated physics, quasi-static and quasi-equilibrium approximations and Maxwell-Boltzmann distribution for carriers are adequate to understand the physics of all non-ideal effects in a quite simplistic manner. This chapter starts with the transport equations derived from Poisson's equation and then gives a overview of various non-ideal effects on the transport parameters i.e. mobility and lifetime. In doing so, physical models that exist in the literature are also presented and discussed.

2.1 Device Equations

2.1.1 Poisson's Equation

The electric field is quasi-static in semiconductor devices i.e. time-derivatives are neglected in non-homogeneous Helmholtz equations as the device dimensions are much smaller than the wavelength associated with the operating frequency. Under this quasi-static assumption, the electric and magnetic fields are decoupled and the Helmholtz equation reduces to well-known Poisson's equation given by,

$$\nabla^2\varphi = -\frac{\rho}{\varepsilon} \tag{2.1}$$

where ρ represents the space-charge density in semiconductors. This density can be calculated from the knowledge of electron and hole concentrations in conduction and valence band respectively and from the net ionized impurity concentration $N = N_D - N_A$ i.e.,

$$\rho = q(p - n + N) \tag{2.2}$$

where n (p) is electron (hole) concentration.

2.1.2 Continuity Equations

Since the knowledge of n, p is defined under thermal equilibrium condition only, continuity equations are needed to describe the model completely. These equations are given as,

$$\nabla\overline{J_n} - q\left(\frac{\partial n}{\partial t}\right) = +qU \tag{2.3a}$$

$$\nabla\overline{J_p} + q\left(\frac{\partial p}{\partial t}\right) = -qU \tag{2.3b}$$

where U represents the net recombination rate per unit volume and J_n, J_p are the electron and hole current densities, respectively. The detailed expressions for these current densities require the understanding of the physical mechanisms involving electron transport in the semiconductors. On the other hand, the net recombination rate includes several mechanisms such as Shockley-Read-Hall (SRH) recombination, Auger recombination, optical generation and impact ionization. Considering these mechanisms, the total recombination rate at equilibrium condition can be given as [20],

$$U = R - G = (R-G)_{SRH} + (R-G)_A + (R-G)_{BB} - G_{II} \tag{2.4}$$

where $(R-G)_{SRH}$ is due to Shockley-Read-Hall (SRH) recombination, $(R-G)_A$ is due to Auger recombination, $(R-G)_{BB}$ is due to band-to-band radiative recombination and G_{II} is due to impact ionization.

In order to develop the analytical modeling for a npn bipolar junction transistor, one dimensional analysis is preferable as three dimensional analysis is difficult and there is no simple way to solve the 3-D differential equations. For one dimensional case, the Equations (2.3) reduce to

$$\frac{dJ_n}{dx} = +q(R-G) \tag{2.5a}$$

$$\frac{dJ_p}{dx} = -q(R-G) \tag{2.5b}$$

2.1.3 Transport Equations

The transport theory is described by the well-known Boltzmann transport equation (BTE). This equation is based on the semi-classical view of carrier transport in semiconductors. That is electron moves through a sequence of drifts in the electric field followed by scattering events. The drifting time, the type of scattering process and the final state are random quantities and are expressed in terms of transition rates due to various processes. Still the free motion of electron is deterministic and depends on the spatial distribution of the electric field. The BTE can be simplified by assuming the interaction among the carriers to be weak (i.e the single-particle approximation), the energy bands to be parabolic, the scattering processes to be elastic or isotropic and the carrier temperature to be uniform in space and time. Applying the band theory and effective-mass theorem, the BTE can be written as,

$$\overline{J_n} = q\mu_n n\overline{F_n} \tag{2.6a}$$

$$\overline{J_p} = q\mu_p p\overline{F_p} \tag{2.6b}$$

where F_n and F_p are quasi-Fermi potentials. Using the definitions of the quasi-Fermi potentials, equations (2.6) can be written in the familiar form:

$$\overline{J_n} = q\mu_n n\overline{E} + qD_n\nabla n \tag{2.7a}$$

$$\overline{J_p} = q\mu_p p\overline{E} - qD_p\nabla p \tag{2.7b}$$

The current densities consist of the drift component caused by the electric field and the

diffusion component caused by the carrier concentration gradient. μ_n, μ_p represent the electron and hole mobility respectively and D_n, D_p represent the electron and hole diffusion coefficient respectively. For non-degenerate semiconductors these parameters are related by the Einstein relations:

$$D_n = \left(\frac{kT}{q}\right)\mu_n \tag{2.8a}$$

$$D_p = \left(\frac{kT}{q}\right)\mu_p \tag{2.8b}$$

where $\frac{kT}{q}$ is called as thermal voltage, V_T, k is the Boltzmann's constant and T is the temperature in Kelvin. In 1-D form, the Equations (2.7) can be represented as,

$$J_n = q\mu_n n\overline{E} + qD_n \frac{dn}{dx} \tag{2.9a}$$

$$J_p = q\mu_p p\overline{E} - qD_p \frac{dp}{dx} \tag{2.9b}$$

2.2 Physical Models

2.2.1 Heavy Doping Effect: Band-gap Narrowing

When doping density is large, band structure changes significantly. This is due to [21] fluctuations of local potential for statistical distribution of impurities within the crystal lattice and interaction between majority carriers and impurity atoms, between impurity atoms themselves and between a minority carrier and the surrounding cloud of majority carriers.

Interaction between impurity atoms at large concentrations causes impurity levels to broaden into a band. This broadening is further enhanced by the statistical fluctuations of the local potential caused by the random distribution of impurities. This impurity-band-formation theory was developed by Morgan [22] using semiclassical approach. The shape of

the impurity band is nearly Gaussian. The width of this band depends on doping density and is affected by the screening of majority carriers. From the work of Mertens *et. el.* [21] it can be inferred that, when impurity concentrations becomes very large, the impurity band starts to shrink and eventually merges into the conduction band. At high doping densities formation of band tails also occur due to the statistical fluctuations of local potential and the interaction of low-energy wave packets. The theory of this band tail formation was developed by Kane [23]. Also, rigid shift of band-edges occur as a consequence of interaction between majority carriers and between the minority and majority carriers.

Combining the above-mentioned effects leads to an effective bandgap narrowing ΔE_G, which in turn increases the product of the equilibrium electron and hole concentrations as follows:

$$n_{ie}^2 = n_{i0}^2 e^{\frac{\Delta E_G}{kT}} \tag{2.10}$$

where $n^2{}_{i0}$ is the product of the equilibrium electron and hole concentrations without considering band-gap narrowing. An empirical expression for ΔE_G was suggested by Slotboom and De Graaf [24-27] as follows:

$$\Delta E_g = E_{bgn}\left[a + \sqrt{a^2 + 0.5)}\right] eV \tag{2.11}$$

where,

$$a = ln\left(\frac{N_i}{N_{n,ref}}\right)$$

and $N_i = N_A + N_d$ represents the total impurity concentration for uncompensated material. The parameter values are given as,

$$E_{bgn} = 0.009eV$$

$$N_{n,ref} = 1.0\times10^{17}\ cm^{-3}$$

Later [27] these values are corrected to

$$E_{bgn} = 0.00692eV$$

$$N_{n,ref} = 1.3\times10^{17}\ cm^{-3}$$

and with these parameters, Equation (2.11) can be applicable for both n-type and p-type materials.

Since base doping density $N_A(x)$ varies from 5×10^{16} to $2\times10^{18}\ cm^{-3}$ in practical use [28], the expression for $n_{ie}(x)$ can be approximated as [28],

$$n_{ie}^2(x) = n_{i0}^2\left[\frac{N_A(x)}{N_{n,ref}}\right]^{\gamma_2} \tag{2.12}$$

where,

$$n_{i0} = 1.194\times10^{10}\ cm^{-3}$$

$$\gamma_2 = 0.5323$$

2.2.2 Carrier Mobility: Position and Field Dependance

Carrier mobility is defined as,

$$\mu = \frac{q\tau}{m_e^*} \tag{2.13}$$

where m_e^* is the effective mass and τ is the mean scattering time. In order to determine τ and hence μ, various scattering mechanisms are included. The most important mechanisms for non-polar semiconductors like Si and Ge are deformation-potential acoustic phonon, non-polar optical phonon and intervalley scattering. Impurity scattering and electron-hole scattering becomes important for these materials when impurity concentration is relatively large. Using Mathiessen's rule, the low-field mobility μ_0 due to these scattering mechanisms can be combined as,

$$\frac{1}{\mu_0} = \frac{1}{\mu_{ac}} + \frac{1}{\mu_{op}} + \frac{1}{\mu_i} \tag{2.14}$$

where μ_{ac}, μ_{op}, μ_i represent mobility due to acoustic phonon, optical phonon and inter-valley scattering respectively. Although Equation (2.14) interprets the general behaviour fairly in a qualitative manner, the quantitative agreement is not satisfactory and hence empirical expressions containing fitting parameters are used for device-simulation purposes. Selberherr [29] exhaustively studied various mobility models proposed in the literature. One of the most widely used mobility model for silicon was proposed by Caughey and Thomas [30] as,

$$\mu_0 = \mu_{min} + \frac{\mu_{max} - \mu_{min}}{1 + \left(\frac{N_i}{N_r}\right)^{\alpha}} \tag{2.15}$$

To include the temperature dependence of the four parameters involved in Equation (2.15), slight modifications are made by several authors [Baccarani and Ostoja [31], Arora et. el. [32] etc.]. Selberherr has shown that the modified equations are entirely equivalent to Equation (2.15), where the parameters are defined as,

$$\mu_{min} = 88\left(\frac{T}{300}\right)^{-0.57}$$

$$\mu_{max} = \mu_{min} + 1252\left(\frac{T}{300}\right)^{-2.33}$$

$$N_r = 1.432\times 10^{7}\left(\frac{T}{300}\right)^{2.546}$$

$$\alpha = 1$$

for electrons and

$$\mu_{min} = 54.3\left(\frac{T}{300}\right)^{-0.57}$$

$$\mu_{max} = \mu_{min} + 407\left(\frac{T}{300}\right)^{-2.33}$$

$$N_{ref} = 2.67\times10^{7}\left(\frac{T}{300}\right)^{2.546}$$

$$\alpha = 1$$

for holes.

These models are not convenient for use in the analytical formulation of the base transit time of bipolar junction transistor. For practical base doping density range mentioned in section (2.2.1) the low-field doping density dependent electron mobility μ_{n0} model is approximated as [28],

$$\mu_{n0} = \frac{D_n(0)}{kT}\left(\frac{N_A(x)}{N_{m,ref}}\right)^{-\gamma_1} \tag{2.16}$$

with

$$D_n(0) = 20.72 cm^2\ (V.s)^{-1}$$

$$N_{m,ref} = 1.0\times10^{17}\ cm^{-3}$$

$$\gamma_1 = 0.42$$

where, $\mu_n(0) = \frac{D_n(0)}{kT}$ is the electron mobility without considering doping and field dependency.

For low-field hole mobility μ_{p0}, Verhoff and Simke [33], Lu and Kuo [34] used equivalent doping dependent model, which can be rearranged in following form

$$\mu_{p0} = \frac{D_p(0)}{kT}\left(\frac{N_A(x)}{N_{m,ref}}\right)^{-\gamma_3} \tag{2.17}$$

with

$$D_p(0) = 12.5727 cm^2\ (V.s)^{-1}$$

$$\gamma_3 = 0.38$$

where, $\mu_p(0) = \frac{D_p(0)}{kT}$ is the hole mobility without considering doping and field dependency.

The electric field dependency of the carrier mobility is expressed by the widely used Caughey-Thomas-Thornber [30, 35] expression given by,

$$\mu = \frac{\mu_0}{\left[1 + \left(\frac{\mu_0 \mid E \mid}{v_s}\right)^{\beta}\right]^{1/\beta}} \tag{2.18}$$

where, v_s is the saturation velocity and E is the electric field with

$$v_{sn} = 1.04 \times 10^7 \ cm/s$$

$$\beta = 2$$

for electrons and

$$v_{sp} = 8.37 \times 10^6 \ cm/s$$

$$\beta = 1$$

for holes.

The field dependent mobility expression for electron μ_n is further simplified for using analytical formulation. This simplification was originally suggested by Kull *et al.* [36] and later modified by Chen and Kuo [37] as,

$$\mu_n = \frac{v_{sn}}{a_e \mid E_n \mid + \frac{v_{sn}}{\mu_{n0}}} \tag{2.19}$$

where, $a_e = 0.7743$ and. This empirical expression is used in the work done by Hassan *et al.* [11] and also in this work. On the other hand, for the field dependent mobility expression for hole μ_p, Equation (2.18) can be rearranged as,

$$\mu_p = \frac{v_{sp}}{|E_p| + \frac{v_{sp}}{\mu_{p0}}} \tag{2.20}$$

2.2.3 Recombination-Generation

Recombination-generation processes in semiconductors are influenced by various mechanisms which includes photon absorption-emission (radiative transitions), trap-assisted recombination, three-particle Auger-impact transitions, plasmon interaction etc.

In direct gap semiconductors i.e. those having conduction and valence band maxima at same crystal momentum, electron transition predominantly occur through photon absorption-emission. But this is not the case for indirect-gap semiconductors, such as Ge and Si. For these materials, electrons at the conduction band edge have nonzero momentum, but holes at the valence band edge have zero momentum and hence, a direct transition that conserves both energy and momentum is impossible without a lattice interaction (phonon) occurring simultaneously i.e. direct transition requires simultaneous interaction of three particles: the electron, the hole and the phonon. The three-particle interaction occurs when electron and hole densities are very high and is generally termed as Auger recombination.

Two-particle interactions are more likely in Si and Ge, as there are ample localized energy states within the forbidden energy gap into which electron or holes can make transitions. These localized states are always available due to crystal imperfections and metallic impurities. There are four processes through which free carriers can interact with localized states: electron capture R_n, electron emission, G_n, hole capture, R_p and hole capture, R_p. At thermal equilibrium, $R_n = G_n$ and $R_p = G_p$, since thermal equilibrium requires every process must be balanced by its reverse process. When non-equilibrium occurs, $R_n \neq G_n$ and $R_p \neq G_p$. Under this situation, the localized state will act as either a trap or a recombination center. In the former case, carriers will return to conduction or valence

band, whereas, in the latter case carriers will recombine at the localized state. Of these two, recombination centers are generally considered.

SRH Recombination

The theory of trap-assisted recombination-generation was developed by Shockley and Read [38] and independently by Hall [39] and therefore the theory was known as "SRH Theory". According to this theory, the overall population of the recombination centers are not greatly affected as the states are nearly full with majority carriers whether equilibrium or non-equilibrium occurs. At steady-state condition, SRH model reads the net recombination rate as (for acceptor-like SRH centers),

$$(R-G)_{SRH} = \frac{pn - n_{ie}^2}{\tau_{p0}(n+n_1) + \tau_{n0}(p+p_1)} \tag{2.21}$$

where,

$$n_1 = n_{ie} e^{\frac{E_t - E_i}{kT}} \tag{2.22a}$$

$$p_1 = n_{ie} e^{\frac{E_i - E_t}{kT}} \tag{2.22b}$$

$$\tau_{n0} = c_n^{-1} \tag{2.22c}$$

$$\tau_{p0} = c_p^{-1} \tag{2.22d}$$

where, E_t is the energy level of traps, $\tau_{n,p0}$ is the electron/hole lifetime and $c_{n,p}$ is the capture probability represented by,

$$c_{n,p} = \sigma_{n,p} v_{th} N_t \tag{2.23}$$

where, $\sigma_{n,p}$ is the electron/hole capture cross-section, v_{th} is the thermal velocity and N_t is the trap density. For metallic impurities the trap density and hence, the carrier lifetime is independent of the doping density, whereas, for nonmetallic impurities they depend on the doping density. Fossum *et. el.* [40] showed that there is an upper limit for carrier lifetime due to presence of some fundamental crystal defects which act as recombination centers. The equilibrium concentration for such defects varies nearly linearly with doping density.

Incorporating these defects Fossum suggested an empirical expression for carrier lifetime $\tau_{n,p}$ as,

$$\tau_{n,p} = \frac{\tau_{n,p}^0}{1+\frac{N_i}{N_{ref}^0}} \tag{2.24}$$

The parameters values are given in the work of Fossum [41] as,

$$\tau_n^0 = 3.95\times10^{-4}\ sec$$

$$\tau_p^0 = 3.52\times10^{-5}\ sec$$

$$N_{ref}^0 = 7.1\times10^{15}\ cm^{-3}$$

A slightly modified expression for lifetime was proposed by Anheier and Engl [42] as,

$$\tau_{n,p} = \tau_{n,p}^0\left[\frac{N_{ref}^0}{N_i}\right]^{\alpha_{n,p}} \tag{2.25}$$

with $\alpha_{n,p} = 0.5$. Later, Engl and Driks [43] suggested a possible range of values for $\alpha_{n,p}$ as $0.3 < \alpha_{n,p} < 0.6$.

Auger Recombination

For a highly doped silicon, the probability of recombination involving direct transitions is negligible as compared with the probability of recombination through traps (SRH recombination). This direct recombination is called Auger recombination. In Auger recombination, three carriers are involved, either two electrons and a hole or two holes and an electron. Two of the carriers recombine and the third carrier carries away the momentum of the incoming carrier and energy released by the recombination process. Because of these three- carrier interaction Auger recombination is likely to occur when doping density is very high.

Auger recombination can be of band-to-band (phonon-assisted) or trap-assisted. A thorough investigation made by Fossum *et.el.* [44] led to the conclusion that, at any impurity concentration, trap-assisted auger recombination does not appreciably change the carrier

lifetime. Therefore, band-to-band Auger recombination gets attention at high doping density. In this work, it has been shown that minority carrier lifetime turns out to be inversely proportional to the square of impurity concentrations, when impurity concentration becomes very high, indicating dominance of Auger recombination.

In the Auger recombination four partial processes are involved:

1. R_n : An electron moves to the valence band from the conduction band where it neutralizes a hole, and delivers the energy between its initial and final states to another conduction band electron.
2. G_n : An electron from the valence band is hit by a high-energy electron, and is excited to the conduction band.
3. R_p : A electron moves to the valence conduction band from the conduction band where it neutralizes a hole, and delivers the energy between its initial and final states to another hole which is excited to high-energy state (deeper in the valence band).
4. G_p : An electron from the valence band is hit by a high-energy hole, and is excited to the conduction band.

At thermal equilibrium, $R_n = G_n$ and $R_p = G_p$. When non-equilibrium occurs, $R_n \neq G_n$ and $R_p \neq G_p$. At steady-state condition, the net Auger recombination rate can be expressed as,

$$(R-G)_A = (C_{An}n + C_{Ap}p)(pn - n_{ie}^2) \tag{2.26}$$

where, $C_{An,p}$ are the Auger coefficients and can be determined from electrical or optical carrier lifetime measurements. Dziewior and Schmid [45] performed determination of these coefficients from photoluminescence decay measurements following laser excitation. Their results show that Auger coefficients are less temperature-sensitive between $77-400$ K with room temperature values being

$$C_{An} = 2.8\times10^{-31}\ cm^6\ sec^{-1}$$

$$C_{Ap} = 9.9\times10^{-32}\ cm^6\ sec^{-1}$$

By including the temperature dependence, the Auger coefficients can be expressed as,

$$C_{An} = 0.67\times10^{-31} + 8.16\times10^{-34}\ T - 2.44E\times10^{-37}\ T^2$$

$$C_{Ap} = 0.72\times10^{-31} - 0.15\times10^{-34}\ T + 2.92\times10^{-37}\ T^2$$

2.3 Conclusion

In this chapter the basic semiconductor equations and the physical models associated with transport parameters are briefly reviewed. These equations are device-independent. Appropriate application of these equations are very important in order to analytically formulate the model of the device characteristics. In the next chapter, these equations are discussed in the context of an npn bipolar transistor with non-uniformly doped base under arbitrary injection level so that the problems of the base transit time modeling can be understood.

Chapter 3

Problems and Challenges of Base Transit Time Modelling

In the previous chapter the fundamental equations and models are discussed that are applicable for any semiconductor device. For an npn bipolar transistor all these are to be reviewed so that the limiting effects on the base transit time can be understood. In this chapter equations and the models are discussed in the context of an npn bipolar transistor under arbitrary injection-level condition and for arbitrary doping profile. The problems and challenges that have to be overcome for accurate modelling are examined.

3.1 Non-Ideal Effects

The base transit time of a bipolar transistor depends on the velocity of minority carriers and the base width. The velocity depends on the mobility and the electric field. Both these factors are strongly influenced by the doping profile and the injection level. The mobility is dependent on the electric field when electric field crosses a critical limit. Furthermore, various non-ideal effects affect the electric field; these include the band-gap narrowing effect, the Webster effect, the Kirk-effect, velocity saturation at the base-collector junction, majority carrier current density in the base, lateral current injection through the base and recombination in the base. Therefore, an accurate model of electric field acting on the minority carriers in the base is almost a formidable task considering all these factors. Since,

high frequency operation of bipolar transistors is mainly limited by the base transit time that gets reduced with increased electric field, a clear physical understanding of electric field and the role of other factors is a must. In this section, this objective is explored.

The problem of modelling electric field in the base for bipolar transistors with low and uniform base doping profile is simple, since all the above-mentioned effects become negligible. Therefore, in this case, the electric field can be assumed to be zero. But when doping profile becomes nonuniform, the electric field can no longer be neglected. Actually, nonuniform base doping profile is often engineered to enhance the minority carrier flow towards the collector. When base doping profile is nonuniform, majority carriers tend to diffuse towards the collector due to concentration gradient. This tendency is counterbalanced by an electric field which retards the majority carrier flow. The electric field is created in a direction such that the minority carriers in the base are quickly swept to the collector. This is termed as built-in electric field. If the doping profile is kept low i.e. of the order of $10^{14}\ cm^{-3}$ to $10^{16}\ cm^{-3}$, the above-mentioned effects, except the injection-level dependency, can still be neglected [1, 2, 5, 13, 14, 49] and the majority carrier current density can be considered as zero. For an npn bipolar transistor this assumption can be read as,

$$J_p = q\mu_p pE - qD_p \frac{dp}{dx} = 0 \tag{3.1}$$

where, J_p is the majority carrier current density, $p(x) = n(x) + N_A$, N_A is the acceptor doping concentration in the p-type base and n(x) is the injection-level dependent minority carrier concentration. This assumption, therefore, can be used to evaluate electric field as,

$$\frac{E}{V_T} = \frac{1}{p}\frac{dp(x)}{dx} = \frac{d}{dx} lnp(x) \tag{3.2}$$

where, V_T is the thermal voltage and is defined in section 2.1.3 as,

$$V_T = \frac{D_n}{\mu_n} = \frac{D_p}{\mu_p} = \frac{kT}{q}$$

Here, the complexity arises due to the injection-level dependency. Fortunately, this is not a severe problem since the injection level can be considered as low i.e, $n(x) << N_A$ for base doping levels less than an order of $10^{17}\ cm^{-3}$ for an operating base-emitter voltage V_{BE} up to 0.75 V. For V_{BE} higher than 0.8 V, high injection effects occur which causes base-widening. Therefore, base width W_B no longer remains constant. Under high-injection conditions, transit-time modelling is done, in the literature, by assuming that $n(x) >> N_A$. Since, the intermediate region between these low and high level regions is very narrow, the consideration of such region for low base doping levels ($<10^{17}\ cm^{-3}$) can be safely neglected. This greatly reduces the complexity of analytical modelling for such base doping levels, since at this intermediate region the assumptions, $n(x) << N_A$ or $n(x) >> N_A$, is no longer valid.

If base doping concentration exceeds the limit of $10^{17}\ cm^{-3}$, none of the non-ideal effects can be neglected. Hence, the physics behind these effects has to be addressed for accurate modelling of base transit time. In the following subsections these effects are briefly described.

3.1.1 Band-gap Narrowing Effect

At high doping level, band-edge shifts for both valence and conduction bands which is known as the band-gap narrowing effect. Since, the doping profile in the base is nonuniform, the band-gap narrowing becomes position-dependent and it decreases from emitter side to the collector side. As a result, the energy band diagram in the base becomes position-dependent for which two important modifications need to be incorporated. One is the modification of the intrinsic carrier concentration and the other is the presence of an electric field that retards the built-in electric field. The effective intrinsic carrier concentration n_{ie} can be modeled by considering the various interactions among the carriers and therefore, the

expression becomes very complex. A simplified expression can be used for n_{ie} at high doping levels, following the empirical expression suggested by Slotboom *et. el.* [24-27], as shown below [Section (2.1)]

$$n_{ie}^2(x) = n_{i0}^2\left[\frac{N_A(x)}{N_{ref}}\right]^{\gamma_2} \tag{3.3}$$

The estimation of the retarding fields caused by band-gap narrowing becomes complicated since both valence and conduction band-edges are shifted by ΔE_C and ΔE_V, respectively. One way to resolve this complexity is to derive the current transport equations by first considering the band-edge shifts and then determine the retarded electric field from the deviation observed from the current transport equations that ignore the band-gap narrowing effect. This derivation was first carried out by Van Overstraeten *et.el.* [46], where the generalization of the transport equations are made for the case of a position-dependent band-gap by employing the Fermi-Dirac distribution function. This generalized transport equations become simplified for Maxwell-Boltzmann distribution and also if equal band-edge shifts are assumed for valence and conduction bands. Since, base doping concentration is limited below $10^{18}\ cm^{-3}$ for device considerations, this simplified transport equations can be employed to describe the effect of band-gap narrowing. From these simplified transport equations, it can be inferred that the electric field acting on minority carriers is less than that acting on majority carriers and the relation between these fields can be expressed as,

$$\frac{E_n}{V_T} = \frac{E_p}{V_T} - \frac{d}{dx} ln(n_{ie}^2) \tag{3.4a}$$

$$\frac{E_p}{V_T} = \frac{d}{dx} lnp(x) \tag{3.4b}$$

for p-type base in an npn transistor and,

$$\frac{E_p}{V_T} = \frac{E_n}{V_T} - \frac{d}{dx} ln(n_{ie}^2) \tag{3.5a}$$

$$\frac{E_n}{V_T} = \frac{d}{dx} ln n(x) \tag{3.5b}$$

for n-type base in a pnp transistor and where, E_n and E_p are the electric fields acting on the electrons and holes, respectively. The logarithmic derivative term in these expressions is due to the position-dependent band-gap narrowing and therefore, represents the retarding component of electric field.

3.1.2 Velocity Saturation Effect

The Velocity saturation of the minority carriers near the base-collector (B-C) junction has to be incorporated in the analytical models. The commonly used assumption of zero minority carrier concentration at B-C junction can no longer be justified at high doping levels because, it leads to an unrealistic situation in which the minority carriers are required to cross the B-C junction at an infinite velocity. For an npn bipolar transistor, this can be explained from the relations given by,

$$J_n(x) = qv(x)n(x) \quad at\ any\ x\ in\ the\ base\ and \tag{3.6a}$$

$$n(W_B) = 0 \tag{3.6b}$$

Since, the minority carriers cross the B-C junction at $x = W_B$, the electron current density J_n at the B-C junction is not zero, which leads to

$$v(W_B) = \infty \tag{3.7}$$

Therefore, the minority carriers that cross the B-C junction should have a finite velocity. Since, the electric field at the base-collector junction is higher than a critical limit, the velocity of the minority carriers must be saturated near the B-C junction. Roulston *et. el.* [47] investigated this phenomena and suggested that the electron current density at the B-C junction for a bipolar transistor can be expressed as,

$$J_n(W_B) = qv_{sn}n(W_B) \quad npn\ bipolar\ transistor \tag{3.8a}$$

$$J_p(W_B) = qv_{sp}p(W_B) \quad pnp\ bipolar\ transistor \tag{3.8b}$$

where, v_{sn} and v_{sp} are the saturation velocities for electron and holes respectively and $x = W_B$ denotes the base-collector junction. Equations (3.8) can be used as a boundary condition for determining minority carrier concentration profile in the base. Although the minority carrier velocity saturates before reaching the B-C junction, there is yet no analytical expression to determine the exact location in the base near the B-C junction where the velocity saturation occurs.

3.1.3 Webster Effect

Webster [48] showed that the electric field in the base is modulated by the minority carriers in the base as injection level increases. This modulation of electric field is negligible for low injection levels in which minority carrier concentration is much smaller than base doping concentration i.e. $n(x) << N_A(x)$. However, as injection level increases, this assumption leads to erroneous results [6, 7, 11].

The pn-product for any extrinsic semiconductor under non-equilibrium condition can be expressed as [1, 49],

$$p(x)n(x) = n_{ie}^2(x)e^{\frac{V(x)}{V_T}} \tag{3.9}$$

where, the effective carrier concentration n_{ie} is used to include the band-gap narrowing effect and the local voltage is V(x). As the electric field in the base region varies from the emitter side to the collector side, so does the local voltage V(x). Since the distribution of minority carriers in the base is unknown, the electric field and hence, the voltage V(x) cannot be determined. However, the voltage across the base-emitter junction V_{BE} is known. Therefore, the equation (3.9) can be used to determine the boundary value of minority carrier concentration. For an npn bipolar transistor, this boundary value can be expressed as,

$$n(0) = \frac{n_{ie}^2(0)}{p(0)} e^{\frac{V_{BE}}{V_T}} \tag{3.10}$$

where, $x = 0$ denotes the base-emitter junction and $V(0) = V_{BE}$. Under low-injection conditions, $p(0) \approx N_A(0)$. Therefore, the equation (3.10) can be approximated as,

$$n_l(0) = \frac{n_{ie}^2(0)}{N_A(0)} e^{\frac{V_{BE}}{V_T}} \tag{3.11}$$

where, $n_l(0)$ denotes the boundary value under low-injection condition. When injection level increases, n(x) cannot be neglected compared to $N_A(x)$ and hence the relation $p(0) = n(0) + N_A(0)$ must be used. Therefore, the equation (3.10) results in a second order linear equation of $n(0)$ as,

$$n^2(0) + n(0)N_A(0) - n_{ie}^2(0)e^{\frac{V_{BE}}{V_T}} = 0 \tag{3.12}$$

The solution of this equation gives the expressions for n(0) and p(0) as,

$$n(0) = -\frac{N_A(0)}{2} + \frac{\sqrt{N_A^2(0) + 4n_{ie}^2(0)e^{\frac{V_{BE}}{V_T}}}}{2} \tag{3.13a}$$

$$p(0) = \frac{N_A(0)}{2} + \frac{\sqrt{N_A^2(0) + 4n_{ie}^2(0)e^{\frac{V_{BE}}{V_T}}}}{2} \tag{3.13b}$$

Substituting the value of p(0) in the equation (3.10) and rearranging the terms in the denominator gives the boundary value of n(x) at the base-emitter junction as,

$$n(0) = \frac{\frac{n_{ie}^2(0)}{N_A(0)} e^{\frac{V_{BE}}{V_T}}}{\frac{1}{2} + \sqrt{\frac{1}{4} + \left[\frac{n_{ie}(0)}{N_A(0)}\right]^2 e^{\frac{V_{BE}}{V_T}}}} = n_l(0) f_w \tag{3.14}$$

where, the factor f_w is expressed by

$$f_w = \frac{1}{\frac{1}{2} + \sqrt{\frac{1}{4} + \left[\frac{n_{ie}(0)}{N_A(0)}\right]^2 e^{\frac{V_{BE}}{V_T}}}} \tag{3.15}$$

reflects the injection-level dependency of the boundary value. Under low-injection this factor becomes unity; but as the injection level increases, this factor decreases from unity. Since, the minority carrier distribution throughout the base region decreases from the value of n(0), this distribution in the base decreases as the injection level increases. This decreasing trend of n(x) with injection level results in a lower gradient of n(x) and hence, of p(x). Since, electric field is the logarithmic derivative of p(x) (Equation 3.2), it can be concluded that the electric fields in the base decrease as injection level increases.

3.1.4 Kirk Effect

Kirk effect [50] occurs at high-injection level condition i.e. when minority carrier concentration becomes greater than the base doping levels. For an npn bipolar transistor, this condition is expressed as $n(x) >> N_A(x)$. Under such condition the number of electrons entering the base-collector depletion region cannot be neglected compared to the concentration of negatively charged acceptor ions present in the B-C depletion region. Thus, the total number of negative charges at the base side of this depletion layer increases significantly. In order to accommodate this increase of negative charges compared to the positive charges at the collector side, the depletion layer at the base side has to shrink which in turn causes the increase in base width. This phenomena is termed as the base-width modulation. The result of this phenomena is the increase of the base transit time. The onset of the Kirk effect is determined from this phenomena, which can be used as an indication of high-injection effects. The Kirk effect occurs when the number of minority carriers that cross the B-C junction $n(W_B)$ is comparable to the base doping concentration N_A. However, for device considerations, N_A must be higher than the collector doping concentration N_C. Therefore, the condition for not triggering the high injection effect for an npn bipolar transistor can be given as,

$$n(W_B) << N_C \tag{3.16}$$

From the Equation (3.9) it is evident that the above condition can be achieved by increasing base doping concentration as minority carrier concentration is inversely proportional to the base doping density. From the same equation it is also evident that $n(W_B)$ becomes

comparable to N_C at higher bias levels for heavy doping since $n(W_B)$ can be increased by increasing the bias. In other words, high injection level occurs at a higher voltage level for heavy base doping. Therefore, the $n(W_B)$ and hence, the electron current density J_n becomes much higher for heavy doping than that found at lower doping. Hence, the current capability of bipolar transistors can be increased up to hundred times using high base doping levels. This increased current capability reduces the base transit time considerably even at the high bias levels despite the retarding effect of high injection effects.

Another significant effect of heavy base doping is that it introduces an intermediate injection level. This intermediate injection level for such doping can no longer be negligible. Under intermediate injection level condition n(x) is comparable to N_A and hence, the analytical model for this region becomes further intractable. This intractability problem can be overcome by first deriving the low injection model which can then be extended to intermediate injection levels by the use of perturbation theory as suggested by Suzuki [28].

3.1.5 Doping and Field Dependence of Mobility

At low base doping density, the minority carrier mobility in the base can be regarded as constant i.e. independent of doping density and independent of electric field. As base doping increases beyond the order of $10^{16}\ cm^{-3}$, the position and field dependency of mobility cannot be neglected. For an npn bipolar transistor with a high doping density, the electron mobility considering both these dependency can be expressed as [section 2.2.2],

$$\mu_n = \frac{v_{sn}}{a_e \mid E_n \mid + \dfrac{v_{sn}}{\mu_{n0}}} \tag{3.17a}$$

$$\mu_{n0} = \frac{D_n(0)}{kT}\left(\frac{N_A(x)}{N_{m,ref}}\right)^{-\gamma_1} \tag{3.17b}$$

where, μ_{n0} represents the low-field electron mobility. For convenience, the equations (3.17a) and (3.17b) can be expressed in terms of diffusivity as,

$$\frac{1}{qD_n} = \frac{1}{qD_{n0}} + \frac{a_e}{qv_{sn}}\left|\frac{E_n}{V_T}\right| \tag{3.18a}$$

$$\frac{1}{qD_{n0}} = \frac{1}{qD_n(0)}\left(\frac{N_A(x)}{N_{m,ref}}\right)^{\gamma_1} \tag{3.18b}$$

3.1.6 Recombination Effects

As discussed in Section (2.2.3), recombination-generation mechanisms include SRH recombination, trap-assisted Auger recombination, radiative recombination and impact ionization. For Si bipolar transistors, the first two mechanisms are significant when the base doping density is high. Of these, Auger recombination becomes more dominant as doping density increases. For indirect semiconductors, such as silicon, the radiative recombination is insignificant [20] due to small photon momentum. The Impact ionization is the reverse process of Auger recombination. For the neutral bulk region this term can be omitted because there is no spontaneous generation in this region. Therefore for the bulk silicon of highly doped base, the total recombination rate can be written as,

$$R-G = (R-G)_{SRH} + (R-G)_{Auger} \tag{3.19}$$

where,

$$(R-G)_{SRH} = \frac{pn-n_{ie}^2}{\tau_p(n+n_1)+\tau_n(p+p_1)} \tag{3.20a}$$

$$(R-G)_{Auger} = (C_{An}n + C_{Ap}p)(pn-n_{ie}^2) \tag{3.20b}$$

where, $\tau_{n,p}$ are the doping-dependent electron and hole lifetime. The empirical expressions of these electron and hole lifetimes given in Section (2.2.3) are rewritten for the base region of an npn bipolar transistor as,

$$\tau_n = \frac{\tau_n^0}{1+\frac{N_A}{N_{ref}^0}} \tag{3.21a}$$

$$\tau_p = \frac{\tau_p^0}{1+\frac{N_A}{N_{ref}^0}} \tag{3.21b}$$

For the neutral base region, traps can be considered as shallow-level i.e trap-centers are very close to the intrinsic Fermi level. Therefore, $n >> n_1$ and $p >> p_1$. Incorporating these

considerations the Equations (3.20) can be modified as,

$$(R-G)_{SRH} = \frac{1}{\tau_p n + \tau_n p} p(n - \frac{n_{ie}^2}{p}) \tag{3.22a}$$

$$(R-G)_{Auger} = (C_{An} n + C_{Ap} p) p(n - \frac{n_{ie}^2}{p}) \tag{3.22b}$$

Applying the charge-neutrality condition in the base i.e $p = n + N_A$, these expressions can be reorganized as,

$$(R-G)_{SRH} = \left[\frac{\frac{1}{\tau_n}}{(1+r_s)n + N_A} \right] p \times (n - \frac{n_{ie}^2}{p}) \tag{3.23a}$$

$$(R-G)_{Auger} = C_{Ap}\{(1+r_a)n + N_A\} p \times (n - \frac{n_{ie}^2}{p}) \tag{3.23b}$$

where,

$$r_s = \frac{\tau_p^0}{\tau_n^0}$$

$$r_a = \frac{C_{An}}{C_{Ap}}$$

Combining these two recombination mechanisms, the current continuity equations in the base region can be expressed as,

$$\frac{dJ_n}{dx} = qR_x(n - \frac{n_{ie}^2}{p}) \tag{3.24a}$$

$$\frac{dJ_p}{dx} = -qR_x(n - \frac{n_{ie}^2}{p}) \tag{3,24b}$$

where,

$$R_x = \left[\frac{\frac{1}{\tau_n}}{(1+r_s)n + N_A} + C_{Ap}[(1+r_a)n + N_A] \right] \times (n + N_A) \tag{3.25}$$

The physical significance of the term R_x can be appreciated if the Equation (3.24a) is compared with the electron continuity equation given in standard text books for electron

continuity equation under low-level injection condition given by

$$\frac{dJ_n}{dx} = \frac{qn}{\tau_n} \tag{3.26}$$

where, τ_n is the minority electron lifetime. The term R_x can be labeled as *Inverse Life Time* in this context.

3.1.7 Lateral Injection Through Base

The work of G.T Wright and P. P Frangos [51], concerning high power npn bipolar junction transistors, has shown that the analysis for minority electron concentration profile and minority electron current density that neglect the lateral base current density for operation in saturation region is not valid. Therefore, the authors have added the majority carrier current density in their analysis.

In order to develop a simple analytical model for bipolar junction transistor, some means must be found to incorporate the lateral injection of base current into the active base region. This can be done by the use of an approximate source function G_b suggested by B. V. Gokhale [52]. The hole current continuity equation in the base region for an npn bipolar junction transistor can be modified as,

$$\frac{dJ_p}{dx} = -qR_x(n - \frac{n_{ie}^2}{p}) + qG_b \tag{3.27}$$

The physical model for the source function G_b is not clearly understood. Gokhale [52] proposed a constant for this function within an effective electrical base width. A better and intuitively acceptable description is to assume that the lateral base current, and hence the source function is proportional to local concentration of the majority carriers in the base [51], as given by

$$G_b = gp(x) \tag{3.28}$$

where the coefficient g is the rate constant which describes the lateral injection of base current. In this way, the physical mechanism of majority carrier current flow can be

incorporated in the model. Divergence of majority (hole) current given by Equation (2.5b) can be reformulated as,

$$\frac{dJ_p}{dx} = -qR_x\left[n(x) - \frac{n_{ie}^2(x)}{n(x)+N_A(x)}\right] + qg\{n(x)+N_A(x)\} \tag{3.29}$$

where locally valid charge-neutrality condition is used.

3.1.8 Majority Carrier Current Dependence

Conventionally the majority carrier current density in the base region is neglected in the analytical modelling of base transit time. This is justified for low base doping densities, since the contribution of this current density towards the electric field and hence, the base transit time is insignificant. But, the contribution becomes increasingly significant as base doping level is increased. Since inclusion of this majority carrier current density makes the analytical modelling rather complicated, this is usually neglected in the literature, even for heavy base doping. The modifications required in this regard are presented in this subsection.

If majority carrier density is not neglected, the hole electric field in the base region of an npn bipolar transistor can be expressed, as an alternative to the expression given in Equation (3.4b), as

$$\frac{E_p}{V_T} = \frac{d}{dx}lnp(x) + \frac{J_p(x)}{qD_p p(x)} \tag{3.30}$$

Due to heavy base doping, the hole mobility is both doping level and electric field dependent. Considering this fact, the hole mobility then can be expressed as [section 2.2.2],

$$\mu_p = \frac{v_{sp}}{|E_p| + \frac{v_{sp}}{\mu_{p0}}} \tag{3.31a}$$

$$\mu_{p0} = \frac{D_p(0)}{kT}\left(\frac{N_A(x)}{N_{m,ref}}\right)^{-\gamma_3} \tag{3.31b}$$

where, μ_{p0} represents the low-field electron mobility. For convenience, the above equations can be expressed in terms of diffusivity as,

$$\frac{1}{qD_p} = \frac{1}{qD_{p0}} + \frac{a_h}{qv_{sn}}\left|\frac{E_p}{V_T}\right| \tag{3.32a}$$

$$\frac{1}{qD_{p0}} = \frac{1}{qD_p(0)}\left(\frac{N_A(x)}{N_{m,ref}}\right)^{\gamma_3} \tag{3.32b}$$

where,

$$a_h = \frac{v_{sn}}{v_{sp}}$$

Since E_p is negative in the base region, a minus sign is used to make it positive i.e. $E_p = -|E_p|$. Substituting the expression of E_p given by Equation (3.30) in the Equation (3.32a) results,

$$\frac{1}{qD_p} = \frac{1}{qD_{p0}} - \frac{a_h}{qv_{sn}}\left[\frac{d}{dx}lnp(x) + \frac{J_p(x)}{qD_p p(x)}\right] \tag{3.33}$$

Now, rearranging the terms in the above equation gives an expression for diffusivity as,

$$\frac{1}{qD_p} = \frac{p(x)\left[\frac{1}{qD_{p0}} - \frac{a_h}{qv_{sn}}\frac{d}{dx}lnp(x)\right]}{p(x) + \frac{a_h}{qv_{sn}}J_p(x)} \tag{3.34}$$

Using this expression for hole diffusivity in the Equation (3.30), the hole electric field E_p can be obtained in terms of $J_p(x)$ and $p(x)$ as,

$$\frac{E_p}{V_T} = \frac{d}{dx}lnp(x) + \frac{J_p(x)\times\left[\frac{1}{qD_{p0}} - \frac{a_h}{qv_{sn}}\frac{d}{dx}lnp(x)\right]}{p(x) + \frac{a_h}{qv_{sn}}\times J_p(x)} \tag{3.35}$$

The simplification of Equation (3.33) results in

$$\frac{E_p}{V_T} = \frac{\frac{dp}{dx} + J_p(x)\times\frac{1}{qD_{p0}}}{p(x) + \frac{a_h}{qv_{sn}}\times J_p(x)} \tag{3.36}$$

Using charge neutrality condition $p(x) = n(x) + N_A(x)$, the Equation (3.36) can be further rearranged as,

$$\frac{E_p}{V_T} = \frac{\frac{dn}{dx} + \frac{dN_A}{dx} + J_p(x) \times \frac{1}{qD_{p0}}}{n(x) + N_A(x) + \frac{a_h}{qv_{sn}} \times J_p(x)} \tag{3.37}$$

The electron electric field E_n can be found from the Equation (3.4a) as,

$$\frac{E_n}{V_T} = \frac{\frac{dn}{dx} + \frac{dN_A}{dx} + J_p(x) \times \frac{1}{qD_{p0}}}{n(x) + N_A(x) + \frac{a_h}{qv_{sn}} \times J_p(x)} - \frac{d}{dx} ln(n_{ie}^2) \tag{3.38}$$

The electron mobility given by Equation (3.18a) can be expressed as,

$$\frac{1}{qD_n} = \frac{1}{qD_{n0}} + \frac{a_e}{qv_{sn}} \left| \frac{\frac{dn}{dx} + \frac{dN_A}{dx} + J_p(x) \times \frac{1}{qD_{p0}}}{n(x) + N_A(x) + \frac{a_h}{qv_{sn}} \times J_p(x)} - \frac{d}{dx} ln(n_{ie}^2) \right| \tag{3.39}$$

which is further rearranged by using the Equation (3.18b) to reflect the dependency of diffusivity on n(x), $N_A(x)$ and $J_p(x)$ as,

$$\frac{1}{qD_n} = \frac{1}{qD_n(0)} \left(\frac{N_A(x)}{N_{m,ref}} \right)^{\gamma_1} + \frac{a_e}{qv_{sn}} \left| \frac{\frac{dn}{dx} + \frac{dN_A}{dx} + J_p(x) \times \frac{1}{qD_{p0}}}{n(x) + N_A(x) + \frac{a_h}{qv_{sn}} \times J_p(x)} - \frac{d}{dx} ln(n_{ie}^2) \right| \tag{3.40}$$

An expression for J_p is required to determine the electric fields and mobilities. In order to obtain this expression for J_p, the hole current continuity equation given by Equation (3.29) can be integrated as,

$$J_p(x) = K - q\int_0^x R_x \left[n(x) - \frac{n_{ie}^2}{n(x) + N_A(x)} \right] dx + qg\int_0^x [n(x) + N_A(x)] dx \tag{3.41}$$

The integration constant K and the generation rate g can be determined from the boundary values of J_p at $x = 0$ and at $x = W_B$ i.e. $J_p(0)$ and $J_p(W_B)$. Of these two constants K can be determined easily as,

$$K = -J_p(0) \tag{3.42}$$

The minus sign is introduced in the above equation as J_p is negative for an npn bipolar transistor. The other constant g can be determined by performing the two integration of the right side of Equation (3.41), which require knowledge of $n(x)$, $N_A(x)$ and R_x.

Considering unform doping profile in the emitter and collector regions, the boundary values for $J_p(x)$ i.e. $J_p(0)$ and $J_p(W_B)$ can be given for the forward-active mode operation of an npn bipolar transistor as,

$$J_p(0) = -\frac{qD_{pE}(0)}{W_E}\frac{n_{ieE}^2}{N_E}e^{\frac{qV_{BE}}{kT}} \tag{3.43a}$$

$$J_p(W_B) = -\frac{qD_{pC}(0)}{W_C}\frac{n_{ieC}^2}{N_C} \tag{3.43b}$$

where,

D_{pE} = the hole mobility in the emitter region

D_{pC} = the hole mobility in the collector region

n_{ieE} = the effective intrinsic concentration in the emitter region

n_{ieC} = the effective intrinsic concentration in the collector region

N_E = the emitter doping concentration

N_C = the collector doping concentration

W_E = the emitter width and

W_C = the collector width

The hole mobility in n-type silicon is different from the hole mobility in p-type silicon. As suggested by the works [53, 54], the mobility ratio for holes can be taken as,

$$\frac{\text{hole mobility in n-type silicon}}{\text{hole mobility in p-type silicon}} = 2.2 \tag{3.44}$$

Using the above relation, $D_{pE}(0)$ and $D_{pC}(0)$ can be calculated from the following relations:

$$D_{pE}(0) = 2.2 \times D_p(0) \times \left[\frac{N_E}{N_{m,ref}}\right]^{-\gamma_3} \tag{3.45a}$$

$$D_{pC}(0) = 2.2 \times D_p(0) \times \left[\frac{N_C}{N_{m,ref}}\right]^{-\gamma_3} \tag{3.45b}$$

For a n^+-p-n transistor, emitter doping level is higher than the base doping level and collector doping level is comparable with the base doping level. Therefore, effective intrinsic carrier concentrations in the emitter and collector regions must include the band-gap narrowing effect. Considering this fact $n_{ieE}(0)$ and $n_{ieC}(0)$ can be calculated from the following relations:

$$n_{ieE}^2(0) = n_{i0}^2\left(\frac{N_E}{N_{n,ref}}\right)^{\gamma_2} \tag{3.46a}$$

$$n_{ieC}^2(0) = n_{i0}^2\left(\frac{N_C}{N_{n,ref}}\right)^{\gamma_2} \tag{3.46b}$$

For the non-unform doping profile in the emitter, the expression for $J_p(0)$ need to be modified. Since the emitter doping level is very high (of the order of $10^{20}\,cm^{-3}$), low-injection condition prevails there under normal operating condition. Therefore, recombination in the emitter can safely be neglected, majority carrier current in the emitter J_n can be assumed as zero and the field-dependency of the carrier mobility can be ignored. All these considerations lead the governing differential equation for minority hole concentration in the emitter

$$\frac{dp}{dx} - p\frac{E_p}{V_T} = -\frac{J_p}{qD_p} \tag{3.47}$$

to

$$\frac{dp}{dx} + p\left[\frac{d}{dx}ln\frac{N_d}{n_{ie}^2}\right] = -\frac{J_p}{qD_p} \tag{3.48}$$

where electric field E_p is expressed considering bandgap narrowing effect as

$$\frac{E_p}{V_T} = \frac{d}{dx}ln\frac{N_d}{n_{ie}^2} \tag{3.49}$$

where N_d is the emitter doping concentration. The boundary conditions for the emitter region are given as

$$p(0) = \frac{n_{ie}^2(0)}{N_d(0)}e^{\frac{V_{BE}}{V_T}} \tag{3.50}$$

$$p(W_E) = 0 \tag{3.51}$$

where $x = 0$ and $x = W_E$ are assumed at the emitter side of the base-emitter junction and the emitter surface side, respectively. Using the boundary conditions result in the expression for J_p as

$$J_p = \frac{1}{\int_0^{W_E} \frac{N_d}{n_{ie}^2} \frac{1}{qD_p} dx} \tag{3.52}$$

This expression for J_p in the emitter region can be used as the boundary value for J_p i.e $J_p(0)$ at the base side of the base-emitter junction in the base region. For uniform doping profile, this expression leads to the expression given by the Equation (3.43a). For exponential and Gaussian doping profiles, $J_p(0)$ can be obtained as,

$$J_{p,exp}(0) = -\frac{qD_{pE}(0)}{W_E} \frac{n_{ieE}^2(0)}{N_E} \frac{\eta_E(1-\gamma_2+\gamma_3)}{1-u_{EW}^{1-\gamma_2+\gamma_3}} e^{\frac{qV_{BE}}{kT}} \tag{3.53a}$$

$$J_{p,gauss}(0) = -\frac{qD_{pE}(0)}{W_E} \frac{n_{ieE}^2(0)}{N_E} \frac{2\sqrt{\eta_E(1-\gamma_2+\gamma_3)}}{\sqrt{\pi} erf\left(\frac{\sqrt{\eta_E(1-\gamma_2+\gamma_3)}}{W_E}\right)} e^{\frac{qV_{BE}}{kT}} \tag{3.53b}$$

where the emitter doping for exponential and Gaussian profile can be assumed as

$$N_{d,exp} = N_E e^{-\eta_E \frac{x}{W_E}} = N_E u_E \tag{3.54a}$$

$$N_{d,gauss} = N_E e^{-\eta_E \left(\frac{x}{W_E}\right)^2} \tag{3.54b}$$

where η_E is the logarithmic slope of the doping profile given by

$$\eta_E = log\left(\frac{N_E}{N_d(W_E)}\right) \tag{3.55}$$

where N_E and $N_d(W_E)$ are the emitter doping concentrations at $x = 0$ and $x = W_E$, respectively.

3.2 Problems and Challenges of Base Transit Time Modelling

In the previous section, the physical models of various non-ideal effects have been briefly reviewed. Inclusion of these models make the analytical modelling complicated. When majority carrier density is considered in the modelling, whether it is intended to do under

low injection condition or intermediate injection level condition, the degree of complexity increases so much that the modelling becomes intractable. In this section, the problems and the difficulty level of this modelling effort are explored.

In order to obtain an expression for the base transit time for an npn bipolar transistor, the minority electron concentration n(x) and the electron current density $J_n(x)$ need to be determined. Conventionally, the determination procedure involves the expression for electron current given by Equation (2.9a), which is recalled here as,

$$J_n = qn\mu_n E_n + qD_n \frac{dn}{dx} \tag{3.56}$$

By dividing each term by qD_n, a first order differential equation of n(x) is formed as,

$$\frac{dn}{dx} + n\frac{E_n}{V_T} = \frac{J_n(x)}{qD_n} \tag{3.57}$$

The solution of this equation gives n(x) and $J_n(x)$. The above equation therefore can be treated as the working differential equation for the base transit modelling. This apparently simple differential equation becomes very much complicated when majority carrier current density, recombination and all other non-ideal effects are included. Using the expression of E_n and D_n transforms the differential equation as,

$$\frac{dn}{dx} + \left[\frac{\frac{dn}{dx} + \frac{dN_A}{dx} + \frac{J_p}{qD_{p0}}}{n + N_A + \frac{a_h J_p}{qv_{sn}}} - \frac{d}{dx} ln(n_{ie}^2) \right] n$$

$$= J_n \left[\frac{1}{qD_n(0)} \left(\frac{N_A(x)}{N_{ref}} \right)^{\gamma_1} + \frac{a_e}{qv_{sn}} \left| \frac{\frac{dn}{dx} + \frac{dN_A}{dx} + \frac{J_p}{qD_{p0}}}{n + N_A + \frac{a_h J_p}{qv_{sn}}} - \frac{d}{dx} ln(n_{ie}^2) \right| \right] \tag{3.58}$$

The above equation can be rearranged as,

$$\left[\frac{2n + N_A + \frac{a_h J_p}{qv_{sn}}}{n + N_A + \frac{a_h J_p}{qv_{sn}}} \right] \frac{dn}{dx} + \left[\frac{\frac{dN_A}{dx} + \frac{J_p}{qD_{p0}}}{n + N_A + \frac{a_h J_p}{qv_{sn}}} - \frac{d}{dx} ln(n_{ie}^2) \right] n$$

$$= J_n \left[\frac{1}{qD_n(0)} \left(\frac{N_A(x)}{N_{ref}} \right)^{\gamma_1} + \frac{a_e}{qv_{sn}} \left| \frac{\frac{dn}{dx} + \frac{dN_A}{dx} + \frac{J_p}{qD_{p0}}}{n + N_A + \frac{a_h J_p}{qv_{sn}}} - \frac{d}{dx} ln(n_{ie}^2) \right| \right] \tag{3.59}$$

The analytical solution of this differential equation is intractable, because

- The differential equation is non-linear and non-homogeneous.
- The expression of J_p requires knowledge of n(x) as is evident from Equation (3.41), which in turn requires the knowledge of J_p.
- As seen from the expression for R_x given by Equation (3.25), inclusion of recombination mechanisms makes the expression a complex one, which requires knowledge of n(x). Therefore, the integration of the term containing R_x of Equation (3.41) becomes intractable.
- The term representing lateral injection through base of Equation (3.41) imposes further complexity in deriving the expression for J_p.
- As recombination is considered, J_n can no longer be treated as constant as used conventionally.
- For low-level injection $n(x) << N_A(x)$ assumption can be used, which simplifies the solution greatly. But for intermediate injection level condition this assumption cannot be used.
- Since, dependency of doping and electric field is considered for electron mobility, the right hand side of the above differential equation is not a simple one as obtained when J_p-dependency of electric field is not considered.
- Since, the base doping profile is non-uniform, the analytical solution becomes impossible.
- Since the coefficients of the differential equation is variable, the determination of integrating factor to solve this equation is not simple and easy.

In order to obtain a tractable solution of the differential equation given by the Equation (3.59), following challenges have to be overcome:

- The differential equation contains two unknown variables $J_n(x)$ and $J_p(x)$. Since

recombination and lateral base injection are considered, both these terms are no longer constant.

- One way to remove $J_n(x)$ from the differential equation is to differentiate the equation (3.59) and then using the electron current continuity equation given by the Equation (3.24a). But the coefficients of n(x) and $J_n(x)$ contain n(x) and its derivative as well as $J_p(x)$. Again, $J_n(x)$ itself is included in the coefficient of $\frac{dn}{dx}$. Therefore, further differentiation makes the non-linearity problem of the differential equation even more complicated and hence, removal of $J_n(x)$ is a big issue.
- Another major issue is the determination of J_p. The expression for $J_p(x)$ given by Equation (3.41) shows that that the integration of the terms is analytically impossible because these terms contain unknown n(x).
- The non-linearity of the differential equation is due to the presence of the terms n(x) and $J_p(x)$. Some means must be made to overcome the problem by approximating n(x) without the loss of generality.
- The non-homogeneity problem can be replaced by removing J_n which is not easy. Moreover, since $\frac{1}{qD_n}$ term is multiplied with $J_n(x)$, a simplified form of this term is needed to resolve the non-homogeneity problem.
- Since the variable coefficients of the above-mentioned differential equations are complicated in nature, these terms must be converted into suitable forms for achieving tractability.
- Resolving all the above-mentioned challenges still leaves an analytically unsolvable differential equation. It is therefore intended to devise some transformation techniques so that the differential equation becomes solvable.

3.3 Conclusion

This chapter briefly describes the various non-ideal effects on base transit time modelling. These non-ideal effects are not strictly additive and therefore, not only make their effects difficult to understand but also present a lot of problems and challenges for analytical modelling. The problems and the challenges that are observed due to these effects have been investigated in this chapter. Resolving the problems and overcoming the challenges is the next job to do. This requires the choice to devise appropriate method and techniques. By explaining the origin and cause of these difficulties, this chapter creates a foundation for successful analytical modelling presented in the following chapter.

Chapter 4
Methodology

In the previous chapter the problems and the challenges that are to be addressed faced in order to derive an analytical model of base transit time have been discussed. The challenges are mainly due to the nonlinearity, non-homogeneity and presence of complicated variable coefficients in the governing differential equation. In order to overcome these challenges, suitable techniques and appropriate approximations are needed. The techniques and approximations must be such that the physics is not ignored while making the model mathematically tractabe. Even then some transformation methods must be devised to make the working differential equation into familiar form. Keeping all these constraints in mind, this chapter aims to find out the roots of the problems and then proposes techniques and approximations to overcome the challenges.

4.1 Nonlinearity Problem: Solution Techniques

The first-order differential equation derived considering all the non-ideal effects in section (3.2) is repeated here for convenience.

$$\left[\frac{2n+N_A+\frac{a_h J_p}{q v_{sn}}}{n+N_A+\frac{a_h J_p}{q v_{sn}}}\right]\frac{dn}{dx}+\left[\frac{\frac{dN_A}{dx}+\frac{J_p}{qD_{p0}}}{n+N_A+\frac{a_h J_p}{q v_{sn}}}-\frac{d}{dx}ln(n_{ie}^2)\right]n$$

$$=J_n\left[\frac{1}{qD_n(0)}\left(\frac{N_A(x)}{N_{ref}}\right)^{\gamma_1}+\frac{a_e}{q v_{sn}}\left|\frac{\frac{dn}{dx}+dN_A}{n+N_A+\frac{a_h J_p}{q v_{sn}}}+\frac{\frac{J_p}{qD_{p0}}}{dx}-\frac{d}{dx}ln(n_{ie}^2)\right|\right] \quad (4.1)$$

The nonlinearity of this differential equations is due to the presence of n(x). Therefore, to overcome the nonlinearity removal of n(x) is a necessary. For this concept of perturbation theory is used. Moreover, presence of J_n term in the coefficient of $\frac{dn}{dx}$ complicates the nonlinearity. This also should be carefully resolved and an approximation for diffusivity is, therefore, needed. In the following subsections, the techniques of overcoming the problems are explored.

4.1.1 The Perturbation Theory

The expression for electron electric field derived in the previous chapter is recalled here:

$$\frac{E_n}{V_T} = \frac{\frac{dn}{dx} + \frac{dN_A}{dx} + J_p(x) \times \frac{1}{qD_{p0}}}{n(x) + N_A(x) + \frac{a_h}{qv_{sn}} \times J_p(x)} - \frac{d}{dx} ln(n_{ie}^2) \tag{4.2}$$

This expression shows that electric field depends on both the concentration and the gradient of the base doping profile, the minority carrier concentration as well as on the band-gap narrowing effect and the majority carrier density. Since, the concentration and the gradient of minority carrier concentration changes as bias voltage changes, the electric field has a strong dependency on the injection level. All of these dependencies need to be identified clearly in the expression for electric field. Concept of perturbation theory using Webster effect [48] can be used for this purpose.

In order to reflect the injection level dependency of electric field, the Equation (3.38) has to be modified further. For this purpose, the perturbation theory is used. Since, the low injection (LI) level solution can be obtained directly, intermediate injection level solution can be obtained from the perturbed LI solution using the Webster effect [48]. Webster showed that the electric field in the quasi-neutral base is modulated by the minority carrier concentration. Again, the injected minority carriers at the base emitter junction (i.e $x = 0$)

$n(0)$ is modified from its low-injection value $n_l(0)$ by a voltage dependent factor f_w (described in the section (3.1.3), which is insignificant under LI conditions but has to be incorporated under intermediate and high level injections, given by

$$n(0) = n_l(0) f_w \tag{4.3}$$

Although this expression holds at $x = 0$, it is expected that the same holds throughout the base region provided a correction term is incorporated. This correction term is needed since the electric field throughout the base is not uniform due to change in the carrier concentration with increased injection level as was shown by Webster. This correction term is therefore both position and voltage dependent. This is the basis for applying perturbation theory and was introduced by Suzuki [7]. According to this theory the minority carrier concentration at any position in the base under any injection level n(x) can be determined provided that the same can be obtained under low-injection condition ($n_l(x)$) and the position and voltage dependent correction term is known. Mathematically, this can be expressed as,

$$n(x) = n_l(x) f_w + \delta_n(x) \tag{4.4}$$

where, $\delta_n(x)$ represents the correction term and f_w is introduced to incorporate Webster effect. Although $\delta_n(x)$ increases with the injection level and with the position in the base, for the accuracy of model derivation, this $\delta_n(x)$ must be such that

$$\delta_n(x) = n_l(x) f_w + N_A \tag{4.5}$$

instead of $\delta_n(x) << n_l(x) f_w$. As a result, the hole concentration in the base can be expressed as,

$$p(x) \approx n_{l2}(x) + N_A \tag{4.6}$$

where, $n_{l2}(x) = n_l(x) f_w$. It is also important to note that the application of the perturbation theory is limited to intermediate injection level only. This is not applicable to high injection

condition since under that condition $n(x) >> N_A(x)$ and therefore, condition (4.5) is not valid. Hence, the intermediate injection model using perturbation theory is limited by the onset of the Kirk effect. However, using the perturbation theory the terms containing $n(x)+N_A(x)$ can be replaced by $n_{l2}(x)+N_A(x)$ and therefore, the non-linearity problem can be resolved.

4.1.2 Approximation of Electron Diffusivity

Using the concept of perturbation theory, the first order differential equation of minority carrier concentration can be rewritten as,

$$\left[\frac{2n_{l1}+N_A+\frac{a_h J_p}{qv_{sn}}}{n_{l1}+N_A+\frac{a_h J_p}{qv_{sn}}}\right]\frac{dn}{dx}+\left[\frac{\frac{dN_A}{dx}+\frac{J_p}{qD_{p0}}}{n_{l1}+N_A+\frac{a_h J_p}{qv_{sn}}}-\frac{d}{dx}ln(n_{ie}^2)\right]n$$
$$=J_n\left[\frac{1}{qD_n(0)}\left(\frac{N_A(x)}{N_{m,ref}}\right)^{\gamma_1}+\frac{a_e}{qv_{sn}}\left|\frac{\frac{dn}{dx}+\frac{dN_A}{dx}+\frac{J_p}{qD_{p0}}}{n_{l1}+N_A+\frac{a_h J_p}{qv_{sn}}}-\frac{d}{dx}ln(n_{ie}^2)\right|\right] \quad (4.7)$$

where, n_{l1} represents n_{l0} and n_{l2} under respective conditions as listed in Table (4.1). The coefficient of J_n, which represents the term $\frac{1}{qD_n}$, contains a a term $\frac{dn}{dx}$ which cannot be known without the knowledge of n(x). An alternative way of representing the above equation is

$$\left[\frac{2n_{l1}+N_A+\frac{a_h J_p}{qv_{sn}}+\frac{a_e J_n}{qv_{sn}}}{n_{l1}+N_A+\frac{a_h J_p}{qv_{sn}}}\right]\frac{dn}{dx}+\left[\frac{\frac{dN_A}{dx}+\frac{J_p}{qD_{p0}}}{n_{l1}+N_A+\frac{a_h J_p}{qv_{sn}}}-\frac{d}{dx}ln(n_{ie}^2)\right]n$$
$$=J_n\left[\frac{1}{qD_n(0)}\left(\frac{N_A(x)}{N_{m,ref}}\right)^{\gamma_1}-\frac{a_e}{qv_{sn}}\left(\frac{\frac{dN_A}{dx}+\frac{J_p}{qD_{p0}}}{n_{l1}+N_A+\frac{a_h J_p}{qv_{sn}}}-\frac{d}{dx}ln(n_{ie}^2)\right)\right] \quad (4.8)$$

where minus sign is used to reflect the negative direction of electron electric field. Here, the coefficient of $\frac{dn}{dx}$ contains the term J_n which can be known if n(x) is known. Either representation [Equation (4.7) or (4.8)] of the governing differential equation suffers with the problem of unknown coefficients. A suitable approximation can resolve this problem. In the representation given by Equation (4.7) the concept of perturbation theory can be used by

approximating the term $\frac{dp}{dx} = \frac{d(n+N_A)}{dx}$ as $\frac{d(n_{l2}+N_A)}{dx}$ in the right hand side of the Equation (4.7). In the representation, given by Equation (4.8), no such approximation can be applied for the unknown term $J_n(x)$ contained in the coefficient of $\frac{dn}{dx}$. The approximation to be applied for the term $\frac{dp}{dx}$ contained in $\frac{1}{qD_n}$ was first used and examined by Suzuki in his work [7], where he showed that this approximation does not lead to any significant error compared to simulation results. Therefore, the electron mobility can be expressed in terms of electron diffusivity as,

$$\frac{1}{qD_n} = \frac{1}{qD_n(0)}\left(\frac{N_A(x)}{N_{m,ref}}\right)^{\gamma_1} - \frac{a_e}{qv_{sn}}\left(\frac{\frac{d(n_{l1}+N_A)}{dx} + \frac{J_p}{qD_{p0}}}{n_{l1}+N_A+\frac{a_h J_p}{qv_{sn}}} - \frac{d}{dx}ln(n_{ie}^2)\right) \tag{4.9}$$

Under the low-injection condition, the above expression is reduced to,

$$\frac{1}{qD_{nl0}} \approx \frac{1}{qD_n(0)}\left(\frac{N_A(x)}{N_{m,ref}}\right)^{\gamma_1} - \frac{a_e}{qv_{sn}}\left(\frac{\frac{dN_A}{dx} + \frac{J_p}{qD_{p0}}}{N_A+\frac{a_h J_p}{qv_{sn}}} - \frac{d}{dx}ln(n_{ie}^2)\right) \tag{4.10}$$

Using the approximated diffusivity, the governing differential equation can be rewritten as,

$$\left[\frac{2n_{l1}+N_A+\frac{a_h J_p}{qv_{sn}}}{n_{l1}+N_A+\frac{a_h J_p}{qv_{sn}}}\right]\frac{dn}{dx} + \left[\frac{\frac{dN_A}{dx}+\frac{J_p}{qD_{p0}}}{n_{l1}+N_A+\frac{a_h J_p}{qv_{sn}}} - \frac{d}{dx}ln(n_{ie}^2)\right]n = \frac{J_n}{qD_n} \tag{4.11}$$

4.2 Derivation of $J_p(x)$

The electron electric field E_n is related to the hole electric field E_p which in turn depends on majority carrier current density J_p. But the knowledge of E_p and D_p is required to obtain J_p. The problem becomes more complicated since D_p and E_p are interrelated. To solve this problem, the hole current continuity equation must be solved, which requires the knowledge of recombination mechanism and lateral base injection mechanism. However, the recombination indeed depends on the minority electron concentration which is a parameter yet to be determined. Under these circumstances, use of the perturbation theory and appropriate approximations resolves the problem.

The hole current continuity considering recombination and lateral base injection is given by

$$\frac{dJ_p}{dx} = -qR_x\left[n - \frac{n_{ie}^2}{p}\right] + qg(n + N_A) \tag{4.12}$$

where,

$$R_x = \left[\frac{\frac{1}{\tau_n}}{(1+r_s)n + N_A} + C_{Ap}[(1+r_a)n + N_A]\right] \times (n + N_A) \tag{4.13}$$

Under low-injection condition $n = N_A$ and using the condition $n ? \frac{n_{ie}^2}{p}$ due to heavy doping, this equation simplifies to

$$\frac{dJ_{pl}}{dx} \approx -qR_{xl}n_l + qg_lN_A \tag{4.14}$$

where, J_{pl}, R_{xl} and g_l are the majority current density, recombination term and generation rate respectively under low-injection condition and

$$R_{xl} \approx \left[\frac{\frac{1}{\tau_n}}{N_A} + C_{Ap}N_A\right] \times N_A$$

$$= \frac{1}{\tau_n} + C_{Ap}N_A^2 \tag{4.15}$$

The equation (4.14) is still analytically unsolvable since $n_l(x)$ has to be known, which in turn cannot be determined without knowing J_{pl}. This problem can be overcome as follows. At first, the recombination mechanism is neglected to determine majority carrier density. This reduces the Equation (4.14) to

$$\frac{dJ_{pl0}}{dx} \approx qg_{l0}N_A \tag{4.16}$$

Using this J_{pl0} in the differential equation results in an expression for $n_{l0}(x)$, the minority carrier concentration under low-injection condition neglecting recombination mechanism. The minority carrier concentration considering recombination $n_l(x)$ cannot be deviated significantly from $n_{l0}(x)$ which neglects recombination under low-injection condition.

Therefore, concept of perturbation theory can be applied to determine $n_l(x)$ and the relation between these two can be expressed as,

$$n_l(x) = n_{l0}(x) + \delta n_0(x) \tag{4.17}$$

where, $\delta n_0(x)$ represents the deviation. Assuming the same consideration for accuracy of model derivation as is made for intermediate injection model derivation, the majority hole concentration under low injection can be given as,

$$\begin{aligned} p_l &= n_l + N_A \\ &= n_{l0}(x) + \delta n_0(x) + N_A \\ &\approx n_{l0} + N_A \end{aligned} \tag{4.18}$$

where,

$$\delta n_0(x) = n_{l0} + N_A \tag{4.19}$$

is assumed as before. Now, this assumption is further extended so that

$$(1+r_s)n_l + N_A \approx (1+r_s)n_{l0} + N_A \tag{4.20a}$$

$$(1+r_a)n_l + N_A \approx (1+r_a)n_{l0} + N_A \tag{4.20b}$$

Therefore, the term R_{xl} can be expressed as

$$R_{xl} = \left[\frac{\frac{1}{\tau_n}}{(1+r_s)n_{l0} + N_A} + C_{Ap}[(1+r_a)n_{l0} + N_A] \right] \times (n_{l0} + N_A) \tag{4.21}$$

The hole continuity equation under low-injection condition given by Equation (4.14) then becomes,

$$\frac{dJ_{pl}}{dx} = -qR_{xl}[n_{l0} + \delta n_0(x)] + qg_l(n_{l0} + \delta n_0(x) + N_A) \tag{4.22}$$

The above equation can be rearranged as,

$$\frac{dJ_{pl}}{dx} = qg_l N_A + q(g_l - R_{xl})n_{l0}(x) + q(g_l - R_{xl})\delta n_0(x) \tag{4.23}$$

Extending the assumption given in (4.19), it can be inferred that

$$g_l N_A + (g_l - R_{xl})n_{l0}(x) ? (g_l - R_{xl})\delta n_0(x) \tag{4.24}$$

This assumption simplifies the hole continuity equation under low-injection as,

$$\frac{dJ_{pl}}{dx} \approx qg_l N_A + q(g_l - R_{xl})n_{l0}(x) \tag{4.25}$$

Integrating the above equation results in an expression for majority carrier current density J_{pl} under low-injection with recombination mechanisms incorporated. Using this expression, minority carrier concentration $n_l(x)$ under the same condition can be estimated.

Following the same procedure, the majority carrier density $J_p(x)$ under intermediate injection-level condition can be derived. The exception that exists between these procedures is that in the former case minority carrier concentration is perturbed by the recombination mechanism, whereas, in the later case the same is perturbed by injection levels based on Webster effect i.e. n_{l0} is now replaced with n_{l2}. The governing equations under intermediate injection-level condition are summarized as follows:

- The term inverse lifetime R_x can be expressed as

$$R_x = \left[\frac{\frac{1}{\tau_n}}{(1+r_s)n_{l2} + N_A} + C_{Ap}[(1+r_a)n_{l2} + N_A] \right] \times (n_{l2} + N_A) \tag{4.26}$$

where following assumptions are made

$$(1+r_s)n + N_A \approx (1+r_s)n_{l2} + N_A \tag{4.27a}$$

$$(1+r_a)n + N_A \approx (1+r_a)n_{l2} + N_A \tag{4.27b}$$

- The hole continuity current equation can be expressed as,

$$\frac{dJ_p}{dx} \approx qgN_A + q(g - R_x)n_{l2}(x) \tag{4.28}$$

where the following assumption is used.

$$gN_A + (g - R_x)n_{l2}(x)?(g - R_x)\delta n(x) \tag{4.29}$$

In summary, the minority carrier concentration, minority carrier current density and the majority carrier density are to be determined is a sequence of three steps, which are tabulated as below:

Step	Minority Carrier Concentration, n(x)	Majority Carrier Current Density, $J_p(x)$	Minority Carrier Current Density, $J_n(x)$
Low-injection level neglecting recombination	n_{l0}	J_{pl0}	J_{nl0}
Low-injection level considering recombination	$n_l = n_{l0} + \delta n_0$	J_{pl}	J_{nl}
Intermediate-injection level	$n = n_{l2} + \delta n$	J_p	J_n

Table 1: Minority carrier concentration, and minority and majority carrier current densities in different steps

4.3 Formation of Modified Electron Current Equation

The equation (4.11) is now rearranged as,

$$\frac{dn}{dx} + \frac{1}{F_1}\left[\frac{\frac{dN_A}{dx} + \frac{J_p}{qD_{p0}}}{n_{l1} + N_A + \frac{a_h J_p}{q v_{sn}}} - \frac{d}{dx} ln(n_{ie}^2)\right] n(x) = \frac{1}{F_1}\frac{J_n}{qD_n} \tag{4.30}$$

where,

$$F_1 = \frac{2n_{l1} + N_A + \frac{a_h J_p}{q v_{sn}}}{n_{l1} + N_A + \frac{a_h J_p}{q v_{sn}}}$$

$$= 1 + \frac{n_{l1}}{n_{l1} + N_A + \frac{a_h J_p}{q v_{sn}}} \tag{4.31}$$

Since F_1 contains injection-level dependent term n_{l2} under intermediate injection level condition in the form of n_{l1}, the new equation (4.30) can be treated as modified electron current equation incorporating the injection-level dependency and is valid for both low and

intermediate injection level conditions. This is shown for the first-time in the literature. In comparison with the original electron current equation given by

$$\frac{dn}{dx}+\frac{E_n}{V_T}n(x)=\frac{J_n}{qD_n}$$

this equation shows that the coefficients of n(x) and $J_n(x)$ are the electron electric field and electron diffusivity, respectively. These terms are then termed as effective electron electric field, $E_{n,eff}$ and $D_{n,eff}$ and can be given by

$$\frac{E_{n,eff}}{V_T}=\frac{1}{F_1}\left[\frac{\frac{dN_A}{dx}+\frac{J_p}{qD_{p0}}}{n_{l1}+N_A+\frac{a_h J_p}{q v_{sn}}}-\frac{d}{dx}ln(n_{ie}^2)\right] \tag{4.32a}$$

$$D_{n,eff}=F_1 D_n \tag{4.32b}$$

From these equations following conclusions can be made:

- The lowest value of F_1 is unity and is obtained under low-level injection.
- This factor increases from unity as injection level increases.
- $E_{n,eff}$ decreases with injection level, as it is determined by dividing the factor F_1.

This means that injection level has a retarding effect on the electron electric field.

- $D_{n,eff}$, the effective mobility, increases with increasing injection level, as the

factor F_1 is multiplied to determine this effective mobility.

Using these effective terms, the modified current equation can be obtained in a simplified form as,

$$\frac{dn}{dx}+\frac{E_{n,eff}}{V_T}n(x)=\frac{J_n}{qD_{n,eff}} \tag{4.33}$$

4.3.1 Effective Electron Electric Field

The effective intrinsic concentration n_{ie} is rewritten as,

$$n_{ie}^2(x)=\frac{n_{i0}^2}{N_{n,ref}^{\gamma 2}}N_A^{\gamma 2}(x) \tag{4.34}$$

The logarithmic derivative of n_{ie}^2 is,

$$\frac{d}{dx} ln(n_{ie}^2) = \gamma_2 \frac{d}{dx} ln(N_A) \tag{4.35}$$

The term $\frac{1}{F_1}$ can be rearranged as,

$$\frac{1}{F_1} = 1 - \frac{n_{l1}}{2n_{l1} + N_A + \frac{a_h J_p}{q v_{sn}}} \tag{4.36}$$

The first term in Equation (4.32a) of the effective electric field can be rearranged as,

$$\begin{aligned} \frac{\frac{dN_A}{dx} + \frac{J_p}{qD_{p0}}}{n_{l1} + N_A + \frac{a_h J_p}{q v_{sn}}} &= \frac{N_A \frac{d}{dx} ln\, N_A + \frac{J_p}{qD_{p0}}}{n_{l1} + N_A + \frac{a_h J_p}{q v_{sn}}} \\ &= \frac{(n_{l1} + N_A + \frac{a_h J_p}{q v_{sn}}) \frac{d}{dx} ln\, N_A + \frac{J_p}{qD_{p0}} - (n_{l1} + \frac{a_h J_p}{q v_{sn}}) \frac{d}{dx} ln\, N_A}{n_{l1} + N_A + \frac{a_h J_p}{q v_{sn}}} \\ &= \frac{d}{dx} ln\, N_A - \frac{(n_{l1} + \frac{a_h J_p}{q v_{sn}}) \frac{d}{dx} ln\, N_A - \frac{J_p}{qD_{p0}}}{n_{l1} + N_A + \frac{a_h J_p}{q v_{sn}}} \end{aligned} \tag{4.37}$$

The effective electric field then can be expressed as,

$$\begin{aligned} \frac{E_{n,eff}}{V_T} = &\left[1 - \frac{n_{l1}}{2n_{l1} + N_A + \frac{a_h J_p}{q v_{sn}}} \right] \times \left[1 - \gamma_2 - \frac{n_{l1} - J_p \left(\frac{\frac{1}{qD_{p0}}}{\frac{d}{dx} ln\, N_A} - \frac{a_h}{q v_{sn}} \right)}{n_{l1} + N_A + \frac{a_h J_p}{q v_{sn}}} \right] \\ &\times \frac{d}{dx} ln\, N_A \end{aligned} \tag{4.38}$$

Finally, the effective electron electric field can be rearranged as,

$$\begin{aligned} \frac{E_{n,eff}}{V_T} = &\left[1 - \gamma_2 + \frac{J_p \left(\frac{\frac{1}{qD_{p0}}}{\frac{d}{dx} ln\, N_A} - \frac{a_h}{q v_{sn}} \right)}{n_{l1} + N_A + \frac{a_h J_p}{q v_{sn}}} \right] \times \frac{d}{dx} ln\, N_A \\ &- \left[2 - \gamma_2 - \frac{n_{l1} - J_p \left(\frac{\frac{1}{qD_{p0}}}{\frac{d}{dx} ln\, N_A} - \frac{a_h}{q v_{sn}} \right)}{n_{l1} + N_A + \frac{a_h J_p}{q v_{sn}}} \right] \times \frac{d}{dx} ln\, N_A \times \frac{n_{l1}}{2n_{l1} + N_A + \frac{a_h J_p}{q v_{sn}}} \end{aligned} \tag{4.39a}$$

$$= E_{n,bi} - E_{n,inj} \tag{4.39b}$$

where $E_{n,bi}$ is the effective built-in electric field and $E_{n,inj}$ is the injection-level dependent electric field and can be given by

$$E_{n,bi} = \left[1 - \gamma_2 + \frac{J_p \left(\frac{\frac{1}{qD_{po}}}{\frac{d}{dx} ln\ N_A} - \frac{a_h}{q v_{sn}} \right)}{n_{l1} + N_A + \frac{a_h J_p}{q v_{sn}}} \right] \times \frac{d}{dx} ln\ N_A \tag{4.40a}$$

$$E_{n,inj} = \left[2 - \gamma_2 - \frac{n_{l1} - J_p \left(\frac{\frac{1}{qD_{po}}}{\frac{d}{dx} ln\ N_A} - \frac{a_h}{q v_{sn}} \right)}{n_{l1} + N_A + \frac{a_h J_p}{q v_{sn}}} \right] \times \frac{d}{dx} ln\ N_A \times \frac{n_{l1}}{2n_{l1} + N_A + \frac{a_h J_p}{q v_{sn}}} \tag{4.40b}$$

It can be inferred from the expression of effective electron electric field given by Equation (4.39a) that the square bracket terms are multiplied by a term $\frac{d}{dx} ln\ N_A$. This term represents a normalized electric field (since logarithmic derivative of concentration is equal to the electric field divided by V_T) and this is the field that is resulted from the non-uniform base doping profile. For practical base doping profile, this field is negative. The terms in the square brackets indeed modulate this field and represents the effects such as band-gap narrowing, majority carrier current density J_p, recombination and injection level. From this equation, it is evident that J_p increases the electric field, since J_p is negative and the logarithmic derivative of base doping profile is negative. The first component $E_{n,bi}$ aids the electric field, whereas, the second component $E_{n,inj}$ retards the electric field. The second component becomes dominant as injection level increases, but is insignificant under low-injection. Retarding effect of band-gap narrowing is included through γ_2 in both these components. It also shows that retarding effect of band-gap narrowing and aiding effect of J_p increases as injection level increases. Since, the value of square-bracket term is greater for $E_{n,inj}$ than that for $E_{n,bi}$, electric field decreases with injection level. For low-injection condition, $E_{n,inj} \to 0$ because $n_{l1} = N_A$ and hence,

$$E_{n1o} \approx \left[1 - \gamma_2 + \frac{J_p \left(\frac{\frac{1}{qD_{po}}}{\frac{d}{dx} ln\ N_A} - \frac{a_h}{q v_{sn}} \right)}{N_A + \frac{a_h J_p}{q v_{sn}}} \right] \times \frac{d}{dx} ln\ N_A \tag{4.41}$$

4.4 Exponential Approximation Technique

The expression of effective electron electric field given by Equation (4.39a) shows that this expression becomes complicated for three reasons. The first one is due to the presence of the field term $\frac{d}{dx} ln\, N_A$. The second occurs due to the presence of the terms containing J_p and the third reason is related to the injection-level dependency.

For an exponential base doping profile, the field term $\frac{d}{dx} ln\, N_A$ is a constant and for other profiles, this term is position-dependent. Clearly, the expression for electric field becomes simpler for exponential base doping profile. Therefore, a suitable approximation technique must be employed to convert the exponential-like doping profiles (i.e. Gaussian, complementary error function etc.) into exponential one and hence, the first issue can be resolved.

A closer look in the electric field expression reveals that the third term in the square brackets is the cause of both the second and third problems. The injection level-dependent term $E_{n,inj}$ causes an additional problem. If these terms can be expressed in a simple function, then both these problems can be resolved. Since, exponential functions has an elegant property that it retains the same after differentiation or integration with constant multiplication factor, the above terms then can be exponentially approximated. This approximation is justified because the terms depend on the doping profile, which takes an exponential form. For the same reasoning, the effective electron diffusivity represented by Equation (4.32b) can be approximated as a simple exponential. Therefore, by devising a suitable exponential approximation technique, the complicated nature of variable coefficients of the modified current equations can be simplified. This approximation technique is described below.

In the work [55], Guoxin Li et. el. has showed that approximating Gaussian doping profile by a simple exponential profile results in only an insignificant error in the charge-

control analysis. This idea can be extended to the doping and field dependent transport parameters and to the expressions which contain two or more exponential terms. The approximation of various quantities by using simple exponential can significantly reduce the mathematical complexity without any significant loss of physical understanding.

The base doping profile is now considered as exponential and can be expressed as,

$$N_A(x) = N_A(0)e^{\frac{-\eta x}{W_B}} \tag{4.42}$$

Introducing a convenient variable u which gives the exponential dependence of the doping profile, the Equation (4.42) becomes,

$$N_A(x) = N_A(0)u(x) \tag{4.43}$$

where,

$$u(x) = e^{\frac{-\eta x}{W_B}} \tag{4.44}$$

where,

$$\eta = log\left[\frac{N_A(0)}{N_A(W_B)}\right] \tag{4,45}$$

is the logarithmic slope of the doping profile and $N_A(0)$ and $N_A(W_B)$ are the doping densities at $x = 0$ and $x = W_B$ i.e. at the base edges of B-E and B-C junctions.

An expression or a transport parameter, which depends on the doping profile given by Eqn. (4.42), is assumed such that

$$f(x) = F_1 u^{\alpha_1} + F_2 u^{\alpha_2} \tag{4.46}$$

This expression can be approximated by a simple exponential function such that

$$f(x) \equiv F_0 u^{\beta_0} \tag{4.47}$$

where, $\eta\beta_0$ is the logarithmic slope and hence, can be obtained from the boundary values of f(x) as,

$$\beta_0 = \frac{1}{\eta} log\left[\frac{f(0)}{f(W_B)}\right] \tag{4.48}$$

and F_0 can be obtained from the fact that the areas under the original curve and the

approximated curve must be equal. Therefore, F_0 can be expressed as,

$$F_0 = \frac{\eta\beta_0}{W_B(1-u_w^{\beta_0})}\int_0^{W_B} f(x)dx \tag{4.49}$$

where, $u_w = u(W_B)$.

4.5 Differential Equation: Solution Techniques

The intractable nonlinear, nonhomogeneous and complicated-variable-coefficient differential equation given by Equation (4.11) can be transformed into a linear, homogeneous and simple-variable-coefficient equation by using the techniques described in the previous sections. Unfortunately, this differential equation is not yet solvable. This section deals the techniques that transforms his equation into a solvable form.

Since, the derivation of $J_p(x)$ is a three-step process as described in the section (4.2), the solution of the differential equation also needs in three steps. The solution technique for each steps are described in the following subsections.

4.5.1 Low-injection Model Neglecting Recombination

Under this condition, $n_{l0}(x) << N_A(x)$ and

$$\frac{dJ_{nl0}}{dx} = qR_{xl0}n_{l0}(x) \approx 0 \tag{4.50}$$

which leads to J_{nl0} as constant. Therefore, non-homogeneous problem does not matter under this condition and the equations remains first order with variable coefficients as,

$$\frac{dn_{l0}(x)}{dx} + \frac{E_{nl0}}{V_T}n_{l0}(x) = \frac{J_{nl0}}{qD_{nl0}} \tag{4.51}$$

where, E_{nl0} and $\frac{1}{qD_{nl0}}$ can be given as,

$$E_{nl0} \approx \left[1 - \gamma_2 + \frac{J_p \left(\frac{\frac{1}{qD_{p0}}}{\frac{d}{dx} ln\, N_A} - \frac{a_h}{qv_{sn}} \right)}{N_A + \frac{a_h J_p}{qv_{sn}}} \right] \times \frac{d}{dx} ln\, N_A \tag{4.52a}$$

$$\frac{1}{qD_{nl0}} \approx \frac{1}{qD_n(0)} \left(\frac{N_A(x)}{N_{ref}} \right)^{\gamma_1} - \frac{a_e}{qv_{sn}} \left(\frac{\frac{dN_A}{dx} + \frac{J_p}{qD_{p0}}}{N_A + \frac{a_h J_p}{qv_{sn}}} - \frac{d}{dx} ln(n_{ie}^2) \right) \tag{4.52b}$$

Since these terms can be exponentially approximated as discussed in section (4), the integrating factor required to solve the differential equation can be determined in the form of exponentials. Finally, the solution of the differential equation can be obtained in terms of confluent hypergeometric functions.

4.5.2 Low-injection Model Considering Recombination

When recombination is included, $J_{nl}(x)$ is no longer a constant, instead it becomes a function of position. A differentiation is used to remove this term from the first order differential equation of n(x) which is rewritten here as,

$$qD_{nl}\left[\frac{dn_l}{dx} + n_l \frac{E_{nl}}{V_T} \right] = J_{nl}(x) \tag{4.53}$$

Differentiating the above equation results in

$$qD_{nl}\left[\frac{d^2 n_l}{dx^2} + n \frac{d}{dx}\left(\frac{E_{nl}}{V_T} \right) + \frac{E_{nl}}{V_T} \frac{dn_l}{dx} \right] + \left[\frac{dn_l}{dx} + n_l \frac{E_{nl}}{V_T} \right] \frac{d}{dx}(qD_{nl})$$

$$= \frac{dJ_{nl}(x)}{dx} = qR_{xl}\left[n_l(x) - \frac{n_{ie}^2}{p_l} \right] \tag{4.54}$$

where electron current continuity equation given by

$$\frac{dJ_{nl}(x)}{dx} = qR_{xl}\left[n_l(x) - \frac{n_{ie}^2}{p_l} \right] \tag{4.55}$$

is used. For heavy base doping, it can be justifiably assumed that

$$n_l(x) >> \frac{n_{ie}^2}{p_l} \tag{4.56}$$

Using this assumption, dividing both sides of the Equation (182) by qD_{nl} and rearranging the results in a second order differential equation as,

$$\frac{d^2n_l}{dx^2}+\left[\frac{E_{nl}}{V_T}-\frac{d}{dx}ln\left(\frac{1}{qD_{nl}}\right)\right]\frac{dn_l}{dx}+\left[\frac{d}{dx}\left(\frac{E_{nl}}{V_T}\right)-\frac{E_{nl}}{V_T}\frac{d}{dx}ln\left(\frac{1}{qD_{nl}}\right)-\frac{qR_{xl}}{qD_{nl}}\right]n_l=0 \quad (4.57a)$$

$$\frac{d^2n_l}{dx^2}+P(x)\frac{dn_l}{dx}+Q(x)n_l(x)=0 \quad (4.57b)$$

where,

$$P(x)=\frac{E_{nl}}{V_T}-\frac{d}{dx}ln\left(\frac{1}{qD_{nl}}\right) \quad (4.58a)$$

$$Q(x)=\frac{d}{dx}\left(\frac{E_{nl}}{V_T}\right)-\frac{E_{nl}}{V_T}\frac{d}{dx}ln\left(\frac{1}{qD_{nl}}\right)-\frac{qR_{xl}}{qD_{nl}} \quad (4.58b)$$

Therefore, the non-homogeneity problem of the differential equation is resolved. But, the problem of intractability still remains. This needs suitable transformation techniques. Since the working differential equation is a second order and there are no analytical formulation to solve a variable-coefficient of second or higher order differential equations other than special functions (i.e. Bessel function, modified Bessel function, Hankel function etc.), transformation to any of these special function has to be made. For this the format of Bessel differential equation can be chosen since the solution of this equation has a quasi-exponential form. The transformation steps ate described below:

1. First, the variable $n_l(x)$ is assumed as a product of two variables v_l and w_l

$$n_l(x)=v_l(x)w_l(x) \quad (4.59)$$

so that the differential equation given by Equation (4.57a) can be expressed as

$$\frac{d^2v_l}{dx^2}+\left[\frac{2}{w_l}\frac{dw_l}{dx}+P(x)\right]\frac{dv_l}{dx}+\frac{1}{w_l}\left[\frac{d^2w_l}{dx^2}+P(x)\frac{dw_l}{dx}+Q(x)w_l(x)\right]v_l(x)=0 \quad (4.60)$$

The governing equation for w_l is given as,

$$\frac{2}{w_l}\frac{dw_l}{dx}+P(x)=constant\,part\,of\;P(x)$$

$$=A_l \quad (Let) \quad (4.61)$$

Using the expression of w_l thus obtained one converts Equation (4.60) into

$$\frac{d^2v_l}{dx^2} + A_l \frac{dv_l}{dx} + [B_l(x) + C_l]v_l(x) = 0 \tag{4.62}$$

where, $B_l(x)$ and constant C_l can be obtained by substituting w_l in the coefficient of $v_l(x)$.

It is worth mentioning that Equation (4.62) is the governing equation for $v_l(x)$. Then $n_l(x) = w_l(x)v_l(x)$ is now solvable.

2. Using the exponential approximation technique, $B_l(x)$ can be expressed as,

$$B_l(x) \equiv B_{0l}u^{\beta_{0l}} \tag{4.63}$$

Therefore, the differential equation of (4.62) turns into

$$\frac{d^2v_l}{dx^2} + A_l \frac{dv_l}{dx} + [B_{0l}u^{\beta_{0l}} + C_l]v_l(x) = 0 \tag{4.64}$$

3. Next, the independent variable x is changed to z by letting

$$z = u^{\frac{\beta_{0l}}{2}} \tag{4.65}$$

This converts the above equation into

$$\frac{d^2v_l}{dz^2} + \frac{a_l}{z}\frac{dv_l}{dz} + \frac{1}{z^2}[b_l^2 + c_l]v_l(z) = 0 \tag{4.66}$$

where a_l, b_l and c_l are constants.

4. Finally, the variable $v_l(z)$ is further assumed as a product of two other variables t_l and y_l

$$v_l(z) = y_l(z)t_l(z) \tag{4.67}$$

so that the differential equation given by Equation (4.66) can be expressed as,

$$\frac{d^2y_l}{dz^2} + \left[\frac{2}{t_l}\frac{dt_l}{dz} + \frac{a_l}{z}\right]\frac{dy_l}{dz} + \frac{1}{t_l}\left[\frac{d^2t_l}{dz^2} + \frac{1}{z}\frac{dt_l}{dz} + \left(\frac{1}{z^2}[b_l^2 + c_l]\right)t_l(z)\right]y_l(z) = 0 \tag{4.68}$$

The variable t_l can be obtained by equating the coefficient of $\frac{dy_l}{dz}$ to unity as,

$$\frac{2}{t_l}\frac{dt_l}{dz}+\frac{a_l}{z}=1 \tag{4.69}$$

Using the expression of t_l thus obtained one converts the differential equation given by the Equation (4.68) into a Bessel differential equation as,

$$\frac{d^2y_l}{dz^2}+\frac{1}{z}\frac{dy_l}{dz}+\frac{1}{z^2}[b_l^2-\beta_l^2]y_l(z)=0 \tag{4.70}$$

where, β_l is the order of the Bessel function. The solution of this equation contains Bessel function of the first and the second kind (J_{β_l} and Y_{β_l}).

5. The total solution of $n_l(x)$ then can be found as,

$$n_l(x)=w_l(x)t_l(x)[C_{1l}J_{\beta_l}+C_{2l}Y_{\beta_l}] \tag{4.71}$$

4.5.3 Intermediate-injection Model

The solution technique under this condition is same as that outlined for the low-injection condition with recombination. The only difference is that here the term n_l is used instead of $n_{l0}(x)$ to determine $J_{pl}(x)$.

4.6 Conclusion

In this chapter, an elaborate discussion of techniques, approximations and transformation methods is presented that are used to overcome the challenges to derive an analytical model of the base transit time. The techniques, approximations and transformation methods are chosen such that the mathematical tractability becomes possible without sacrificing the underlying physics of the non-ideal effects and without loss of generality. Therefore, the model thus derived is indeed general and can be useful for understanding the physics of base transport mechanisms. Moreover, the model can be applicable to other devices that use the principle of bipolar transistor operation.

Chapter 5
Model Derivations

From the rigorous discussions of the previous chapters, it should be very obvious that the analytical modeling of base transit time by including the majority carrier current density in the base, is indeed a challenging job. These challenges occur not only from the complicated physics behind the underlying mechanisms and physical models that exist in the literature, but also from the mathematical intractability of the resulting equations. Keeping the physical models intact often makes the mathematical tractability as impossible a feat. Therefore, assumptions and approximations must be made so that the underlying physics will not be compromised while keeping the mathematics as simple as possible. A thorough but thoughtful and careful research is, therefore, carried out to preserve the physics as well as to make the mathematics tractable. This chapter deals with the analytical development of the base transit time model using the techniques described in the previous chapter.

This chapter starts with the development of the required equations for exponential base doping profile from the general equations for arbitrary doping profile. Then the three-step process of model development will be elaborated in the subsequent sections.

5.1 Modified Equations for Exponential Doping Profile

In the previous chapter, the differential equation and all other related equations have been derived for arbitrary doping profile. Since, the logarithmic derivative of exponential doping profile becomes constant, these equations for this doping profile becomes relatively easy to handle. Moreover, using the exponential approximation technique, [section (4.4)], any exponential-like doping profile i.e. Gaussian, Complementary error function etc. can also be approximated by an exponential function. Therefore, an exponential base doping profile is assumed for model derivation. For this profile, the fundamental relations are:

$$N_A(x) = N_A(0)u(x) \tag{5.1a}$$

$$u(x) = e^{-\frac{\eta x}{W_B}} \tag{5.1b}$$

$$\frac{d}{dx} ln\, N_A = -\frac{\eta}{W_B} \tag{5,1c}$$

$$\frac{d}{dx} ln\,(n_{ie}^2) = -\frac{\eta\gamma_2}{W_B} \tag{5.1d}$$

where, η is the logarithmic slope of the profile and can be defined in section (4.4) as,

$$\eta = log\left[\frac{N_A(0)}{N_A(W_B)}\right] \tag{5.2}$$

Using these relations, the effective electron electric field $E_{n,eff}$ can be given as,

$$\frac{E_{n,eff}}{V_T} = -\frac{\eta}{W_B}\left[1-\gamma_2 - \frac{J_p(F_h u^{\gamma_3} + G_h)}{\frac{\eta}{W_B}(n_{l1}+N_A)+J_pG_h}\right]$$

$$+\frac{\eta}{W_B}\left[2-\gamma_2 - \frac{J_p(F_h u^{\gamma_3} + G_h)}{\frac{\eta}{W_B}(n_{l1}+N_A)+J_pG_h}\right]\times\frac{\frac{\eta}{W_B}n_{l1}}{\frac{\eta}{W_B}(2n_{l1}+N_A)+J_pG_h} \tag{5.3a}$$

$$= \frac{1}{F_1}\frac{E_{n,apparent}}{V_T} \tag{5.3b}$$

where,

$$\frac{1}{F_1} = 1 - \frac{\frac{\eta}{W_B} n_{l1}}{\frac{\eta}{W_B}(2n_{l1} + N_A) + J_p G_h} \tag{5.4a}$$

$$\frac{E_{n,apparent}}{V_T} = \frac{\eta}{W_B}\left[1 - \gamma_2 - \frac{\frac{\eta}{W_B} n_{l1} + J_p(F_h u^{\gamma_3} + G_h)}{\frac{\eta}{W_B}(n_{l1} + N_A) + J_p G_h}\right] \tag{5.4b}$$

The effective electron diffusivity can be expressed as,

$$\frac{1}{qD_{n,eff}} = \frac{1}{F_1}\left[F_e u^{\gamma_1} + \frac{W_B G_e}{\eta}\left|\frac{E_{n,approx}}{V_T}\right|\right] \tag{5.5a}$$

$$= \frac{1}{F_1}\frac{1}{qD_n} \tag{5.5b}$$

where,

$$\frac{1}{qD_n} = F_e u^{\gamma_1} + \frac{W_B G_e}{\eta}\left|\frac{E_{n,approx}}{V_T}\right| \tag{5.6a}$$

$$\frac{E_{n,approx}}{V_T} = -\frac{\eta}{W_B}\left[1 - \gamma_2 - \frac{\frac{dn_{l1}}{dx} + \frac{\eta}{W_B} n_{l1} + J_p(F_h u^{\gamma_3} + Gh)}{\frac{\eta}{W_B}(n_{l1} + N_A) + J_p G_h}\right] \tag{5.6b}$$

In these equations [Equation (5.3) to Equation (5.6)], the constants F_e, F_h, G_e and G_h are defined as,

$$F_e = \frac{1}{qD_n(0)}\left(\frac{N_A(0)}{N_{m,ref}}\right)^{\gamma_1} \tag{5.7}$$

$$F_h = \frac{1}{qD_p(0)}\left(\frac{N_A(0)}{N_{m,ref}}\right)^{\gamma_3} \tag{5.8}$$

$$G_e = \frac{\eta}{W_B}\frac{a_e}{qv_{sn}} \tag{5.9}$$

$$G_h = \frac{\eta}{W_B}\frac{a_h}{qv_{sn}} \tag{5.10}$$

The majority hole current density J_p can be estimated from the following equation which is obtained by integrating the hole continuity equation given by (4.28) as,

$$J_p(x) = K - q\int_0^x R_x n_{l1}(x)dx + qg\int_0^x [n_{l1}(x) + N_A(x)]dx \tag{5.11}$$

where, K and g can be determined using the boundary conditions for J_p and the inverse lifetime R_x can be expressed as,

$$R_x = \left[\frac{\frac{1}{\tau_n}}{(1+r_s)n_{l1} + N_A} + C_{Ap}[(1+r_a)n_{l1} + N_A]\right] \times (n_{l1} + N_A) \tag{5.12}$$

The perturbed n_{l1} represents n_{l0} under low-level injection condition with recombination neglected and n_{l2} under intermediate injection level condition using Webster effect. This J_p can be used to determine $E_{n,eff}$ and $D_{n,eff}$. Finally, the minority electron concentration can be derived from the following differential equation:

$$\frac{dn}{dx}+\frac{E_{n,eff}}{V_T}n(x)=\frac{J_n}{qD_{n,eff}} \tag{5.13}$$

The minority electron current density J_n is the source of non-homogeneity of the differential equation. Therefore, the electron current continuity equation is used to overcome the problem of non-homogeneity. For exponential doping profile, this continuity equation can be expressed as,

$$\frac{dJ_n}{dx}=R_x n_{l1}(x) \tag{5.14}$$

5.2 Low Injection Level Model Derivation Without Considering Recombination

The development of low-injection (LI) model is a two-step process. First the effect of lateral base injection is considered, while recombination is excluded in the analysis. All other effects and considerations are used. Second, the recombination mechanism is then included using a perturbation approach.

Since, recombination mechanism is neglected in the first step, the minority electron current density J_{nl0} can be regarded as constant. But this does not hold true for $J_{pl0}(x)$, since the presence of lateral base injection current. Therefore, the hole continuity equation must be solved to determine $J_{pl0}(x)$. Equation (219) under low injection condition [$p(x)\approx N_A(x)$] gives,

$$J_{pl0}(x)=K+qg_{l0}\frac{W_B}{\eta}N_A(0)(1-u) \tag{5.15}$$

Applying the boundary conditions for hole current density at $x=0$ and $x=W_B$ gives,

$$K=-J_{pl0}(0) \tag{5.16}$$

$$g_{l0}=\frac{\eta}{W_B}\frac{J_{pl0}(0)-J_{pl0}(W_B)}{qN_A(0)(1-u_w)} \tag{5.17}$$

The majority hole current density then can be rearranged as,

$$J_{pl0}(x) = J_{0l0} - J_{1l0}u \tag{5.18}$$

where,

$$J_{0l0} = \frac{J_{pl0}(0)u_w - J_{pl0}(W_B)}{1-u_w} \tag{5.19}$$

$$J_{1l0} = \frac{J_{pl0}(0) - J_{pl0}(W_B)}{1-u_w} \tag{5.20}$$

Under low-injection condition $n = N_A$ and hence,

$$F_1 \to 1 \tag{5.21}$$

$$\frac{d}{dx}(n_{l1} + N_A) \to \frac{d}{dx}N_A \tag{5.22}$$

These approximations reduce the $E_{n,apparent}$ term in the effective electron field $E_{n,eff}$ [Equation (5.3)] and the approximate electric field term $E_{n,approx}$ in the effective electron diffusivity $D_{n,eff}$ [Equation (5,5)] to low-injection electric field E_{nl0} as follows:,

$$\frac{E_{nl0}}{V_T} = -\frac{\eta}{W_B}\left[1-\gamma_2 - \frac{J_{pl0}(x)(F_h u^{\gamma_3} + G_h)}{\frac{\eta}{W_B}N_A + J_{pl0}(x)G_h}\right] \tag{5.23a}$$

$$= -\frac{\eta}{W_B}[b + b_{dxl0}(x)] \tag{5.23b}$$

where,

$$b = 1-\gamma_2 \tag{5.24a}$$

$$b_{dxl0}(x) = -\frac{J_{pl0}(x)(F_h u^{\gamma_3} + G_h)}{\frac{\eta}{W_B}N_A + J_{pl0}(x)G_h} \tag{5.24b}$$

At this stage, the required parameters needed to solve the first order differential equation [Equation (5.13)] are found. Using their approximations and rearranging the terms results in a first order variable-coefficient differential equation of minority electron concentration n(x) as,

$$\frac{dn_{l0}}{dx} + n_{l0}\frac{E_{nl0}}{V_T} = J_{nl0}F_e u^{\gamma_1} + J_{nl0}\frac{W_B G_e}{\eta}\left|\frac{E_{nl0}}{V_T}\right| \tag{5.25}$$

The integrating factor (I.F.) of this equation is given as,

$$I.F. = e^{\int \frac{E_{nl0}}{V_T}}$$

$$= e^{-\frac{\eta}{W_B}\int b\,dx - \frac{\eta}{W_B}\int b_{dxl0}(x)dx}$$

$$= \left[e^{-\frac{\eta x}{W_B}} \right]^{b_{l0}} \times e^{-\frac{\eta}{W_B}\int b_{dxl0}(x)dx}$$

$$= u^{b_{l0}} \times e^{v_{l0}(x)} \tag{5.26}$$

where,

$$v_{l0}(x) = -\frac{\eta}{W_B}\int b_{dxl0}(x)dx \tag{5,27}$$

Integrating the differential equation (5.25) w.r.t x gives,

$$n_{l0}(x)u^{b_{l0}}e^{v_{l0}} = \left[n_{l0}(x)e^{v_{l0}}\right]_{x=0} + J_{nl0}F_e\int_0^x u^{b_{l0}+\gamma_1}e^{v_{l0}}dx \tag{5.28}$$

$$+\frac{W_B J_{nl0} G_e}{\eta}\int_0^x u^{b_{l0}}\left|\frac{E_{nl0}}{V_T}\right|e^{v_{l0}}dx \tag{5.29}$$

The integral terms are non-integrable because of the complex form of b_{dxl0} and also of $\frac{E_{nl0}}{V_T}$.

Using the exponential approximation of these terms transforms these into simple exponential terms and therefore, makes the integral possible. Now, in order to obtain a tractable closed form solution of the differential equation (5.25), the terms $b_{dxl0}(x)$ and $\frac{E_{nl0}}{V_T}$ can be approximated using an exponential form:

$$b_{dxl0}(x) \equiv b_{dl0}u^{\beta_{0l}} \tag{5.30a}$$

$$\left|\frac{E_{nl0}(x)}{V_T}\right| \equiv \frac{\eta}{W_B}F_{1l}u^{\beta_{1l}} \tag{5.30b}$$

where,

$$\beta_{0l} = \frac{1}{\eta}log\left[\frac{b_{dxl0}(0)}{b_{dxl0}(W_B)}\right] \tag{5.31a}$$

$$\beta_{1l} = \frac{1}{\eta}log\left[\frac{\frac{E_{nl0}(0)}{V_T}}{\frac{E_{nl0}(W_B)}{V_T})}\right] \tag{5.31b}$$

and,

$$b_{dl0} = \frac{\eta\beta_{0l}}{W_B(1-u_w^{\beta_{0l}})}\int_0^{W_B} b_{dxl0}(x)dx \tag{5.32a}$$

$$F_{1l} = \frac{W_B}{\eta}\left[\frac{\eta\beta_{1l}}{W_B(1-u_w^{\beta_{1l}})}\int_0^{W_B}\left|\frac{E_{nl0}(x)}{V_T}\right|dx\right] \tag{5.32b}$$

Using the exponentially approximated form of $bdxl0(x)$ [Equation (5.30a)], the term $v_{l0}(x)$

can be expressed as,

$$v_{l0}(x) = V_{0l} u^{\beta_{0l}} \tag{5.33}$$

where,

$$V_{0l} = \frac{b_{dl0}}{\beta_{0l}} \tag{5.34}$$

Using these exponential approximations, results in a solvable form of the equation given by (5.29) as ,

$$n_{l0}(x) u^{b_{l0}} e^{v_{l0}} = \left[n_{l0}(x) e^{v_{l0}} \right]_{x=0} + J_{nl0} F_e \int_0^x u^{b_{l0}+\gamma_1} e^{v_{l0}} dx \tag{5.35}$$

$$+ J_{nl0} G_e F_{1l} \int_0^x u^{b_{l0}+\beta_{1l}} e^{v_{l0}} dx \tag{5.36}$$

The general form of the integration terms results in a confluent hypergeometric functions as [Appendix (A.1)]

$$I = \int_0^x u^{\alpha} e^{v_{l0}} dx = -\frac{W_B}{\eta\alpha} \left[u^{\alpha} M\left(\frac{\alpha}{\beta_{0l}}; \frac{\alpha}{\beta_{0l}} + 1; v_l \right) \right]_{V_{0l}}^{v_{l0}} \tag{5.37}$$

where $M(x)$ is the confluent hypergeometric function. Using this result along with Kummar's relation [56, 57],

$$e^{v} M_l(a;b;v) = M(b-a;b;-v) \tag{5.38}$$

and solving for appropriate boundary conditions at $x = 0$ and $x = W_B$ given by,

$$n(0) = \frac{\frac{n_{ie}^2(0)}{N_A(0)} e^{\frac{V_{BE}}{V_T}}}{\frac{1}{2} + \sqrt{\frac{1}{4} + \left[\frac{n_{ie}(0)}{N_A(0)} \right]^2 e^{\frac{V_{BE}}{V_T}}}} \tag{5.39a}$$

$$n(W_B) = \frac{J_n(W_B)}{q v_{sn}} \tag{5.39b}$$

and finally, rearranging the terms, an expression of minority carrier concentration n(x) can be obtained as,

$$n_{l0}(x) = -J_{nl0} \left[A_{1l} u^{\gamma_1} M_{1l}(x) + A_{2l} u^{\beta_1} M_{2l}(x) + A_{3l} u^{-b_{l0}} e^{-v_{l0}} \right] \tag{5.40}$$

where,

$$M_{1l}(x) = M\left(1; \frac{b_{l0} + \gamma_1}{\beta_{0l}} + 1; -v_{l0}(x)\right) \tag{5.41a}$$

$$M_{2l}(x) = M\left(1; \frac{b_{l0} + \beta_{1l}}{\beta_{0l}} + 1; -v_{l0}(x)\right) \tag{5.41b}$$

and,

$$J_{nl0} = -A_{low} n_l(0) \tag{5.42}$$

$$A_{low} = \frac{u_w^{-b_{l0}} e^{V_{0l} - V_{wl}}}{\frac{1}{qv_s} - H_{wl} + H_{0l} u_w^{-b_{l0}} e^{V_{0l} - V_{wl}}} \tag{5.43}$$

$$H_{wl} = A_{1l} u_w^{\gamma_1} M_{1lw} + A_{2l} u_w^{\beta_{1l}} M_{2lw} \tag{5.44}$$

$$H_{0l} = A_{1l} M_{1l0} + A_{2l} M_{2l0} \tag{5.45}$$

Here 'w' in the subscript denotes the value at $x = W_B$ and

$$A_{1l} = \frac{W_B F_e}{\eta(b_{l0} + \gamma_1)} \tag{5.46}$$

$$A_{2l} = \frac{W_B F_{1l} G_e}{\eta(b_{l0} + \beta_{1l})} \tag{5.47}$$

$$A_{3l} = \left(\frac{1}{A_{low}} - A_{1l} M_{1l0} - A_{2l} M_{2l0}\right) e^{V_{0l}} \tag{5.48}$$

5.3 Low Injection Level Model Derivation Considering Recombination

In order to develop a low injection that includes recombination, the minority carrier concentration n_{l0} obtained for $J_p \neq 0$ and without considering recombination is extended by adding a correction term such that $n_l(x) = n_{l0}(x) + \delta n_0(x)$. Here n_l is minority carrier concentration for $J_p \neq 0$ and Recombination $\neq 0$. For the accuracy of derivation $\delta n_0(x)$ must be $= (n_{l0} + N_A)$. Therefore the inverse lifetime R_x given by Equation (5.12) becomes as,

$$R_{xl} = \left[\frac{\frac{1}{\tau_n}}{(1+r_s)n_{l0} + N_A} + C_{Ap}[(1+r_a)n_{l0} + N_A] \right] \tag{5.49}$$

$$\times (n_{l0} + N_A) \tag{5.50}$$

and the Equation (5.11) reduces to,

$$J_{pl}(x) = K - q\int_0^x R_{xl} n_{l0}(x)dx + qg\int_0^x [n_{l0}(x) + N_A(x)]dx \tag{5.51}$$

Taking the exponential approximation of the terms (since there is no direct closed form integral), the right hand side of the Equation (5.51) results in,

$$J_{pl}(x) = K - q\frac{W_B}{\eta m_{0l}} R_{0l}(1 - u^{m_{0l}}) + qg_l \frac{W_B}{\eta k_{1l}} p_{1l}(1 - u^{k_{1l}}) \tag{5.52}$$

where, $R_{xl}n_{l1}$ and $p \approx n_{l0} + N_A$ are exponentially approximated as,

$$R_{xl}n_{l0} \equiv R_{0l}u^{m_{0l}} \tag{5.53}$$

$$n_{l0} + N_A \equiv p_{1l}u^{k_{1l}} \tag{5.54}$$

where,

$$m_{0l}(k) = \frac{1}{\eta} log\left[\frac{R_{xl}(0)n_{l0}(0)}{R_{xl}(W_B)n_{l0}(W_B)} \right] \tag{5.55}$$

$$k_{1l} = \frac{1}{\eta} log\left[\frac{n_l(0) + N_A(0)}{n_l(W_B) + N_A(W_B)} \right] \tag{5.56}$$

and,

$$R_{0l} = \frac{\eta m_{0l}}{W_B(1 - u_w^{m_{0l}})} \int_0^{W_B} R_{xl}(x) n_{l0}(x)dx \tag{5.57}$$

$$p_{1l} = \frac{\eta k_{1l}}{W_B(1-u_w^{k_{1l}})}\int_0^{W_B}(n_{l0}(x)+N_A(x))(x)dx \tag{5.58}$$

Applying the boundary conditions for hole current density at $x = 0$ and $x = W_B$ gives,

$$K = -J_{pl}(0) \tag{5.59}$$

$$g_l = \frac{J_{pl}(0) - J_{pl}(W_B) + b_{1l}(1-u_w^{m0l})}{b_{2l}(1-u_w^{k_{1l}})} \tag{5.60}$$

where,

$$b_{1l} = \frac{W_B}{\eta}\frac{qR_{0l}}{m_{0l}} \tag{5.61}$$

$$b_{2l} = \frac{W_B}{\eta}\frac{qp_{1l}}{k_{1l}} \tag{5.62}$$

The majority hole current density then can be rearranged as,

$$J_{pl}(x) = J_{0l} - J_{1l}u^{k_{1l}} + b_{1l}u^{m_{0l}} \tag{5.63}$$

where,

$$J_{0l} = -J_{pl}(0) - b_{1l} + g_l b_{2l} \tag{5.64}$$

$$J_{1l} = g_l b_{2l} \tag{5.65}$$

5.3.1 Derivation of Electric Field

The expression for effective electron electric field given by Equation (5.3) can be rearranged as,

$$\frac{E_{n,eff}}{V_T} = -\frac{\eta}{W_B}\left[1-\gamma_2 - \frac{\frac{\eta(2-\gamma_2)}{W_B}n_{l0}(x) + J_{pl}(x)(F_h u^{\gamma_3} + G_h)}{\frac{\eta}{W_B}(2n_{l0}(x)+N_A(x)) + J_{pl}(x)G_h}\right]$$

$$= -\frac{\eta}{W_B}[b + b_{dxl}(x)] \tag{5.66}$$

where,

$$b = 1-\gamma_2 \tag{5.67a}$$

$$b_{dxl}(x) = -\frac{\frac{\eta(2-\gamma_2)}{W_B} n_{l0}(x) + J_{pl}(x)(F_h u^{\gamma_3} + G_h)}{\frac{\eta}{W_B}(2n_{l0}(x) + N_A(x)) + J_{pl}(x)G_h} \tag{5.67b}$$

5.3.2 Solution of Differential Equation

Differentiating the electron current density equation given by (5.13) and then combining with the Equation (5.14) results in a a second order variable-coefficient differential equation of minority electron concentration $n_l(x)$ given as,

$$\frac{d^2 n_l}{dx^2} + G_{1l}(x)\frac{dn_l}{dx} + G_{2l}(x)n_l = 0 \tag{5.68}$$

where,

$$G_{1l}(x) = \frac{E_{nl,eff}}{V_T} - \frac{d}{dx} ln\left(\frac{1}{F_{1l}}\frac{1}{qD_{nl}}\right) \tag{5.69a}$$

$$G_{2l}(x) = \frac{d}{dx}\left(\frac{E_{nl,eff}}{V_T}\right) - \frac{1}{F_{1l}}\frac{qR_{xl}}{qD_{nl}} - \frac{E_{nl,eff}}{V_T}\frac{d}{dx} ln\left(\frac{1}{F_{1l}}\frac{1}{qD_{nl}}\right) \tag{5.69b}$$

Using the electric field expression given by Equation (5.66), the terms G_{1l} and G_{2l} can be expressed as,

$$G_{1l}(x) = -\left[\frac{\eta}{W_B}(b_l + b_{dxl}) + \frac{d}{dx} ln\left(\frac{1}{F_{1l}}\frac{1}{qD_{nl}}\right)\right] \tag{5.70a}$$

$$G_{2l}(x) = \frac{\eta}{W_B}(b_l + b_{dxl})\frac{d}{dx} ln\left(\frac{1}{F_{1l}}\frac{1}{qD_{nl}}\right) - \frac{\eta}{W_B}\frac{db_{dxl}}{dx} - \frac{1}{F_{1l}}\frac{qR_{xl}}{qD_{nl}} \tag{5.70b}$$

Letting $n_l(x) = v_l(x)w_l(x)$ in the Equation (5.68) results in a second order differential equation of $v_l(x)$ as,

$$\frac{d^2 v_l}{dx^2} + \left[\frac{2}{w_l}\frac{dw_l}{dx} + G_{1l}(x)\right]\frac{dv_l}{dx} + \frac{1}{w_l}\left[\frac{d^2 w_l}{dx^2} + G_{1l}(x)\frac{dw_l}{dx} + G_{2l}(x)w_l\right]v_l = 0 \tag{5.71}$$

In order to make the variable coefficient of $\frac{dv_l}{dx}$ a constant, let

$$\frac{2}{w_l}\frac{dw_l}{dx} + G_{1l}(x) = -\frac{\eta b_l}{W_B} \tag{5.72}$$

Substituting $G_{1l}(x)$ from Equation (5.70a) gives,

$$\frac{2}{w_l}\frac{dw_l}{dx}-\left[\frac{\eta}{W_B}(b_l+b_{dxl})+\frac{d}{dx}ln\left(\frac{1}{F_{1l}}\frac{1}{qD_{nl}}\right)\right]=-\frac{\eta b_l}{W_B} \tag{5.73}$$

Rearranging the terms results,

$$\frac{dw_l}{dx}=\frac{w_l}{2}\left[\frac{d}{dx}ln\left(\frac{1}{F_{1l}}\frac{1}{qD_{nl}}\right)+\frac{\eta}{W_B}b_{dxl}\right]$$

$$\Rightarrow\frac{dw_l}{w_l}=\left[\frac{d}{dx}ln\left(\frac{1}{F_{1l}}\frac{1}{qD_{nl}}\right)^{\frac{1}{2}}\right]dx+\frac{1}{2}\int\frac{\eta}{W_B}b_{dxl}dx$$

$$\Rightarrow ln\,w_l=ln\left(\frac{1}{F_{1l}}\frac{1}{qD_{nl}}\right)^{\frac{1}{2}}+\frac{1}{2}\int\frac{\eta}{W_B}b_{dxl}dx\quad[Integrating\ both\ sides\ w.r.t.\ respective\ variables]$$

$$\Rightarrow w_l(x)=e^{\left[ln\left(\frac{1}{F_{1l}}\frac{1}{qD_{nl}}\right)^{\frac{1}{2}}+\frac{1}{2}\int\frac{\eta}{W_B}b_{dxl}dx\right]}$$

$$\Rightarrow w_l(x)=\left(\frac{1}{F_{1l}}\frac{1}{qD_{nl}}\right)^{\frac{1}{2}}e^{\frac{1}{2}\int\frac{\eta}{W_B}b_{dxl}dx}$$

$$\Rightarrow w_l(x)=\left(\frac{1}{F_{1l}}\frac{1}{qD_{nl}}\right)^{\frac{1}{2}}e^{\frac{-b_{il}(x)}{2}} \tag{5.74}$$

where, $b_{il}(x)$ can be obtained from Equation (5.67b) as follows:

$$b_{il}(x)=-\int\frac{\eta}{W_B}b_{dxl}dx \tag{5.75}$$

Since b_{dxl} is not integrable, integration in the above equation can be performed on the exponentially approximated form of b_{dxl}. This leads to,

$$b_{il}(x)=\frac{b_{dl}}{m_{dl}}u^{m_{dl}} \tag{5.76}$$

where,

$$m_{dl}=\frac{1}{\eta}\left[\frac{b_{dxl}(0)}{b_{dxl}(W_B)}\right] \tag{5.77}$$

$$b_{dl}=\frac{\eta m_{dl}}{W_B(1-u_w^{m_{dl}})}\int_0^{W_B}b_{dxl}dx \tag{5.78}$$

Then, upon substituting the expression for $w_l(x)$ in the differential equation of $v_l(x)$ [Equation (5.71)] results,

$$\frac{d^2v_l}{dx^2}-\frac{\eta b_l}{dx}\frac{dv_l}{dx}+G_{3l}(x)v_l=0 \tag{5.79}$$

where

$$G_{3l}(x) = -\frac{1}{4}\left[\frac{d}{dx} ln\left(\frac{1}{F_{1l}}\frac{1}{qD_{nl}}\right)\right]^2 - \frac{1}{4}\left(\frac{\eta b_{dxl}}{W_B}\right)^2$$
$$-\frac{1}{2}\frac{\eta}{W_B}\frac{db_{dxl}}{dx} + \frac{1}{2}\frac{d^2}{dx^2} ln\left(\frac{1}{F_{1l}}\frac{1}{qD_{nl}}\right)$$
$$-\frac{1}{F_{1l}}\frac{qR_{xl}}{qD_{nl}} + \frac{1}{2}\frac{\eta b_{dxl}}{W_B}\left[\frac{\eta b_l}{W_B} - \frac{d}{dx} ln\left(\frac{1}{qD_{nl}}\right)\right] \tag{5.80}$$

G_{3l} contains derivatives, logarithmic derivatives and derivative of logarithmic derivatives. Since the terms $\frac{1}{qD_{nl}}$, F_{1l} and b_{dxl} are not simple functions, these types of derivative become cumbersome. Exponential approximation can be used for the terms whose logarithmic derivatives are required to reduce the complexity, since logarithmic derivative of exponential functions is a constant. For this purpose, the exponential approximation of $\frac{1}{qD_{nl}}$ and F_{1l} are determined as follows:

$$\frac{1}{qD_{nl}} \equiv F_{nl} u^{m_{nl}} \tag{5.81}$$

$$F_{1l} \equiv F_{1l0} u^{m_{0l}} \tag{5.82}$$

where,

$$m_{nl} = \frac{1}{\eta} log\left[\frac{\frac{1}{qD_{nl}(0)}}{\frac{1}{qD_{nl}(W_B)}}\right] \tag{5.83}$$

$$m_{0l} = \frac{1}{\eta} log\left[\frac{F_{1l}(0)}{F_{1l}(W_B)}\right] \tag{5.84}$$

and,

$$F_{nl} = \frac{\eta m_{nl}}{W_B(1-u_w^{m_{nl}})}\int_0^{W_B}\frac{1}{qD_{nl}(x)}dx \tag{5.85}$$

$$F_{1l0} = \frac{\eta m_{1l}}{W_B(1-u_w^{m_{1l}})}\int_0^{W_B}F_{1l}(x)dx \tag{5.86}$$

where, $\frac{1}{qD_{nl}}$ can be expressed as,

$$\frac{1}{qD_{nl}} = F_e u^{\gamma_1} + G_e\left[1-\gamma_2 - \frac{\frac{dn_{l0}}{dx} + \frac{\eta}{W_B}n_{l0} + J_{pl}(F_h u^{\gamma_3} + Gh)}{\frac{\eta}{W_B}(n_{l0}+N_A) + J_{pl}G_h}\right] \tag{5.87}$$

where,

$$\frac{dn_{l0}}{dx} = \frac{\eta}{W_B}J_{nl0}\left[\gamma_1 A_{1l} u^{\gamma_1} M_{1l} + \beta_{1l} A_{2l} u^{\beta_{1l}} M_{2l} - b_{l0} A_{3l} u^{-b_{l0}} e^{-v_{l0}}\right]$$

$$-\frac{\eta}{W_B} J_{nl0}\left[\frac{\beta_{0l} v_{l0} A_{1l} u^{\gamma_1} H_{1l}}{\frac{b_{l0}+\gamma_1}{\beta_{0l}}+1}+\frac{A_{2l} u^{\beta_{1l}} H_{2l}}{\frac{b_{l0}+\beta_{1l}}{\beta_{0l}}+1}+A_{3l} u^{-b_{l0}} e^{-v_{l0}}\right] \tag{5.88}$$

where, H's are the confluent hypergeometric functions given by,

$$H_{1l}(x) = M\left(1;\frac{b_{l0}+\gamma_1}{\beta_{0l}}+2;-v_{l0}(x)\right) \tag{5.89a}$$

$$H_{2l}(x) = M\left(1;\frac{b_{l0}+\beta_{1l}}{\beta_{0l}}+2;-v_{l0}(x)\right) \tag{5.89b}$$

Using the exponential approximation technique for the term G_{3l}, a position dependent term F_{3l} and a constant term 'c' can be separated as,

$$F_{3l}(x) = -\frac{1}{4}\left(\frac{\eta b_{dxl}}{W_B}\right)^2 - \frac{1}{2}\frac{\eta}{W_B}\frac{db_{dxl}}{dx}$$

$$-\frac{1}{2}\left(\frac{\eta}{W_B}\right)^2 (b_l + m_{nl} - m_{0l}) b_{dxl} - \frac{1}{F_{1l}}\frac{qR_{xl}}{qD_{nl}} \tag{5.90a}$$

$$c = \frac{1}{2}\left[\frac{\eta}{W_B}(m_{nl} - m_{0l})\right]^2 \tag{5.90b}$$

In order to convert the differential equation into a solvable form $F_{3l}(x)$ is exponentially approximated as,

$$F_{3l}(x) \equiv F_{30l} u^{\beta_{3l}} \tag{5.91}$$

where,

$$\beta_{3l} = \frac{1}{\eta} log\left[\frac{F_{3l}(0)}{F_{3l}(W_B)}\right] \tag{5.92}$$

and,

$$F_{30l} = \frac{\eta\beta_{3l}}{W_B(1-u_w^{\beta_{3l}})}\int_0^{W_B} F_{3l}(x)dx \tag{5.93}$$

The differential equation [Equation (5.79)] can be rewritten as

$$\frac{d^2 v_l}{dx^2} - \frac{\eta b_l}{dx}\frac{dv_l}{dx} + [F_{3l}(x) - c]v_l = 0 \tag{5.94}$$

Changing the independent variable x to z by letting

$$z = u^{\beta_{3l}/2} \tag{5.95}$$

the differential equation [Equation (5.94)] becomes as,

$$\frac{d^2 v_l}{dz^2} + \frac{a_{0l}}{z}\frac{dv_l}{dz} + \frac{1}{z^2}[b_{0l}^2 - c_1]v_l = 0 \tag{5.96}$$

where,

$$a_{0l} = 1 + \frac{2b_l}{\beta_{3l}} \tag{5.97}$$

$$b_{0l} = \frac{2W_B}{\eta\beta_{3l}}\sqrt{F_{30l}} \tag{5.98}$$

$$c_1 = \left(\frac{2W_B}{\eta\beta_{3l}}\right)c \tag{5.99}$$

Letting

$$v_l(x) = y_l(x)t_l(x) \tag{5.100}$$

gives a second order differential equation of y_l in terms of, t_l as

$$\frac{d^2 y_l}{dz^2} + \left[\frac{2}{t_l}\frac{dt_l}{dz} + \frac{a_{0l}}{z}\right]\frac{dy_l}{dz} + \frac{1}{t_l}\left[\frac{d^2 t_l}{dz^2} + \frac{a_{0l}}{z}\frac{dt_l}{dz} + \frac{1}{z^2}[b_{0l}^2 - c_1]t_l\right]y_l = 0 \tag{5.101}$$

Then, letting the coefficient of first derivative of y_l as,

$$\frac{2}{t_l}\frac{dt_l}{dz} + \frac{a_{0l}}{z} = \frac{1}{z} \tag{5.102}$$

gives,

$$\frac{dt_l}{dz} = \frac{1}{2}\left[\frac{1 - a_{0l}}{z}\right]t_l \tag{5.103}$$

The solution of this differential equation gives an expression for $t_l(x)$ as,

$$t_l = u^{-\frac{b_l}{2}} \tag{5.104}$$

Substituting the expression for t_l in the differential equation [Equation (5.101)] results in a Bessel equation as,

$$\frac{d^2 y_l}{dz^2} + \frac{1}{z}\frac{dy_l}{dz} + \frac{1}{z^2}\left[b_{0l}^2 - \beta_l^2\right] y_l = 0 \tag{5.105}$$

where,

$$\beta_l = \frac{b_l + m_{nl} - m_{1l}}{\beta_{3l}} \tag{5.106}$$

The solution of the Bessel equation consists of Bessel functions of the first and the second kind (J_β and Y_β) and can be given as,

$$y_l(x) = C_{1l} J_{\beta_l}(b_{0l} z) + C_{2l} Y_{\beta_l}(b_{0l} z) \tag{5.107}$$

Therefore, the minority carrier concentration under low injection case can be obtained from the relation $n_l(x) = w_l t_l y_l$ as,

$$n_l(x) = u^{\frac{-b_l}{2}} \left(\frac{1}{F_{1l}} \frac{1}{qD_{nl}}\right)^{\frac{1}{2}} [C_{1l} J_{\beta_l}(b_{0l} z) + C_{2l} Y_{\beta_l}(b_{0l} z)] \tag{5.108}$$

The minority electron current density can be obtained from the following relation [after arranging the Equation (5.13)],

$$J_{nl}(x) = qD_{nl}(x)\left[F_{1l}(x)\frac{dn_l}{dx} + \frac{E_{nl,apparent}(x)}{V_T} n_l(x)\right] \tag{5.109}$$

where,

$$\frac{E_{n,apparent}}{V_T} = -\frac{\eta}{W_B}\left[1 - \gamma_2 + \frac{\frac{\eta}{W_B} n_{l0} + J_{pl}(F_h u^{\gamma_3} + Gh)}{\frac{\eta}{W_B}(n_{l0} + N_A) + J_{pl} Gh}\right] \tag{5.110}$$

$$\frac{dn_l}{dx} = \frac{1}{2}\frac{\eta \beta_{3l}}{W_B} w_l t_l [C_{1l} f_{1l}(x) + C_{2l} f_{2l}(x)] \tag{5.111}$$

where,

$$f_{1l} = \frac{\eta}{W_B}(b_{0l}z)\left[J_{\beta_l+1}(b_{0l}z) - J_{\beta_l-1}(b_{0l}z)\right] + \frac{\left[\frac{d}{dx}ln\left(\frac{1}{F_{1l}}\frac{1}{qD_{nl}}\right) - \frac{1}{F_{1l}}\frac{E_{nl,apparent}}{V_T}\right]}{\frac{\eta}{W_B}\beta_{3l}} J_{\beta_l}(b_{0l}z) \tag{5.112a}$$

$$f_{2l} = \frac{\eta}{W_B}(b_{0l}z)\left[Y_{\beta_l+1}(b_{0l}z) - Y_{\beta_l-1}(b_{0l}z)\right] + \frac{\left[\frac{d}{dx}ln\left(\frac{1}{F_{1l}}\frac{1}{qD_{nl}}\right) - \frac{1}{F_{1l}}\frac{E_{nl,apparent}}{V_T}\right]}{\frac{\eta}{W_B}\beta_{3l}} Y_{\beta_l}(b_{0l}z) \tag{5.112b}$$

Using the appropriate boundary conditions at $x = 0$ and $x = W_B$, the constants C_{1l} and C_{2l} can be obtained as,

$$C_{2l} = -\beta_{sl}C_{1l} \tag{5.113}$$

$$C_{1l} = \frac{\frac{n(0)}{w_{l1}(0)}}{J_{\beta_l}(b_{0l}) - \beta_{sl}Y_{\beta_l}(b_{0l})} = n(0)C_{0l} \tag{5.114}$$

where,

$$\beta_{sl} = \frac{f_{1lw} + A_{lw}J_{\beta_l}(b_{0l}z_w)}{f_{2lw} + A_{lw}Y_{\beta_l}(b_{0l}z_w)} \tag{5.115}$$

$$A_{lw} = \frac{2W_B}{\eta}\frac{S_l + E_{nlw}}{\beta_{3l}} \tag{5.116}$$

$$S_l = \frac{qv_s}{qD_{nlw}} \tag{5.117}$$

$$C_{0l} = \frac{\frac{1}{w_{l1}(0)}}{J_{\beta_l}(b_{0l}) - \beta_{sl}Y_{\beta_l}(b_{0l})} \tag{5.118}$$

and,

$$f_{1lw} = \frac{W_B}{\eta}\left[\frac{\frac{d}{dx}ln\left(\frac{1}{F_{1lw}}\frac{1}{qD_{nlw}}\right) - \frac{1}{F_{1lw}}\frac{E_{nl1w}}{V_T}}{\beta_{3l}}\right] J_{\beta_l}(b_{0l}z_w) \tag{5.119}$$

$$+ (b_{0l}z_w)\left[\frac{J_{\beta_l+1}(b_{0l}z_w) - J_{\beta_l-1}(b_{0l}z_w)}{2}\right] \tag{5.120}$$

$$f_{2lw} = \frac{W_B}{\eta}\left[\frac{\frac{d}{dx}ln\left(\frac{1}{F_{1lw}}\frac{1}{qD_{nlw}}\right) - \frac{1}{F_{1lw}}\frac{E_{nl1w}}{V_T}}{\beta_{3l}}\right] Y_{\beta_l}(b_{0l}z_w) \tag{5.121}$$

$$+ (b_{0l}z_w)\left[\frac{Y_{\beta_l+1}(b_{0l}z_w) - Y_{\beta_l-1}(b_{0l}z_w)}{2}\right] \tag{5.122}$$

The minority electron concentration then can be expressed as,

$$n_l(x) = n(0)\mu^{\frac{-b_l}{2}}\left(\frac{1}{F_{1l}}\frac{1}{qD_{nl}}\right)^{\frac{1}{2}}[J_{\beta_l}(b_{0l}z) - \beta_{sl}Y_{\beta_l}(b_{0l}z)]C_{0l} \tag{5.123}$$

5.3.3 Intermediate Injection Level Model Derivation

The low injection (LI) minority carrier concentration, $n_{l1}(x)$ can be extended to the intermediate regime by using perturbation theory. Using this theory, the LI minority carrier concentration can be expressed as

$$n(x) = n_{l1}f_w + \delta n(x) = n\,l2 + \delta n(x) \tag{5.124}$$

where n_{l2} is obtained using the Webster effect. For the accuracy of model derivation, δn is chosen such that $\delta n = n_{l2} + N_A$.

Changing the variable n_{l0} to n_{l2}, the LI model developed in section (5.3) with considering recombination can be used for intermediate level model derivation. Therefore, the model equations under intermediate injection level are exactly same as those for the model described in section (5.3), with 'l' dropped in the subscript of all the equations.

5.4 Model Derivation Considering Separate Effects of J_p and Recombination Mechanisms

In order to investigate the separate effects of majority carrier current density J_p and the recombination mechanisms, other than the model derived in the previous sections, models considering J_p only and considering recombination mechanisms only have to be developed. In the following sections, these models are presented. The first model concerns only the J_p to reflect the role of base current by incorporating the lateral base injection. The second model deals with only the recombination mechanisms. In both cases, first a low-injection (LI) model is deduced, which is later used to derive the intermediate-level (II) model.

5.4.1 Model Derivation Considering J_p Only

In this model, only the effect of lateral base injection is considered. Recombination is excluded in the analysis. All other effects and considerations are used. In order to develop the model, the LI model developed in Section (5.2) is extended by using perturbation theory to derive the intermediate-injection level model.

Integration of Eqn. (4.28) under intermediate injection condition [n(x)is comparable with $N_A(x)$] and using Equation (4.6) gives

$$J_p(x) = K + qg\frac{W_B}{\eta k_1} p_1(1-u^{k_1}) \tag{5.125}$$

where $p \approx n_{l2} + N_A$ is exponentially approximated as $p_1 u^{k_1}$. Applying the boundary conditions for hole current density at $x = 0$ and $x = W_B$ gives

$$K = -J_p(0) \tag{5.126}$$

$$g = \frac{\eta}{W_B}\frac{J_p(0)-J_p(W_B)}{qp_1(1-u_w^{k_1})} \tag{5.127}$$

The majority hole current density then can be rearranged as

$$J_p(x) = J_0 - J_1 u^{k_1} \tag{5.128}$$

where

$$J_0 = \frac{J_p(0)u_w^{k_1} - J_p(W_B)}{1-u_w^{k_1}} \tag{5.129}$$

$$J_1 = \frac{J_p(0)-J_p(W_B)}{1-u_w^{k_1}} \tag{5.130}$$

Using this expression for J_p in the term $E_{n,11}$

$$E_{n,11} = -\frac{\eta}{W_B}\left[\frac{(J_1u^{k_1} - J_0)(F_h u^{\gamma_3} + G_h)}{(\frac{\eta}{W_B}p_1 - J_1G_h)u^{k_1} + J_0G_h}\right] \tag{5.131}$$

Since, $(\frac{\eta}{W_B}p_1 - J_1G_h)u^{k_1}$?$J_0G_h$, the denominator term can be expanded into a binomial series. Neglecting the second and higher order terms, the Equation (5.131) can be

approximated as

$$E_{n,11} \approx -\frac{\eta}{W_B}[b + b_{d0}(x)] \tag{5.132}$$

where

$$b = 1 - \gamma_2 + \gamma_0 \tag{5.133}$$

$$b_{d0}(x) = \sum_{k=1}^{5} a_h(k) u^{g_h(k)} \tag{5.134}$$

where $\gamma_0 = J_1 J_2 G_h$, $J_2 = \dfrac{1}{gp_1 - J_1 G_h}$, $J_3 = J_0 G_h J_2^2$,

$$a_h(1) = -(J_1 J_3 + J_0 J_2) G_h \tag{5.135}$$

$$a_h(2) = J_0 J_3 G_h \tag{5.136}$$

$$a_h(3) = J_1 J_2 F_h \tag{5.137}$$

$$a_h(4) = -(J_1 J_3 + J_0 J_2) F_h \tag{5.138}$$

$$a_h(5) = J_0 J_3 F_h \tag{5.139}$$

and $g_h(1) = -k_1$, $g_h(2) = -2k_1$, $g_h(3) = \gamma_3$, $g_h(4) = \gamma_3 - k_1$ and $g_h(5) = \gamma_3 - 2k_1$.

In order to obtain analytical tractability, the terms $b_d(x)$ and $b_e(x)$ are exponentially approximated as

$$\sum_{k=0}^{5} b_d(k) \equiv \sum_{k=0}^{5} b_{d1} u^{r_d(k)} \tag{5.140}$$

$$b_e(x) \equiv b_{e1} u^{r_e} \tag{5.141}$$

Therefore, electric field term, $\dfrac{E_{n,eff}}{V_T}$ given by Equation (5.66) can be given as

$$\frac{1}{F_1}\frac{E_{n1}}{V_T} = -\frac{\eta}{W_B}\left[1 - \gamma_2 + \gamma_0 + b_{d0} + \sum_{k=1}^{5} b_d(k) - b_e\right] \tag{5.142}$$

Using the above equation for electric field and the the mobility (Equation 4.9) in the electron current density equation (5.13) results in a first order variable-coefficient differential

equation of minority electron concentration n(x) as

$$\frac{dn}{dx}+n\frac{1}{F_1}\frac{E_{n1}}{V_T}=J_n\left(\frac{F_e u^{\gamma_1}}{F_1}\right)+J_n\frac{W_B G_e}{\eta}\frac{\left|\frac{E_{n3}}{V_T}\right|}{F_1} \tag{5.143}$$

The integrating factor of this equation is given as

$$I.F.=e^{\int\frac{1}{F_1}\frac{E_{n1}}{V_T}}=u^b e^{b_i(x)} \tag{5.144}$$

where

$$b_i(x)=\sum_{k=1}^{5}\left[\frac{a_h(k)u^{g_h(k)}}{g_h(k)}+\frac{b_{d1}(k)u^{r_d(k)}}{r_d(k)}\right]+\frac{b_{e1}u^{r_e}}{r_e} \tag{5.145}$$

Integrating the differential equation (5.194) w.r.t x gives

$$n(x)u^b e^v=\left[n(x)e^v\right]_{x=0}+J_n F_2\int_0^x u^{\beta_1}e^v dx \tag{5.146}$$

$$+\frac{W_B G_e}{\eta}J_n F_2\int_0^x u^{\beta_2}e^v dx \tag{5.147}$$

where the terms $b_i(x)$, $\frac{F_e u^{\gamma_1}}{F_1}$ and $\frac{\left|\frac{E_{n1}}{V_T}\right|}{F_1}$ are exponentially approximated to obtain a solvable form for the differential equation and are given by

$$b_i(x)\equiv V_0 u^{\beta_0}=v(x) \tag{5.148}$$

$$\frac{F_e u^{\gamma_1}}{F_1}\equiv F_2 u^{\beta_2} \tag{5.149}$$

$$\frac{\left|\frac{E_{n3}}{V_T}\right|}{F_1}\equiv F_3 u^{\beta_3} \tag{5.150}$$

Following the same procedure outlined for LI model, an expression of minority carrier concentration n(x) for intermediate injection level can be obtained as

$$n(x)=-J_n\left[A_1 u^{\beta_1}M_1(x)+A_2 u^{\beta_2}M_2(x)+A_3 u^{-b}e^{-v}\right] \tag{5.151}$$

where

$$J_n = -A_{high} n(0) \tag{5.152}$$

$$A_{high} = \frac{u_w^{-b} e^{V_0 - V_w}}{\frac{1}{q v_s} - H_w + H_0 u_w^{-b} e^{V_0 - V_w}} \tag{5.153}$$

$$H_w = A_1 u_w^{\beta_2} M_{1w} + A_2 u_w^{\beta_3} M_{2w} \tag{5.154}$$

$$H_0 = A_1 M_{10} + A_2 M_{2l0} \tag{5.155}$$

and

$$A_1 = \frac{W_B F_2}{\eta(b+\beta_2)} \tag{5.156}$$

$$A_2 = \frac{W_B F_3 G_e}{\eta(b+\beta_3)} \tag{5.157}$$

$$A_3 = \left(\frac{1}{A_{high}} - A_1 M_{10} - A_2 M_{20} \right) e^{V_0} \tag{5.158}$$

5.4.2 Model Derivation Considering Recombination Only

In this model, only the effect of recombination mechanisms is considered. The effect of J_p is neglected in developing this model. All other effects and considerations are used. Again, in order to develop the model, first LI is model is derived and then, this LI model is extended by using perturbation theory to derive the intermediate-injection level model.

Low Injection Level Model Derivation

Under low injection condition, $n_l = N_A$. Therefore the R_x term in the electron current continuity equation becomes as

$$R_{xl} = \frac{1}{\tau_n} + C_{Ap} N_A^2 \tag{5.159}$$

and the Equation (3.24) reduces to

$$\frac{dJ_{nl}}{dx} = q R_{xl} n_l \tag{5.160}$$

where for heavy doping, $n >> \frac{n_{ie}^2}{N_A}$ is assumed.

Now, differentiating the electron current density equation given by (2.9a) and then combining with the Equation (5.14) results in a a second order variable-coefficient differential equation of minority electron concentration n(x) as

$$\frac{d^2 n_l}{dx^2} + \left[\frac{E_{nl}}{V_T} - \frac{d}{dx} ln\left(\frac{1}{qD_{nl}} \right) \right] \frac{dn_l}{dx} \tag{5.161}$$

$$+ \left[\frac{d}{dx}\left(\frac{E_{nl}}{V_T} \right) - \frac{E_{nl}}{V_T} \frac{d}{dx} ln\left(\frac{1}{qD_{nl}} \right) - \frac{qR_{xl}}{qD_{nl}} \right] n_l = 0 \tag{5.162}$$

Using the electric field expression for LI case, the above equation becomes

$$\frac{d^2 n_l}{dx^2} - \left[\frac{\eta b_l}{W_B} + \frac{d}{dx} ln\left(\frac{1}{qD_{nl}} \right) \right] \frac{dn_l}{dx} \tag{5.163}$$

$$+ \left[\frac{\eta b_l}{W_B} \frac{d}{dx} ln\left(\frac{1}{qD_{nl}} \right) - \frac{qR_{xl}}{qD_{nl}} \right] n_l = 0 \tag{5.164}$$

where $b_l = 1 - \gamma_2$. Now, letting $n_l(x) = v_l(x) w_l(x)$ results in a second order differential equation of v(x) as

$$\frac{d^2 v_l}{dx^2} - \left[\frac{2}{w_l} \frac{dw_l}{dx} + G_{1l}(x) \right] \frac{dv_l}{dx} \tag{5.165}$$

$$+ \frac{1}{w_l} \left[\frac{d^2 w_l}{dx^2} + G_{1l}(x) \frac{dw_l}{dx} + G_{2l}(x) w_l \right] v_l = 0 \tag{5.166}$$

where

$$G_{1l}(x) = -\left[\frac{\eta b_l}{W_B} + \frac{d}{dx} ln\left(\frac{1}{qD_{nl}} \right) \right] \tag{5.167}$$

$$G_{2l}(x) = \frac{\eta b_l}{W_B} \frac{d}{dx} ln\left(\frac{1}{qD_{nl}} \right) - \frac{qR_{xl}}{qD_{nl}} \tag{5.168}$$

In order to make the variable coefficient of $\frac{dv_l}{dx}$ a constant, it can be assumed that

$$\frac{2}{w_l} \frac{dw_l}{dx} + G_{1l}(x) = -\frac{\eta b_l}{W_B} \tag{5.169}$$

This gives

$$w_l(x) = \left(\frac{1}{qD_{nl}} \right)^{\frac{1}{2}} \tag{5.170}$$

and the differential equation of $v_l(x)$ as

$$\frac{d^2v_l}{dx^2} - \frac{\eta b_l}{dx}\frac{dv_l}{dx} - F_{3xl}v_l = 0 \tag{5.171}$$

where

$$F_{3xl} = \frac{1}{4}\left[\frac{d}{dx} ln\left(\frac{1}{qD_{nl}}\right)\right]^2 - \frac{1}{2}\frac{\eta b_l}{W_B}\frac{d}{dx} ln\left(\frac{1}{qD_{nl}}\right) \tag{5.172}$$

$$-\frac{1}{2}\frac{d^2}{dx^2} ln\left(\frac{1}{qD_{nl}}\right) + \frac{qR_{xl}}{qD_{nl}} \tag{5.173}$$

Using the exponential approximation of F_{3xl} as $F_{3l}u^{\beta_{3l}}$ and then changing the independent variable x to z by letting $z = u^{\beta_{3l}/2}$, the differential equation of $v_l(x)$ becomes

$$\frac{d^2v_l}{dz^2} + \frac{a_{0l}}{z}\frac{dv_l}{dx} - b_{0l}^2 v_l = 0 \tag{5.174}$$

where,

$$a_{0l} = 1 + \frac{2b_l}{\beta_{3l}} \tag{5.175}$$

$$b_{0l} = \frac{qW_B}{\eta\beta_{3l}}\sqrt{F_{3l}} \tag{5.176}$$

Again, assuming $v_l(x) = y_l(x)t_l(x)$ gives a second order differentia equation of y_l in terms of t_l. Then, letting the coefficient of first derivative of y_l to unity results in a modified Bessel equation of y_l as

$$\frac{d^2y_l}{dz^2} + \frac{1}{z}\frac{dy_l}{dx} - \frac{1}{z^2}\left[b_{0l}^2 + \beta_l^2\right]y_l = 0 \tag{5.177}$$

where

$$t_l = u^{-\frac{b_l}{2}} \tag{5.178}$$

$$\beta_l = \frac{b_l}{\beta_{3l}} \tag{5.179}$$

The solution of the modified Bessel equation consists of Bessel functions of first and second kind (I_β and K_β) and can be given as

$$y_l = C_{1l}I_{\beta_l}(b_{0l}z) + C_{2l}K_{\beta`_l}(b_{0l}z) \tag{5.180}$$

Therefore, the minority carrier concentration under LI case can be obtained from the relation

$n_l(x) = w_l t_l y_l$ as

$$n_l(x) = u^{\frac{-b_l}{2}} \left(\frac{1}{qD_{nl}} \right)^{\frac{1}{2}} [C_{1l} I_{\beta_l}(b_{0l} z) + C_{2l} K_{\beta`_l}(b_{0l} z)] \tag{5.181}$$

Using the appropriate boundary conditions, the constants C_{1l} and C_{2l} can be obtained as

$$C_{2l} = -\beta_{sl} C_{1l} \tag{5.182}$$

$$C_{1l} = \frac{\frac{n(0)}{w_l(0)}}{I_{\beta_l}(b_{0l}) - \beta_{sl} K_{\beta_l}(b_{0l})} \tag{5.183}$$

where

$$\beta_{sl} = \frac{f_{1wl} + A_{wl} I_{\beta_l}(b_{0l} z_w)}{f_{2wl} + A_{wl} K_{\beta_l}(b_{0l} z_w)} \tag{5.184}$$

$$A_{wl} = \frac{2W_B}{\eta} \frac{S_l + E_{nlw}}{\beta_{3l}} \tag{5.185}$$

$$S_l = \frac{q v_s}{q D_{nlw}} \tag{5.186}$$

and

$$f_{1lw} = \left[\frac{b_l + \frac{W_B}{\eta} \frac{d}{dx} ln\left(\frac{1}{qD_{nlw}} \right)}{\beta_{3l}} \right] I_{\beta_l}(b_{0l} z_w) \tag{5.187}$$

$$-(b_{0l} z_w) \left[\frac{I_{\beta_l+1}(b_{0l} z_w) + I_{\beta_l-1}(b_{0l} z_w)}{2} \right] \tag{5.188}$$

$$f_{2lw} = \left[\frac{b_l + \frac{W_B}{\eta} \frac{d}{dx} ln\left(\frac{1}{qD_{nlw}} \right)}{\beta_{3l}} \right] K_{\beta_l}(b_{0l} z_w) \tag{5.189}$$

$$+(b_{0l} z_w) \left[\frac{K_{\beta_l+1}(b_{0l} z_w) + K_{\beta_l-1}(b_{0l} z_w)}{2} \right] \tag{5.190}$$

Intermediate Injection Level Model Derivation

Under intermediate injection condition, $n(x)$ is comparable with N_A. In this case, the R_x term in the electron current continuity equation becomes

$$R_x = \left[\frac{\frac{1}{\tau_n}}{(1+r_s)n_{l2} + N_A} + C_{Ap}[(1+r_a)n_{l2} + N_A] \right] \tag{5.191}$$

$$\times (n_{l2} + N_A) \tag{5.192}$$

and the Equation (3.24) reduces to

$$\frac{dJ_n}{dx} = qR_x n \tag{5.193}$$

where for heavy doping, $n >> \frac{n_{ie}^2}{N_A}$ is assumed.

Now, differentiating the electron current density equation given by (5.13) and then combining with the Equation (5.14) results in a a second order variable-coefficient differential equation of minority electron concentration n(x) as

$$\frac{d^2n}{dx^2} + \left[\frac{1}{F_1}\frac{E_{n1}}{V_T} - \frac{d}{dx} ln\left(\frac{1}{F_1}\frac{1}{qD_n} \right) \right] \frac{dn}{dx} \tag{5.194}$$

$$+ \left[\frac{d}{dx}\left(\frac{1}{F_1}\frac{E_{n1}}{V_T} \right) - \frac{1}{F_1}\frac{E_{n1}}{V_T}\frac{d}{dx} ln\left(\frac{1}{F_1}\frac{1}{qD_n} \right) - \frac{1}{F_1}\frac{qR_x}{qD_n} \right] n = 0 \tag{5.195}$$

Using the electric field expression and rearranging the terms, the above equation becomes

$$\frac{d^2n}{dx^2} - \left[\frac{\eta}{W_B}(b - b_e) + \frac{d}{dx} ln\left(\frac{1}{F_1}\frac{1}{qD_n} \right) \right] \frac{dn}{dx} \tag{5.196}$$

$$+ \left[-\frac{\eta}{W_B}\frac{db_e}{dx} + \frac{\eta}{W_B}(b - b_e)\frac{d}{dx} ln\left(\frac{1}{F_1}\frac{1}{qD_n} \right) - \frac{1}{F_1}\frac{qR_x}{qD_n} \right] n = 0 \tag{5.197}$$

where $b_l = 1 - \gamma_2$. Now, letting $n(x) = v(x)w(x)$ results in a second order differential equation of v(x) as

$$\frac{d^2v}{dx^2} + \left[\frac{2}{w}\frac{dw}{dx} + G_1(x) \right] \frac{dv}{dx} \tag{5.198}$$

$$+ \frac{1}{w}\left[\frac{d^2w}{dx^2} + G_1(x)\frac{dw}{dx} + G_2(x)w \right] v = 0 \tag{5.199}$$

where

$$G_1(x) = -\left[\frac{\eta}{W_B}(b - b_e) + \frac{d}{dx} ln\left(\frac{1}{qD_n}\right)\right] \tag{5.200}$$

$$G_2(x) = -\frac{\eta}{W_B}\frac{db_e}{dx} + \frac{\eta}{W_B}(b - b_e)\frac{d}{dx} ln\left(\frac{1}{F_1}\frac{1}{qD_n}\right) - \frac{qR_x}{qD_n} \tag{5.201}$$

In order to make the variable coefficient of $\frac{dv}{dx}$ a constant,

$$\frac{2}{w}\frac{dw}{dx} + G_1(x) = -\frac{\eta b}{W_B} \tag{5.202}$$

is assumed. This gives

$$w(x) = \left(\frac{1}{F_1}\frac{1}{qD_n}\right)^{\frac{1}{2}} e^{\frac{b_i(x)}{2m_i}} \tag{5.203}$$

and the differential equation of $v(x)$ as

$$\frac{d^2v}{dx^2} - \frac{\eta b}{dx}\frac{dv}{dx} - G_3(x)v = 0 \tag{5.204}$$

where $b_e(x)$ is exponentially approximated to $b_i(x) = b_{i0}u^{m_i}$ in order to obtain the integral of its non-integrable form, and

$$G_3(x) = \frac{1}{4}\left[\frac{d}{dx} ln\left(\frac{1}{F_1}\frac{1}{qD_n}\right)\right]^2 + \frac{1}{4}\left(\frac{\eta b_e}{W_B}\right)^2 \tag{5.205}$$

$$-\frac{1}{2}\frac{\eta}{W_B}\frac{db_e}{dx} - \frac{1}{2}\frac{d^2}{dx^2} ln\left(\frac{1}{F_1}\frac{1}{qD_n}\right) \tag{5.206}$$

$$+\frac{1}{F_1}\frac{qR_x}{qD_n} + \frac{1}{2}\frac{\eta b_e}{W_B}\left[\frac{\eta b}{W_B} - \frac{d}{dx} ln\left(\frac{1}{qD_n}\right)\right] \tag{5.207}$$

To obtain an analytically tractable solution of the differential equation (5.204), the exponential approximation of $\frac{1}{qD_n}$ as $F_n u^{m_n}$, $b_e(x)$ as $b_{e0}u^{m_e}$, and F_1 as $F_{10}u^{m_1}$. This makes the logarithmic terms of $G_3(x)$ position independent. Therefore, the term G_3 can be decomposed into a variable $F_3(x)$ and a constant term c as given by

$$F_3(x) = \frac{1}{4}\left(\frac{\eta b_e}{W_B}\right)^2 - \frac{1}{2}\frac{\eta}{W_B}\frac{db_e}{dx} \tag{5.208}$$

$$+\frac{1}{2}\left(\frac{\eta}{W_B}\right)^2 (b + m_n - m_1)b_e + \frac{1}{F_1}\frac{qR_x}{qD_n} \tag{5.209}$$

$$c = \frac{1}{2}\left[\frac{\eta}{W_B}(m_n - m_1)\right]^2 \tag{5.210}$$

$F_3(x)$ can be exponentially approximated as $F_{30}u^{\beta_3}$ to convert the differential equation into a solvable form as,

$$\frac{d^2v}{dx^2} - \frac{\eta b}{dx}\frac{dv}{dx} + [F_3(x) - c]v = 0 \tag{5.211}$$

Changing the independent variable x to z by letting $z = u^{\beta_3/2}$, the differential equation becomes

$$\frac{d^2v}{dz^2} + \frac{a_0}{z}\frac{dv}{dx} + \frac{1}{z^2}[b_0^2 - c_1]v = 0 \tag{5.212}$$

where,

$$a_0 = 1 + \frac{2b}{\beta_3} \tag{5.213}$$

$$b_0 = \frac{2W_B}{\eta\beta_3}\sqrt{F_{30}} \tag{5.214}$$

$$c_1 = \left(\frac{2W_B}{\eta\beta_3}\right)c \tag{5.215}$$

Again, assuming $v(x) = y(x)t(x)$ gives a second order differential equation of y in terms of t. Then, letting the coefficient of first derivative of y to unity results in a Bessel equation of y as

$$\frac{d^2y}{dz^2} + \frac{1}{z}\frac{dy}{dx} + \frac{1}{z^2}\left[b_0^2 - \beta^2\right]y = 0 \tag{5.216}$$

where,

$$t = u^{-\frac{b}{2}} \tag{5.217}$$

$$\beta = \frac{b + m_n - m_1}{\beta_3} \tag{5.218}$$

The solution of the Bessel equation consists of Bessel functions of first and second kind (J_β and Y_β) and can be given as

$$y(x) = C_1J_\beta(b_0z) + C_2Y_\beta(b_0z) \tag{5.219}$$

Therefore, the minority carrier concentration under intermediate injection case can be

obtained from the relation $n(x) = wty$ as

$$n(x) = u^{\frac{-b}{2}}\left(\frac{1}{F_1}\frac{1}{qD_n}\right)^{\frac{1}{2}}[C_1 J_\beta(b_0 z) + C_2 Y_\beta(b_0 z)] \tag{5.220}$$

Using the appropriate boundary conditions, the constants C_1 and C_2 can be obtained as

$$C_2 = -\beta_s C_1 \tag{5.221}$$

$$C_1 = \frac{\frac{n(0)}{w(0)}}{J_\beta(b_0) - \beta_s Y_\beta(b_0)} \tag{5.222}$$

where

$$\beta_s = \frac{f_{1w} + A_w J_\beta(b_0 z_w)}{f_{2w} + A_w Y_\beta(b_0 z_w)} \tag{5.223}$$

$$A_w = \frac{2W_B}{\eta}\frac{S + E_{mw}}{\beta_3} \tag{5.224}$$

$$S = \frac{qv_s}{qD_{mw}} \tag{5.225}$$

and

$$f_{1lw} = \frac{W_B}{\eta}\left[\frac{\frac{d}{dx}ln\left(\frac{1}{F_{1lw}}\frac{1}{qD_{nlw}}\right) - \frac{1}{F_{1lw}}\frac{E_{nl1w}}{V_T}}{\beta_{3l}}\right] J_{\beta_l}(b_{0l} z_w) \tag{5.226}$$

$$+ (b_{0l} z_w)\left[\frac{J_{\beta_l+1}(b_{0l} z_w) - J_{\beta_l-1}(b_{0l} z_w)}{2}\right] \tag{5.227}$$

$$f_{2lw} = \frac{W_B}{\eta}\left[\frac{\frac{d}{dx}ln\left(\frac{1}{F_{1lw}}\frac{1}{qD_{nlw}}\right) - \frac{1}{F_{1lw}}\frac{E_{nl1w}}{V_T}}{\beta_{3l}}\right] Y_{\beta_l}(b_{0l} z_w) \tag{5.228}$$

$$+ (b_{0l} z_w)\left[\frac{Y_{\beta_l+1}(b_{0l} z_w) - Y_{\beta_l-1}(b_{0l} z_w)}{2}\right] \tag{5.229}$$

5.5 Conclusion

In this chapter, the model equations for base transit time for an npn bipolar transistor are derived. In doing so, position and field dependence of transport parameters are considered. Moreover, heavy-doping effects such as band-gap narrowing, high injection effects such as the Webster and the Kirk effects and velocity saturation at the base-collector junction are

also considered in this model. Although considering all these effects makes the modeling effort more intractable, appropriate application of the exponential approximation technique and perturbation theory allows one to arrive at a closed-form solution.

Chapter 6
Results and Discussion

The presence of majority carrier current and recombination in the quasi-neutral base has an influence on the value of the base transit time of a BJT. This impact is due to the alteration of minority carrier profile which affects the electric field and hence the minority carrier current density. These changes then results in a significant change on the base transit time.

In this chapter, a quantitative analysis of the effects of the majority carrier current and the recombination process in the base is presented. Also, presented in this chapter is the deviations of these results compared with the results obtained without considering these factors. Justifications of these results are finally analyzed, which will establish the relative importance and significance of the majority carrier current and recombination on the base transit time.

A recently published work by Hassan *et. al.* [11] is chosen as reference to compare the results obtained using the proposed model of this work. Both this model and the developed models consider the same factors i.e. the velocity saturation at the base collector junction, the Webster and the Kirk effects, the bandgap narrowing effect and doping and field dependance of the mobility.

6.1 Results

This section presents the results of the developed model that include the majority carrier current density and the recombination process in the base. This will be called the Present Model for the rest of the thesis. The results are compared against the model developed by Hassan *et. al.* [11] where $J_p = 0$ is assumed and the recombination mechanism in the base is neglected. Henceforth, Ref. [11] will be called the Previous Model. All other effects are same in both these models.

In this section, first, the results of both the present and previous models are compared. The effects of the variation of two important parameters (i.e. the peak base doping density and the logarithmic slope of the base doping profile) are also presented and analyzed in this section.

6.1.1 The Present Model vs. The Previous Model [11]

Estimation of the majority carrier density, $J_p(x)$, is a major challenge due to the reasons mentioned in Section (3.2). However, a technique is utilized in the present model to overcome this challenge [Section (4.2)]. Figure (6.1) shows the plot of $J_p(x)$ using this technique, where the base doping density is considered as a parameter. Although the boundary conditions $J_p(0)$ and $J_p(W_B)$ are related to the emitter and collector parameters (doping level and width) respectively, $J_p(W_B)$ is almost unaffected by the collector parameters. This is because $J_p(W_B) \approx 0$ under active-mode operation of an npn BJT. Hence, the plot for $J_p(x)$ is affected both by the emitter doping level, N_E as well as the emitter width, W_E. In this work, a uniform emitter doping profile is assumed. However, the shape of the J_p-plot in the base region is affected by the minority carrier injection level and by the base doping level. The figure shows that the higher is the peak doping level, the lower is the J_p within the base. This is due to the increase in the majority hole current density gradient when $N_A(0)$ increases [Equation (3.29)].

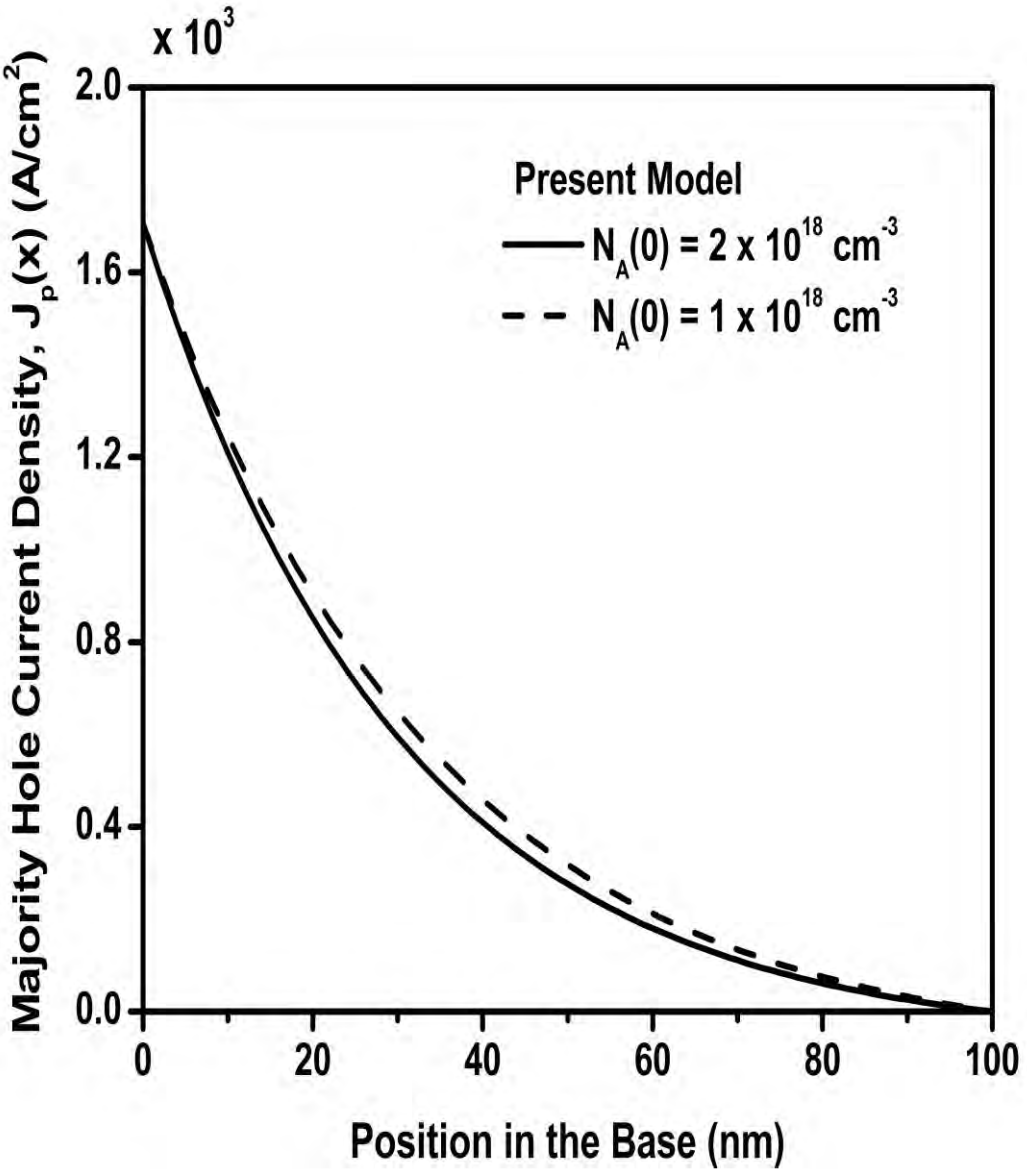

Figure 6.1: Majority Hole Current Density in the base for $N_A(0)=1\times10^{18}cm^{-3}$ and $N_A(0)=2\times10^{18}cm^{-3}$.

In the following subsections, simulation results for the electric field, the minority electron concentration, the minority electron current density, the collector current density and the base transit time are presented. The simulation uses a base width of 100 nm and a base emitter voltage of 0.9 V. Two peak doping densities are considered: $N_A(0)=1\times10^{18}cm^{-3}$ and $N_A(0)=2\times10^{18}cm^{-3}$. In both cases, two values of logarithmic slope of the doping profile is chosen. These are: $\eta=3.00$ and $\eta=3.69$, respectively.

Effects on the Electron Electric Field

The majority carrier current density J_p aids the electric field in the base, as explained in the section (4.3.1). On the other hand, due to the recombination mechanism the minority electron concentration in the base is reduced, which in turn increases the minority carrier concentration gradient, $\frac{dn}{dx}$, thereby increasing the electric field [Equation (3.38)]. Furthermore, the recombination decreases the majority carrier density gradient in the base [Equation (3.29)]. This results in an increase of majority carrier current in the base, which further enhances the electric field in the base [(Equation 3.38)]. Therefore, when both recombination and majority carrier current density are incorporated in the analytical modeling, the electric field is found to be higher than that when one or both or are not considered. Figure (6.2) shows the variation of electron electric field E_n in the base. In this figure, E_n is shown as negative to reflect its actual direction in the base. As expected, the calculated electric field is found to be higher throughout the base region than that obtained using the previous model.

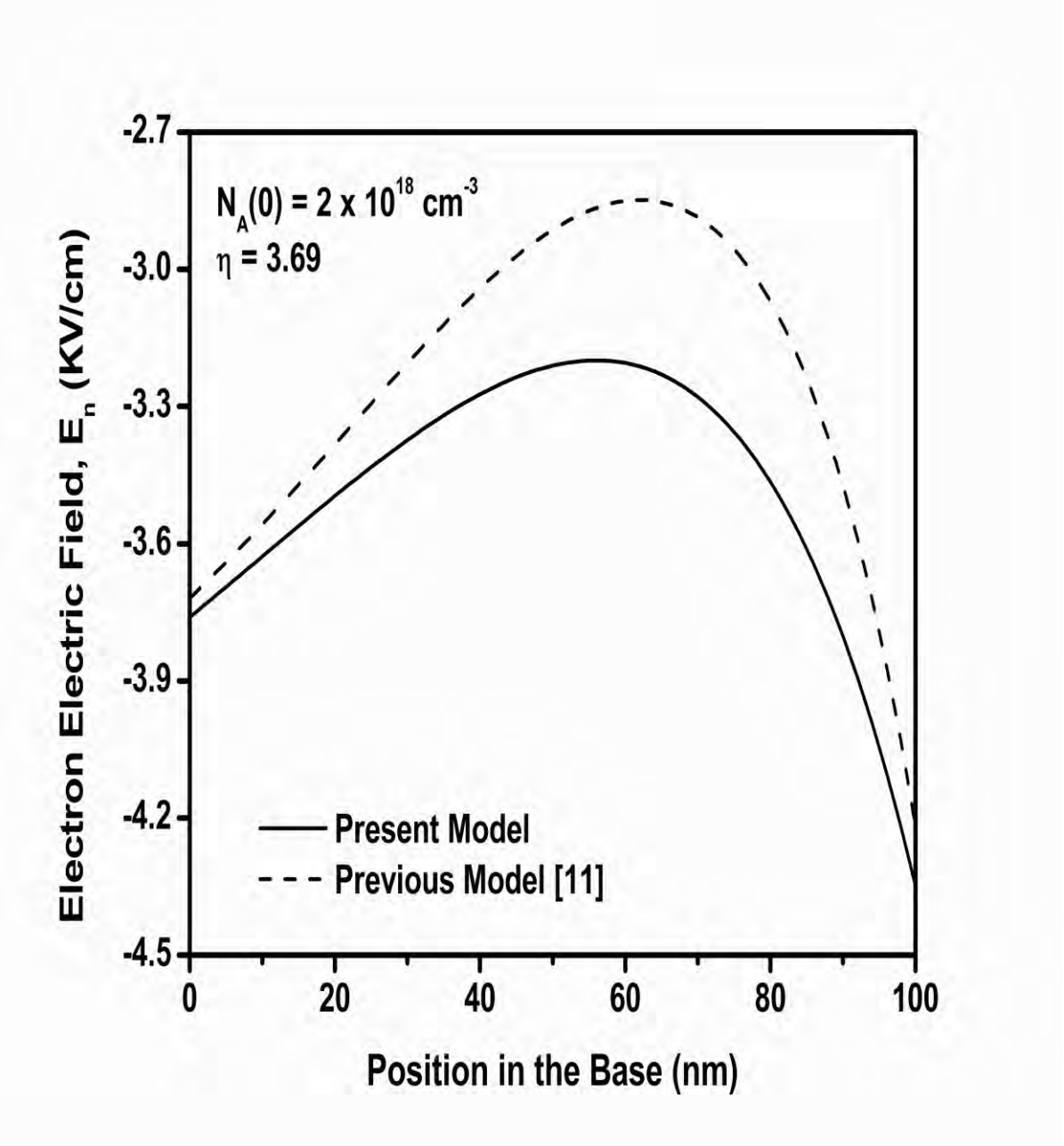

Figure 6.2: Electron Electric Field variation in the base for $N_A(0) = 2 \times 10^{18} cm^{-3}$.

Effects on n(x) and $J_n(x)$

Figures (6.3) and (6.4) show variations of the minority carrier density n(x) and the minority carrier current density $J_n(x)$, respectively. The latter figure displays the absolute value of J_n. Since both J_p and recombination aid the electric field in the base, more electrons are swept to the collector side. This decreases the base stored charge and increases the current. In comparison with the previous model the present model, therefore, shows a lower electron density in Figure (6.3) and a higher electron current density J_n in most of the base region in Figure (6.4).

The Figure (6.4) also shows that J_n decreases near the collector side and becomes lower than the value of J_n of the previous model. The first effect is due to the lowering of the electron mobility due to increased electric field [Equations (3.18a) and (3.18b)] near the collector side as seen in Figure (6.2). The second one is expected since the present model includes the recombination mechanism for which a negative gradient for J_n is used [Equation (3.24a) where J_n is negative for an npn BJT]. The previous model neglects the recombination mechanism in the base.

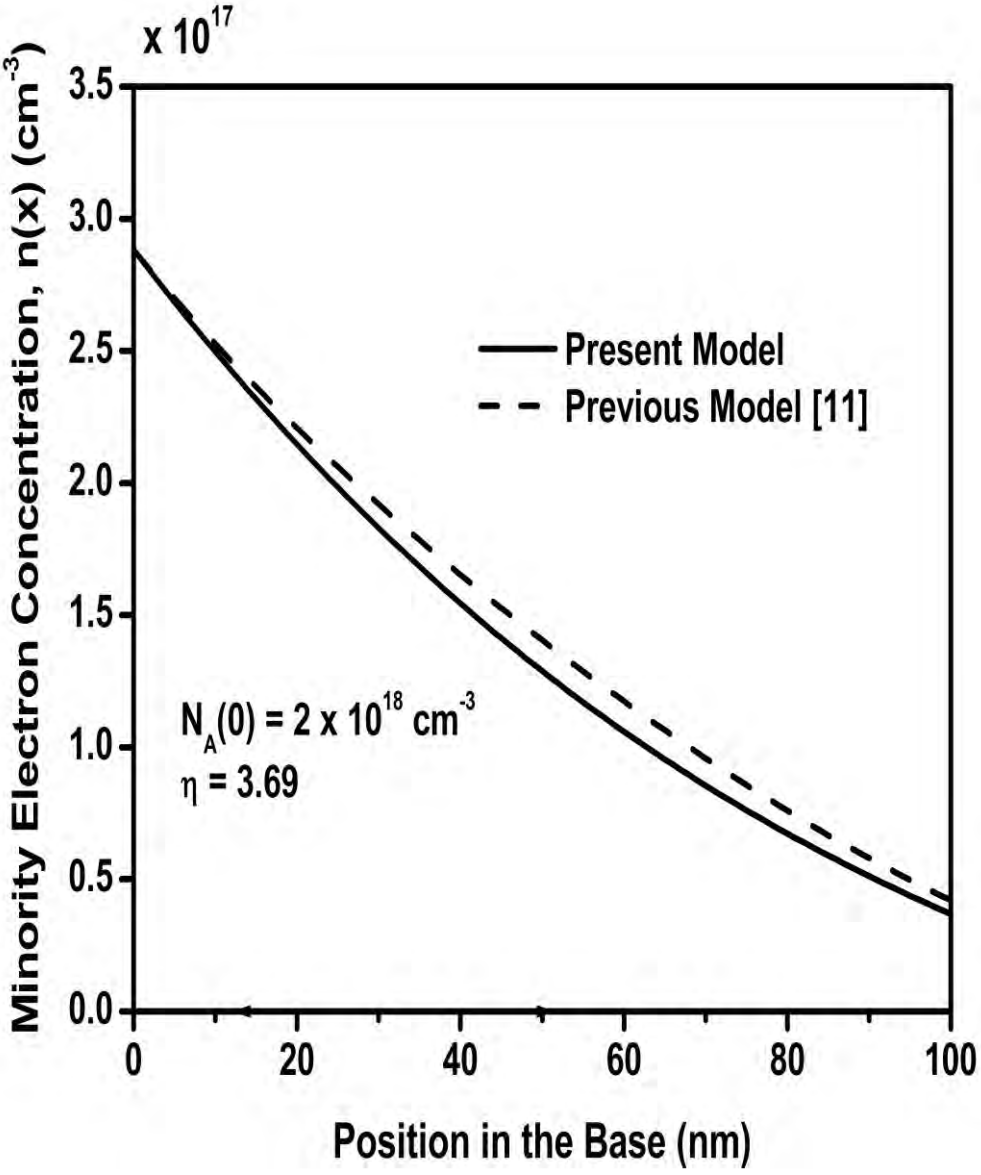

Figure 6.3: Minority Electron Concentration in the base for $N_A(0) = 2\times10^{18} cm^{-3}$

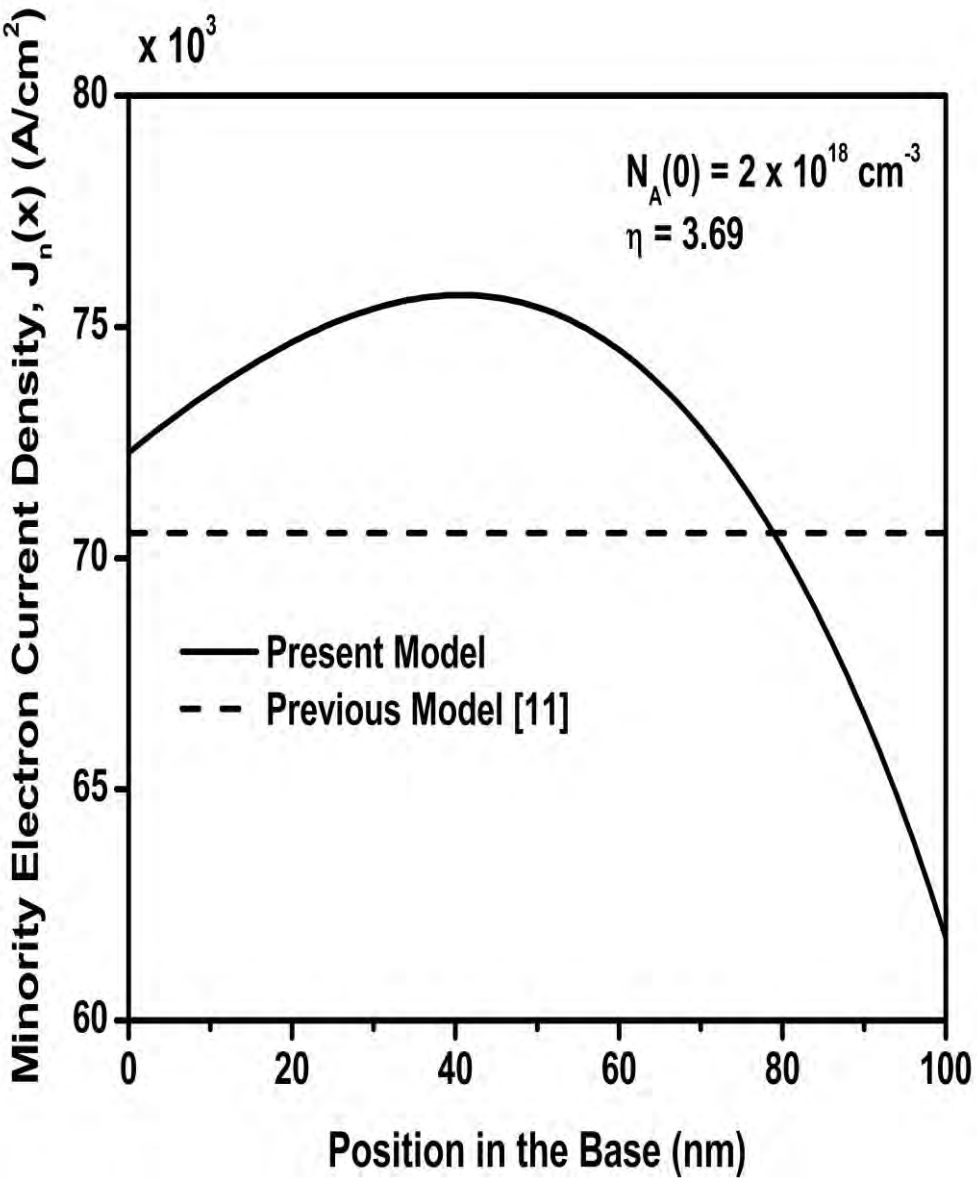

Figure 6.4: Minority Electron Current Density in the base for $N_A(0) = 2 \times 10^{18} cm^{-3}$.

6.1.2 Effects on the Collector Current Density

The collector current density J_C can be expressed as,

$$J_C = J_n(W_B) + J_p(W_B)$$
$$\approx J_n(W_B) \tag{6.1}$$

where,

$$J_n(W_B) = qv_{sn}n(W_B) \tag{6.2}$$

From the above equations it is evident that J_C is directly proportional to $n(W_B)$. On the other hand, using Equations (3.14) and (5.123), it can be inferred that $n(W_B)$ varies exponentially with V_{BE}. Therefore, J_C has an exponential dependence on V_{BE}. This exponential dependence is observed in the Figure (6.5) which plots the collector current density J_c against the variation of base-emitter voltage V_{BE}. These figures also indicate that J_C for the present model is lower than that for the previous model. This is expected since $J_C \approx J_n(W_B)$ and $J_n(x)$ is brought down as one approaches to the collector (as explained in the previous subsection).

The lowering of J_C in the present model compared to the previous model suggests that the emitter efficiency and hence, the current gain for an npn BJT transistor is lower than those of the previous model. In fact, inclusion of both the J_p dependency and the recombination mechanism leads to a decrease in the current gain. Therefore, the previous model overestimates the emitter efficiency and the current gain, since it neglects both the J_p dependency and the recombination mechanism. The lowering tendency of J_n as collector is approached may lead to an erroneous conclusion that J_n will be zero if base-width is increased. But this will not be the case, since $n(W_B)$ is reduced due to recombination (which causes J_n to reduce) and never be zero, as then electron has to cross the B-C junction with infinite velocity.

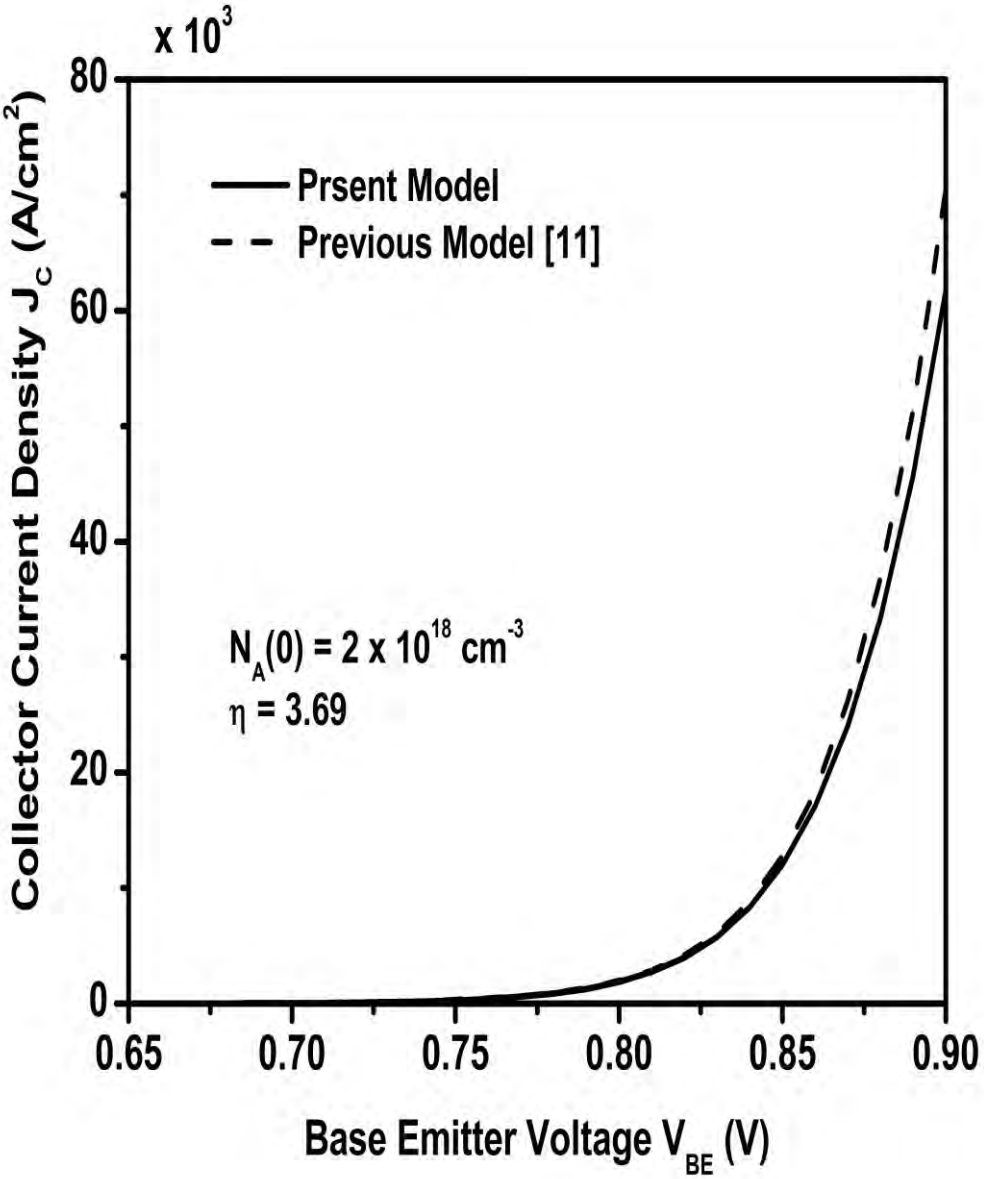

Figure 6.5: Collector Current Density vs. base emitter voltage for $N_A(0)=2\times10^{18}cm^{-3}$.

6.1.3 Effects on the Base Transit Time

For convenience the definition of the base transit time is recalled as,

$$\tau_B = -q\int_0^{W_B} \frac{n(x)}{J_n(x)}\,dx \tag{6.3}$$

For the previous model, J_n becomes position independent and hence, can be taken out of the integral term. Since the present model includes both the J_p dependency and the recombination mechanism, J_n is position dependent and therefore must remain within the integral term of Equation (6.3). Therefore, the lowering of J_n near the collector side for the current model does not lead to an increase of τ_B. Instead, the base transit time τ_B should decrease for the present model since J_n is observed to be higher in most part of the base (except for a narrow region near the collector side)[Figure (6.4)] and n(x) is observed lower throughout the base [Figure (6.3)] due to the aiding electric field. The expected decrease in τ_B is observed in the Figure (6.7).

From the above discussion, the simulation proves that the inclusion of both the J_p and the recombination mechanism decreases both the the collector current density J_C and the base transit time τ_B. The reduction of J_C means a corresponding reduction in the emitter efficiency as well as in the small-signal common base and common emitter current gains. On the other hand, the reduction of τ_B results in a decrease in the total transit time, τ_{ec} and hence, in an increase in the unity-gain-bandwidth frequency, f_T [Equations (1.5) and (1.6)]. This is expected since the gain-bandwidth product is equal to f_T and hence, a decrease in the gain results in a corresponding increase in the bandwidth. Furthermore, the inclusion of both the J_p and the recombination mechanism in the analytical modeling results in more improved gain-bandwidth product than that obtained neglecting those dependencies.

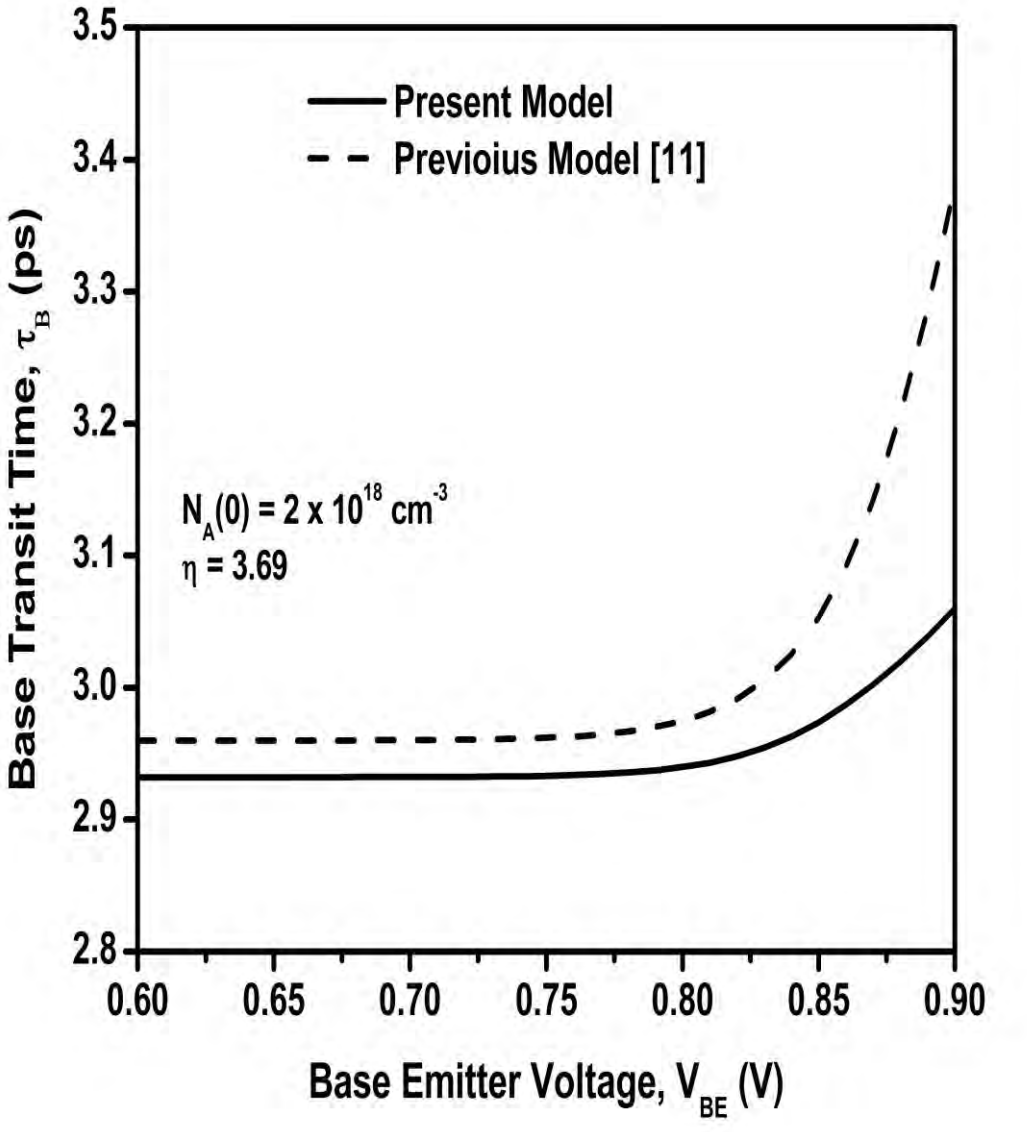

Figure 6.6: Base transit time vs. base emitter voltage for $N_A(0) = 2 \times 10^{18} cm^{-3}$.

6.1.4 Effects Due to the Variation of Peak Base Doping Density, $N_A(0)$

In this subsection, the effects of peak doping density $N_A(0)$ on the base transit time is investigated. For this analysis, the logarithmic slope of the doping profile (η) is kept constant. Therefore increasing $N_A(0)$ results in a corresponding increase in $N_A(W_B)$ to maintain the η constant.

Increased $N_A(0)$ results in more doping concentration in the base and hinders the carrier movement which results in a decrease in the carrier mobility [Equations (3.18a) and (3.18b)]. The electron electric field in the base is dependent on the logarithmic slope of the base doping profile (for exponential doping profile which is defined as η and is affected by the band-gap narrowing effect, the injection level and the majority carrier current density [Section (4.3.1)]. The increased $N_A(0)$ results in a decrease of the injection level and thereby decreasing the retarding field caused by the injection level. Since $J_p(x)$ in the base decreases when $N_A(0)$ increases [Figure (6.1)], it has a lowered aiding effect on the electric field. The electric field can be greatly affected by the base doping gradient η since electric field is proportional to η [Equation (3.38)]. For this case, $N_A(0)$ increases keeping η as constant. Therefore when $N_A(0)$ increases, the increase in the electric field is less dominant over the decrease in the carrier mobility. This causes the minority electron current density $J_n(x)$ to decrease more than the decrease in the minority carrier concentration [when $N_A(0)$ increases, n(x) decreases since $pn \propto n_{ie}^2$ for a fixed bias as seen in the Equation (3.14)]. Thus, when $N_A(0)$ increases while keeping η as constant, the base transit time increases. Figure (6.7) also shows this increase of τ_B. This results are consistent with those shown in Ref. [11].

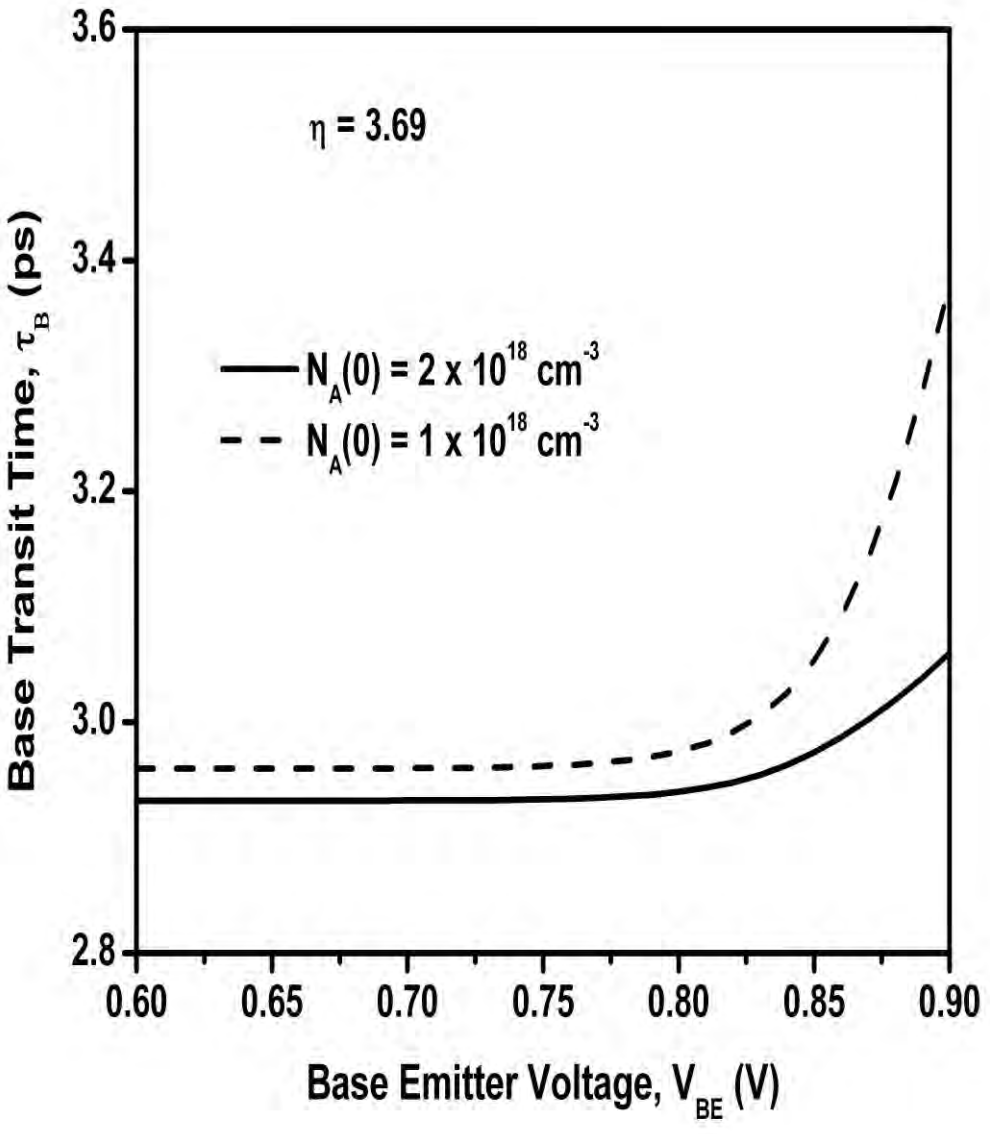

Figure 6.7: Base transit time vs. base emitter voltage for $N_A(0)=1\times10^{18}cm^{-3}$ and $N_A(0)=2\times10^{18}cm^{-3}$. Here η is kept as constant.

6.1.5 Effects Due to the Variation of Logarithmic Slope of the Base Doping Profile, η

The logarithmic slope of the doping profile can be increased by increasing the peak doping density $N_A(0)$ while keeping the $N_A(W_B)$ as constant. From the arguments presented in the previous subsection, it can be inferred that the increase in the electric field for the present case dominates over the decrease in the carrier mobility, since both η and $N_A(0)$ are increased. For this case, the base transit time decreases when $N_A(0)$ increases. This fact is observed in the Figure (6.8). The same is also supported by the Ref. [14].

From the Figure (6.8), it is observed that the base transit time τ_B increases when $N_A(0)$ increases from $N_A(0)=1\times10^{18}cm^{-3}$ to $N_A(0)=2\times10^{18}cm^{-3}$ keeping η as constant ($\eta=3.00$). On the other hand, τ_B decreases if η is increased from 3.00 to 3.69 keeping $N_A(0)$ as constant ($N_A(0)=2\times10^{18}cm^{-3}$). Therefore, both $N_A(0)$ and η must be increased in order to reduce the base transit time.

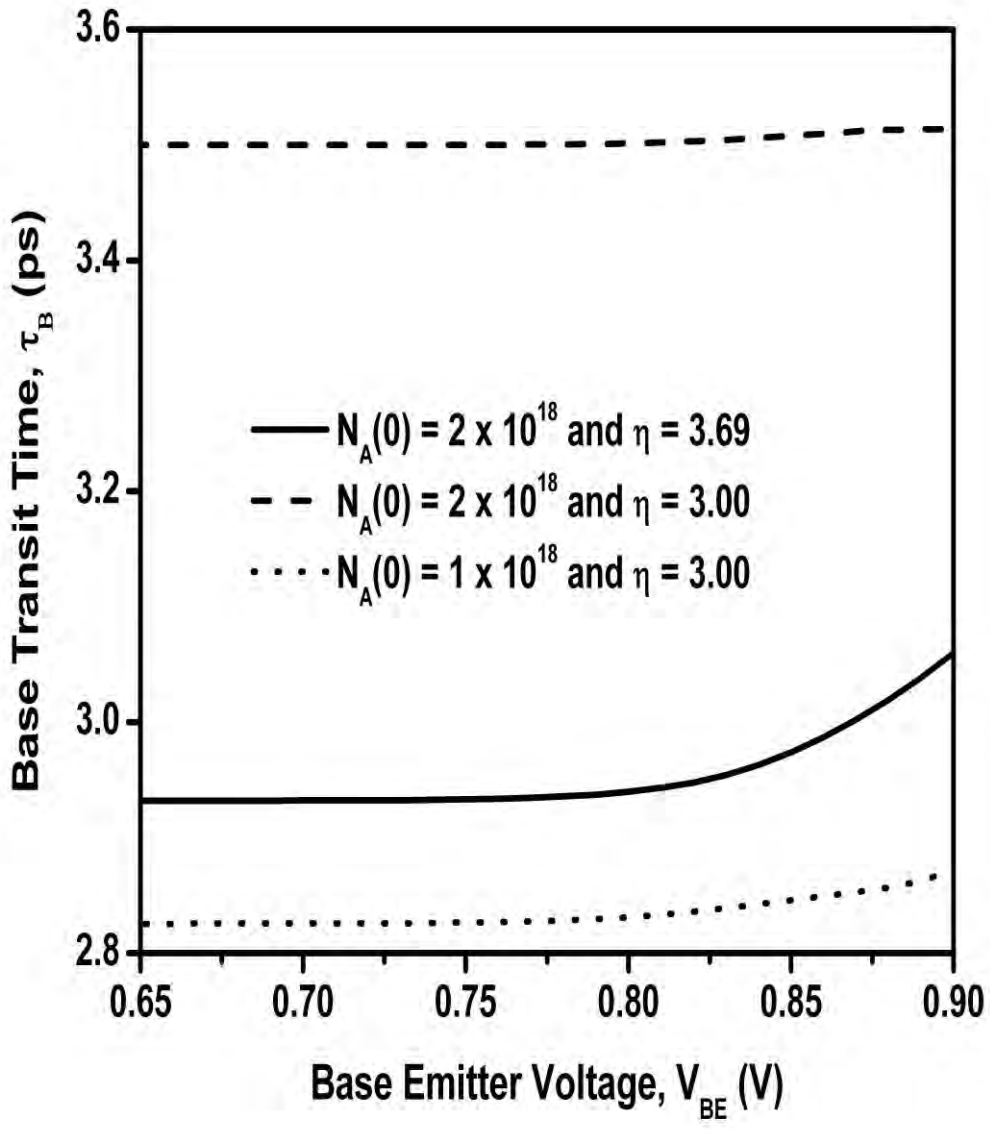

Figure 6.8: Base transit time vs. base emitter voltage for the variation of $N_A(0)$ and η.

6.2 Model Verification

The proposed model in this thesis has been verified by the simulation results and also by an experimental data. The verifications are presented in this section.

6.2.1 Comparison with the Numerical Simulation Results

A numerical simulation was carried out to verify the current model. The procedure for this simulation is detailed in the Appendix (A.2). The approximations that include the application of perturbation theory to overcome the nonlinearity problem, and the approximation for electron diffusivity and the exponential approximation to overcome the mathematical intractability are used in the present model. However, no additional approximations were used while performing this numerical simulation. In this subsection numerically computed results are compared against the results of the present analytical model.

Figures (6.9) and (6.10) show the comparison of the base transit times obtained from the current model and the simulation result for the two values of logarithmic slope of the base doping profile. The Figure (6.9) shows the results for a peak doping concentration of $N_A(0)=2\times10^{18}cm^{-3}$, while the Figure (6.10) shows the results for a peak doping concentration of $N_A(0)=1\times10^{18}cm^{-3}$. Both of these figures show better agreements in the base transit time with the simulation results when η is lower i.e. $\eta=3.00$. However, when η is high and the base doping level is low, the results of the present model deviates from the numerical simulation results to some extent. An error analysis for these plots are also presented in the Figures (6.11) and (6.12) respectively. The error is defined as the percentage deviation in the base transit time τ_B of the present model from that of the numerical simulation as a fraction of τ_B of the numerical simulation i.e.

$$\%\,of\ Error=\frac{\tau_{B,\,numerical\ simulation}-\tau_{B,\,present\ model}}{\tau_{B,\,numerical\ simulation}}\times100\% \tag{6.4}$$

For the peak doping level of $N_A(0)=2\times10^{18}cm^{-3}$ with $\eta=3.69$, the highest error is found as $\approx 2.8\%$. Even this error is within the limit of 3% and is found for a narrow range of bias levels ($0.86-0.9$ V). For other cases, the error is within a limit of $\pm 2\%$. Therefore, the approximations made in developing the present model are well justified.

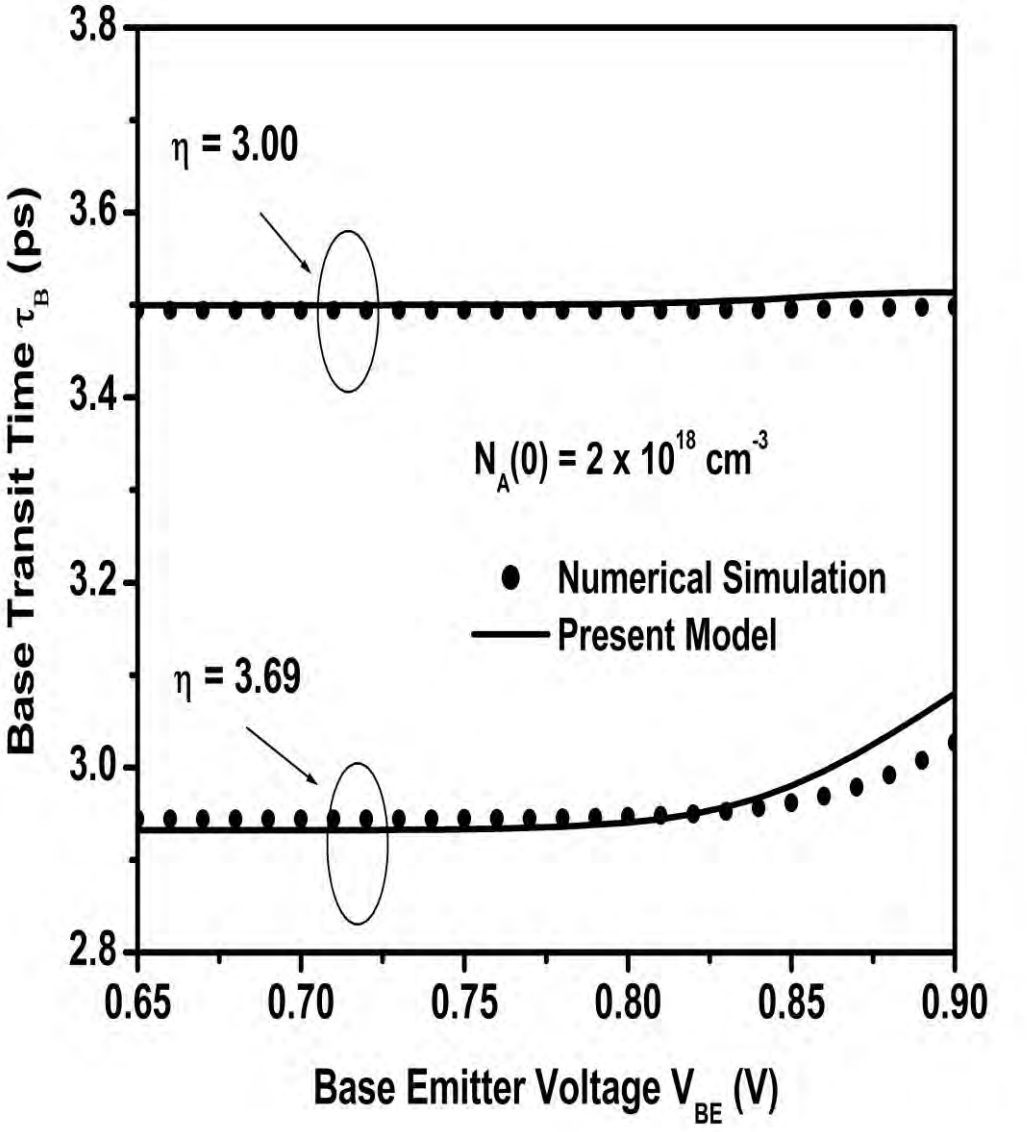

Figure 6.9: Base transit time vs. base emitter voltage for the current model and for the numerical simulation for $N_A(0) = 2\times10^{18} cm^{-3}$.

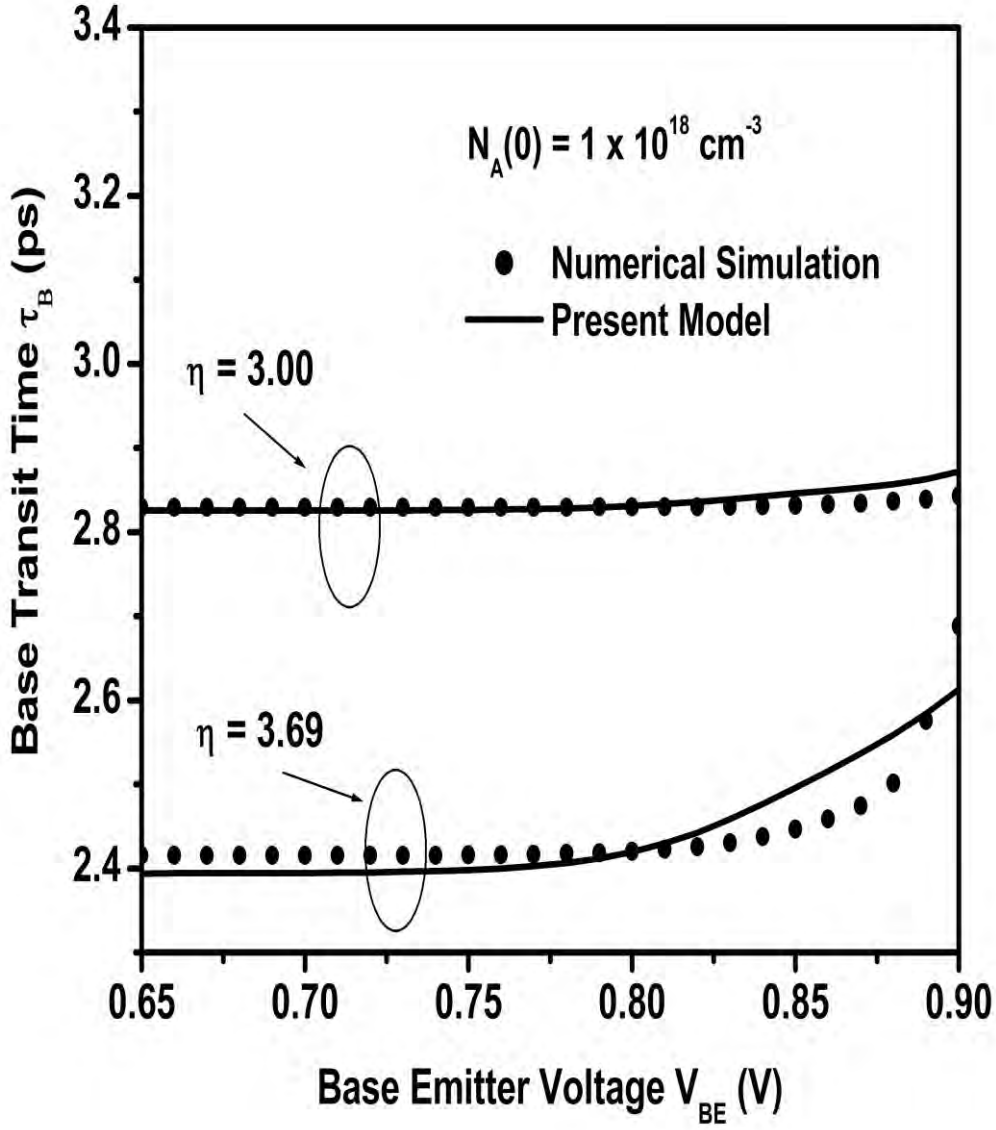

Figure 6.10: Base transit time vs. base emitter voltage for the current model and for the numerical simulation for $N_A(0)=1\times10^{18}cm^{-3}$.

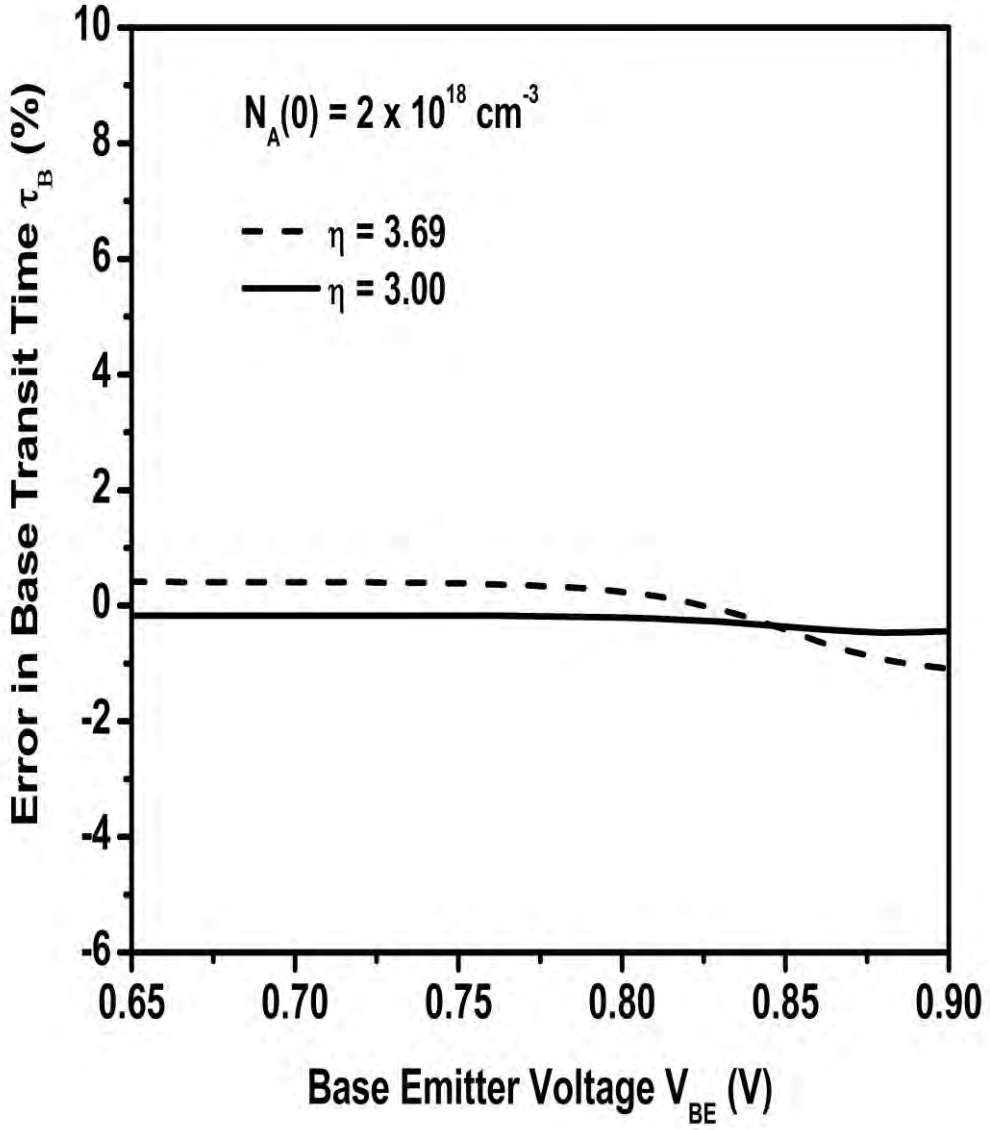

Figure 6.11: Relative error in the base transit time compared against the simulation. Here $N_A(0) = 2 \times 10^{18} cm^{-3}$.

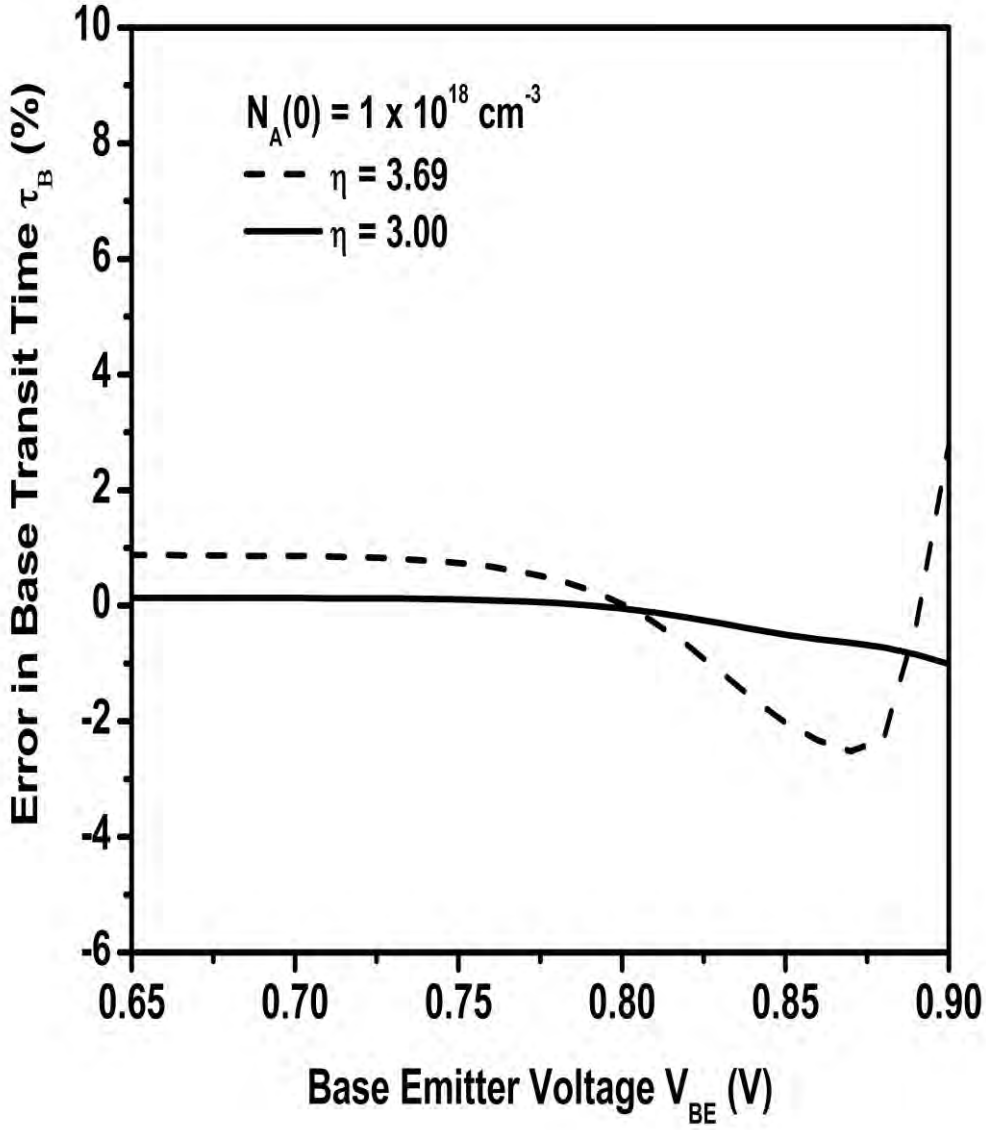

Figure 6.12: Relative error in the base transit time compared against the simulation. Here $N_A(0)=1\times10^{18}cm^{-3}$.

6.2.2 Experimental Verification

The present model proposed in this work is verified against two experimental setups. The first setup was done by H. St*ü* bing and H. M. Rein [58, 59] is used and the second one by T. Fuse [60].

First Experimental Setup

The doping profile used in the first setup [58, 59] is shown in Figure (6.13). The physical parameters for this experimental setup are listed in the Table (6.1).

Parameter	Feature Size
W_E	$0.24\mu m$
W_B	$0.26\mu m$
W_C	$0.50\mu m$
E-B Area	$50\mu m^2$
N_{B0}	$4.8\times10^{17}\ cm^{-3}$
N_C	$1.0\times10^{16}\ cm^{-3}$
N_E	$2.0\times10^{20}\ cm^{-3}$

Table 6.1: Physical parameters for the experimental setup carried out in Ref. [58, 59]

Figure (6.14) shows the experimental data obtained from Reference [59] to validate the proposed model. This figure also presents the results of the previous model [11]. From this figure it is evident that the proposed model agrees with the experimental data in the most part except for a narrow region of $0.70 < V_{BE} < 0.75$ V. The discrepancy observed in the low-injection region can be attributed to the approximations made for low-injection modeling. However, as injection level increases the present model matches more closely with the experimental data. It is also observed that the results for the current model is in better agreement with the experimental data when compared with those of the the previous model.

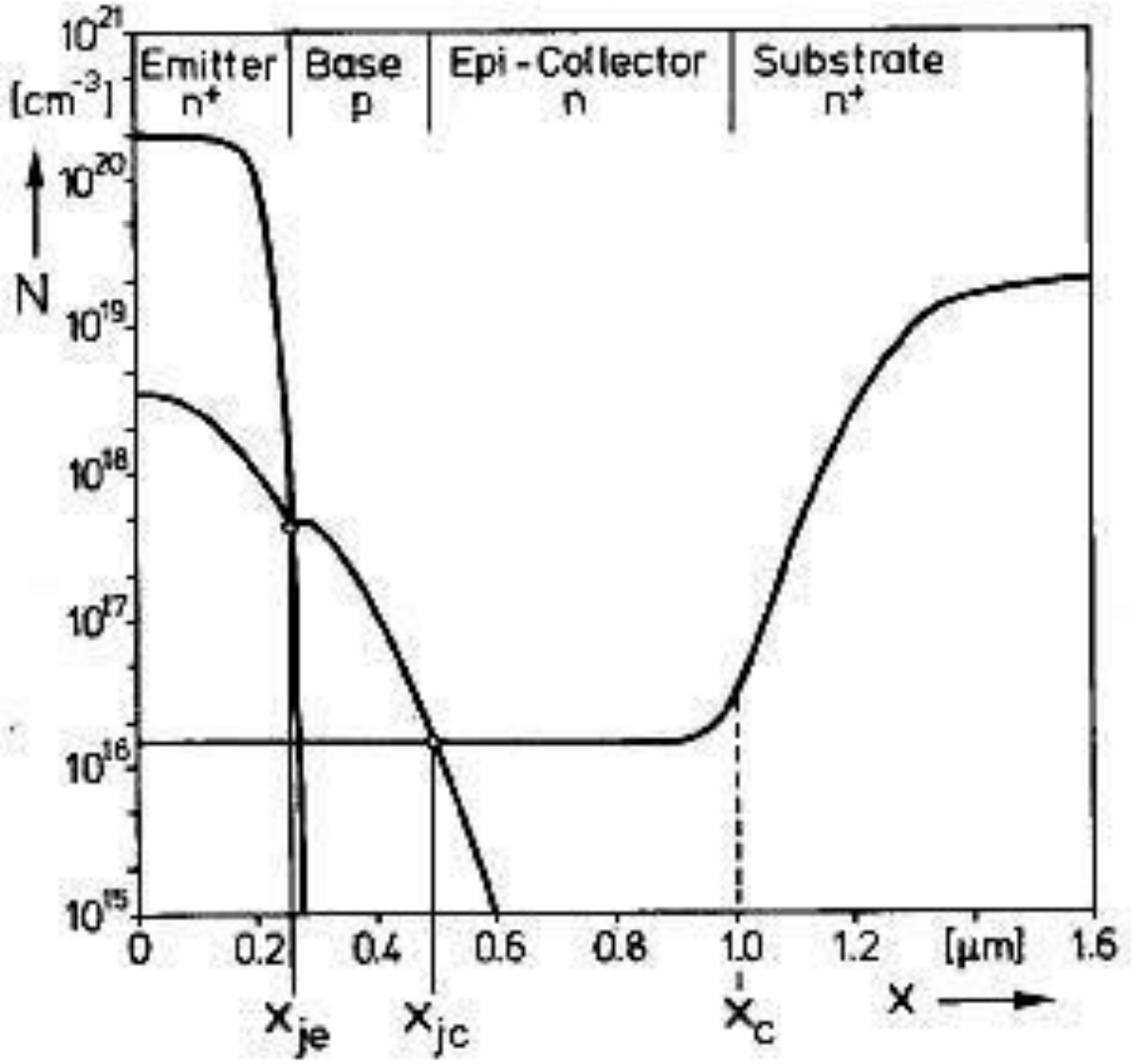

Figure 6.13: Profile of the Doping Concentration used in the Experiment done in [58, 59].

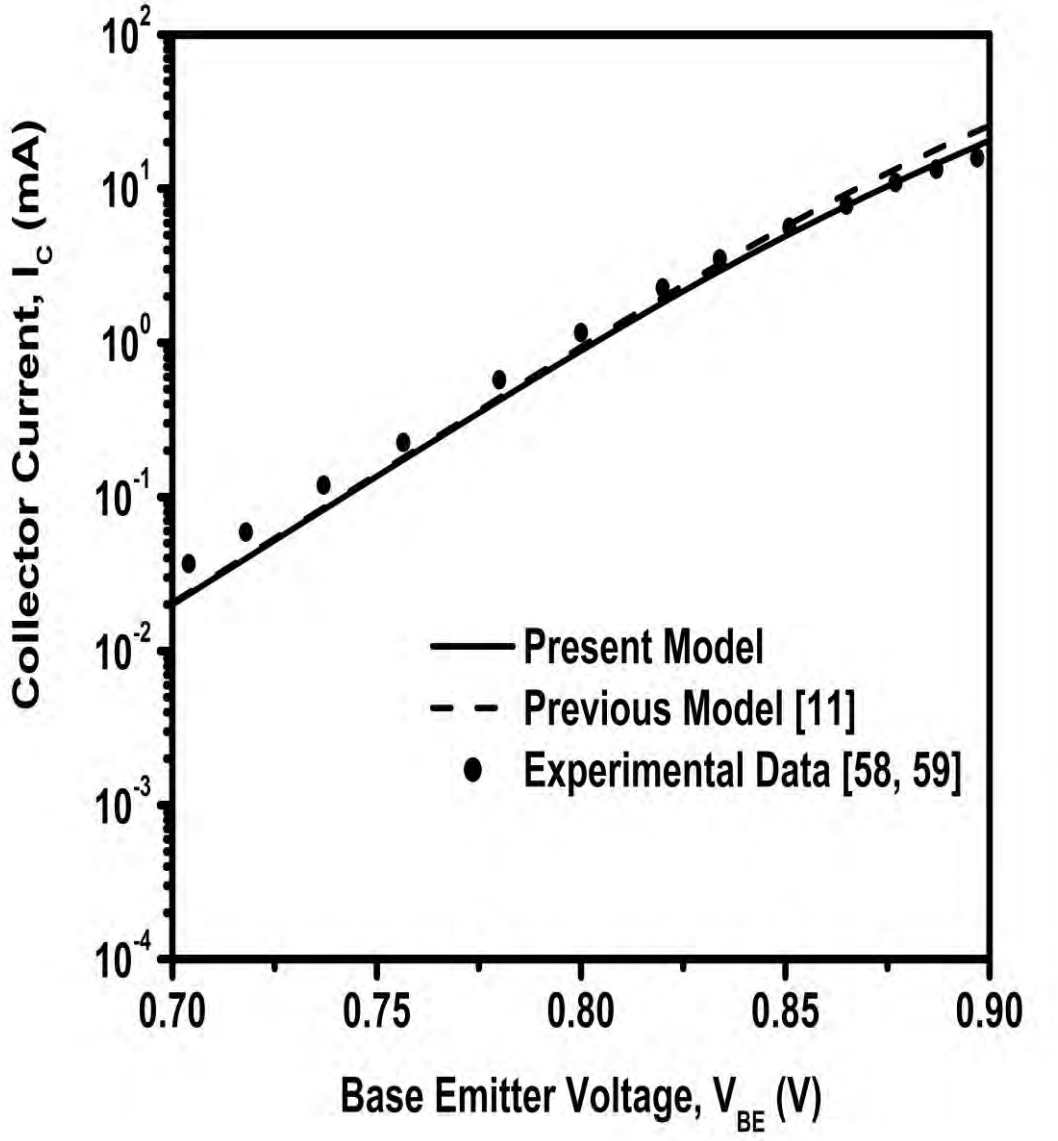

Figure 6.14: Collector current vs. Base Emitter Voltage. The plot compares the data for the current model with the Experimental data from Ref. [59]. The figure also shows the data for the previous model [11].

Second Experimental Setup

In this setup [60], the emitter-to-collector transit time (τ_{ec}) was calculated from the measured cutoff frequency (f_T) using the following definition:

$$\tau_{ec} = \frac{1}{2\pi f_T} \tag{6.5}$$

The model [60] was developed by considering the base pushout in the presence of velocity overshoot and also, the emitter current-crowding and carrier-spreading effects. The model defined τ_{ec} as a sum of four different components, namely

1. Base-emitter junction capacitance charging time, τ_{BE}
2. Base transit time, τ_B
3. Epi-collector space-charge region transit time, τ_{SCR}
4. Base-collector junction capacitance charging time, τ_{BC}

and, which can be expressed as,

$$\tau_{ec} = \tau_{BE} + \tau_B + \tau_{SCR} + \tau_{BC} \tag{6.6a}$$

$$\tau_{BE} = \frac{V_T}{I_E} C_{jE} \tag{6.6b}$$

$$\tau_B = f_{BM}\tau_F \tag{6.6c}$$

$$\tau_{SCR} = \frac{W_C - \Delta W_C}{v} \tag{6.6d}$$

$$\tau_{BC} = R_C C_{jC} \tag{6.6e}$$

where, C_{jE}, R_C and C_{jC} are the base-emitter junction capacitance, buried collector resistance and base-collector junction capacitance, respectively. f_{BM} represents the two-dimensional base pushout factor, τ_F is the low-current forward-base transit time and $W_C - \Delta W_C$ is the epi-collector space charge region width due to base pushout. The velocity v

is the maximum overshoot velocity and is corrected later by Liou [61] as,

$$v = 2v_{max} \tag{6.7}$$

where, $v_{max} = 1.1\times10^{7}\ cm/s$. The related physical parameters for this setup are listed in the Table (6.2).

Parameter	Feature Size
W_E	$0.03\mu m$
W_B	$0.17\mu m$
W_C	$0.80\mu m$
E-B Area	$7.5\mu m^2$
B-C Area	$7.5\mu m^2$
N_{B0}	$2.1\times10^{18}\ cm^{-3}$
N_C	$1.0\times10^{16}\ cm^{-3}$
N_E	$2.1\times10^{20}\ cm^{-3}$
C_{jE}	$10.0(fF)$
C_{jC}	$13.0(fF)$
R_C	$30.0(\Omega)$

Table 6.2: Physical parameters for the experimental setup carried out in Ref. [60]

Figure (6.15) shows the experimental data obtained from Reference [60] as well as the results of the the present model. From this figure it is evident that the proposed model closely matches with the experimental data in almost all collector-current densities except for a region where base push-out condition commences. This slight deviation is due to the fact that the proposed model did not critically consider the effects of the emitter current crowding and the collector current-spreading. However, this result is consistent with the results of the model developed in Ref. [61].

In the present model recombination in the base is considered which results in position dependent J_n in the base. Therefore, τ_{BE} can be calculated from $I_E = J_n(0)A_{BE}$ instead of

$I_E \approx I_C = J_n(W_B)A_{BE}$, where, A_{BE} is the base-emitter area. A better result may be obtained if the I_E can be calculated from the emitter current modelling.

From the verifications of the present model with the above-mentioned experimental setups, it is proved that the majority carrier current density which is enhanced by the recombination mechanism should not be neglected in the analytical modelling of the base transit time.

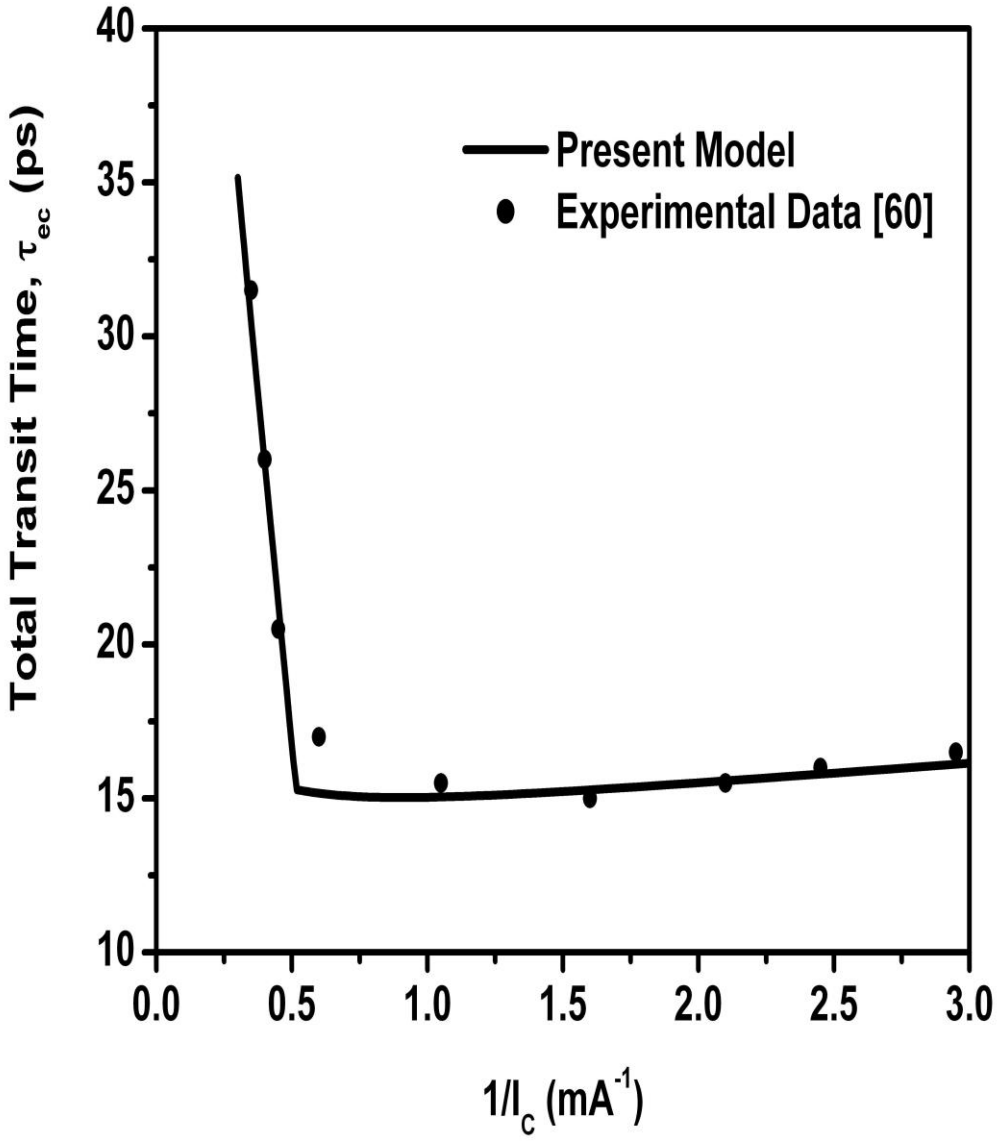

Figure 6.15: Comparison of emitter-to-collector transit time τ_{ec} for the present model and the Experimental data from Ref. [60].

Investigation of Further Effects

In the previous sections the proposed model has been compared against a model developed in [11]. In this section the proposed model is compared against the J_p-only model and the recombination-only model to investigate the separate effects of J_p and the recombination mechanisms. Effects of emitter doping profile and the base doping level are also observed and analyzed in this section.

6.2.3 Separate Effects of J_p and Recombination

This section presents the effects of J_p and recombination on the transit times and high frequency parameters of BJT along with that on electric fields, energy band and currents.

Effects on the Electric Field and on the Energy Band

In the previous section, it has been mentioned that J_p has an aiding effect on the electron electric field, E_n. The recombination mechanism has also aiding effect on E_n, since recombination causes an increase in the carrier density gradient. Therefore, for the model that considers only J_p, only recombination mechanisms or both J_p and recombination, an increase in E_n is expected over the model that does not consider any of these factors. The expected increase is observed in Figure (6.16) compared with that of the previous model.

Since gradient of potential i.e. energy represents the existance of an electric field and the quasi-neutral base region has electric fields due to non-uniform doping profile and also due to the carrier-density gradient, the energy band diagram must have a gradient in the quasi-neutral base. This gradient in the energy band is observed in Figure (6.17) for all four models. The depletion layer for base-emitter junction is entirely due to base doping, since emitter doping is almost of two-order higher magnitude. Moreover, this length is excluded

from the base width since the length is negligible when compared with the base width. The figure also shows that the band diagram is almost identical for all the four models. This is due to the fact that the change in energy band is negligible when compared to the total band diagram of the transistor. The change are evident if the band diagram is zoomed to the base region only. A closer view for the base region plotted in Figure (6.18) reveals that the higher the electric field the higher the gradient in the energy band. Therefore, the most bending is observed in the recombination-only model whereas the least bending is found for the previous model.

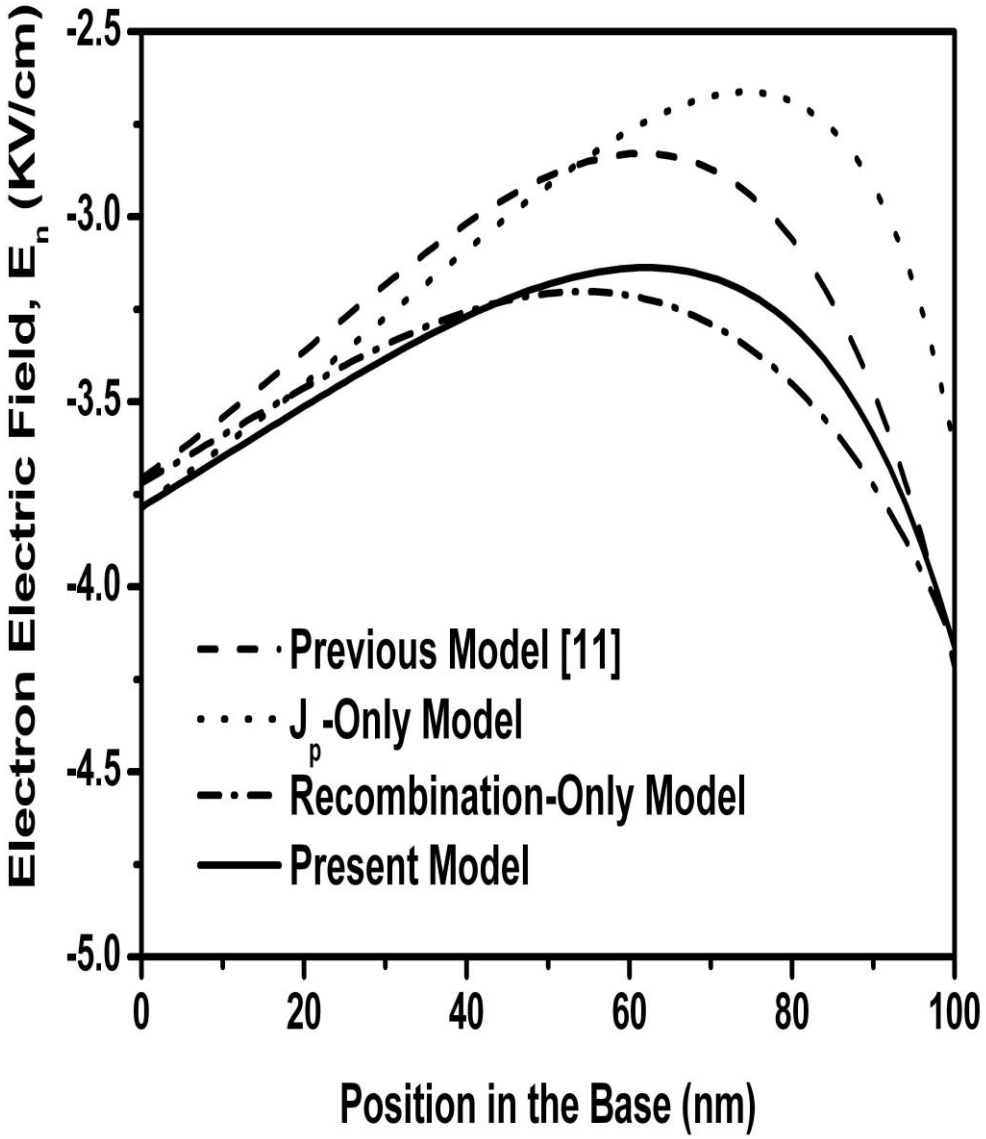

Figure 6.16: Comparison of electron electric field $E_n(x)$ for the present model, previous model [11], J_p-only model and recombination-only model. In this figure, $N_A(0) = 2\times10^{18}\ cm^{-3}$, $\eta = 3.69$ and $V_{BE} = 0.9V$. Uniform emitter doping profile is assumed.

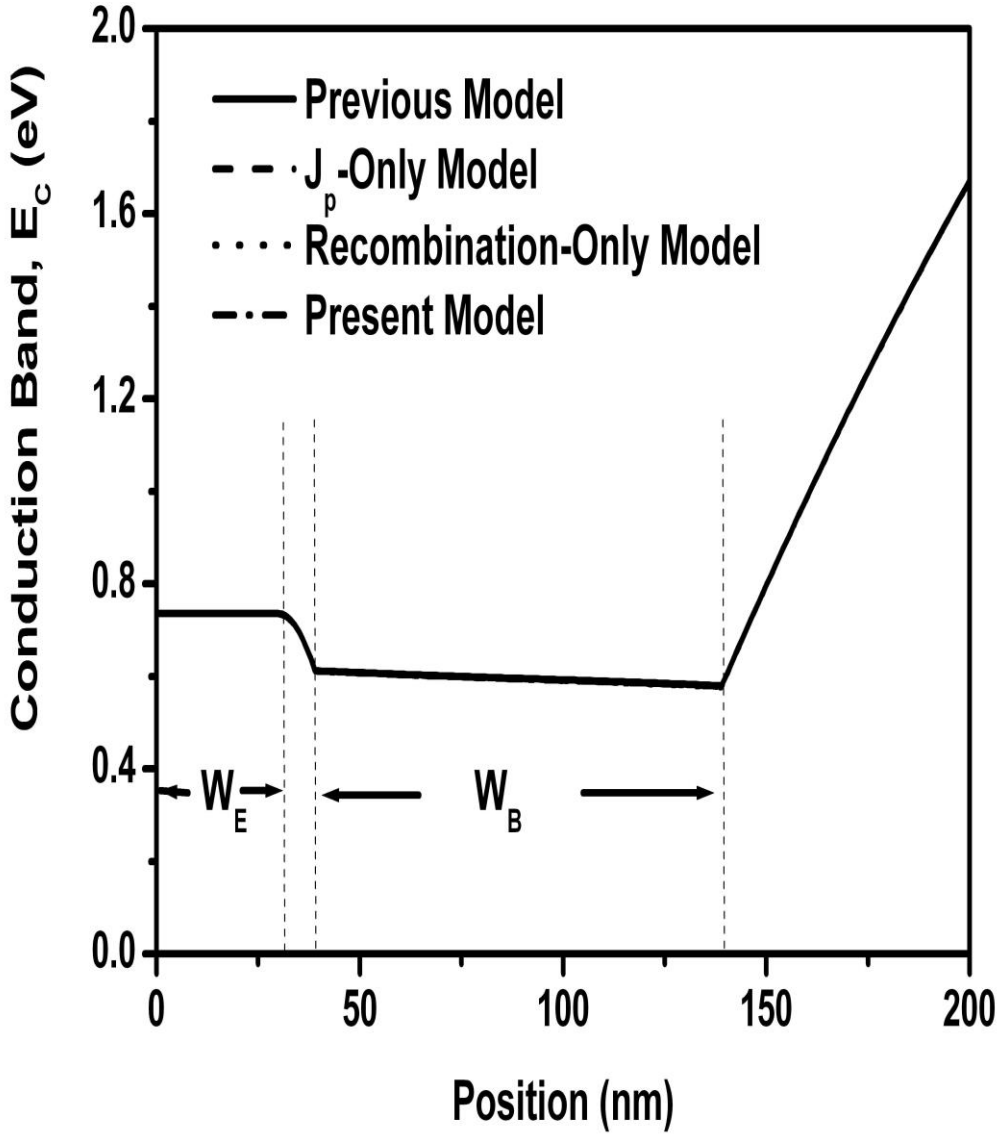

Figure 6.17: Comparison of energy band diagram for conduction band E_C for the present model, previous model [11], J_p-only model and recombination-only model. In this figure, $N_A(0) = 2\times10^{18}\ cm^{-3}$, $\eta = 3.69$ and $V_{BE} = 0.9V$. Uniform emitter doping profile is assumed.

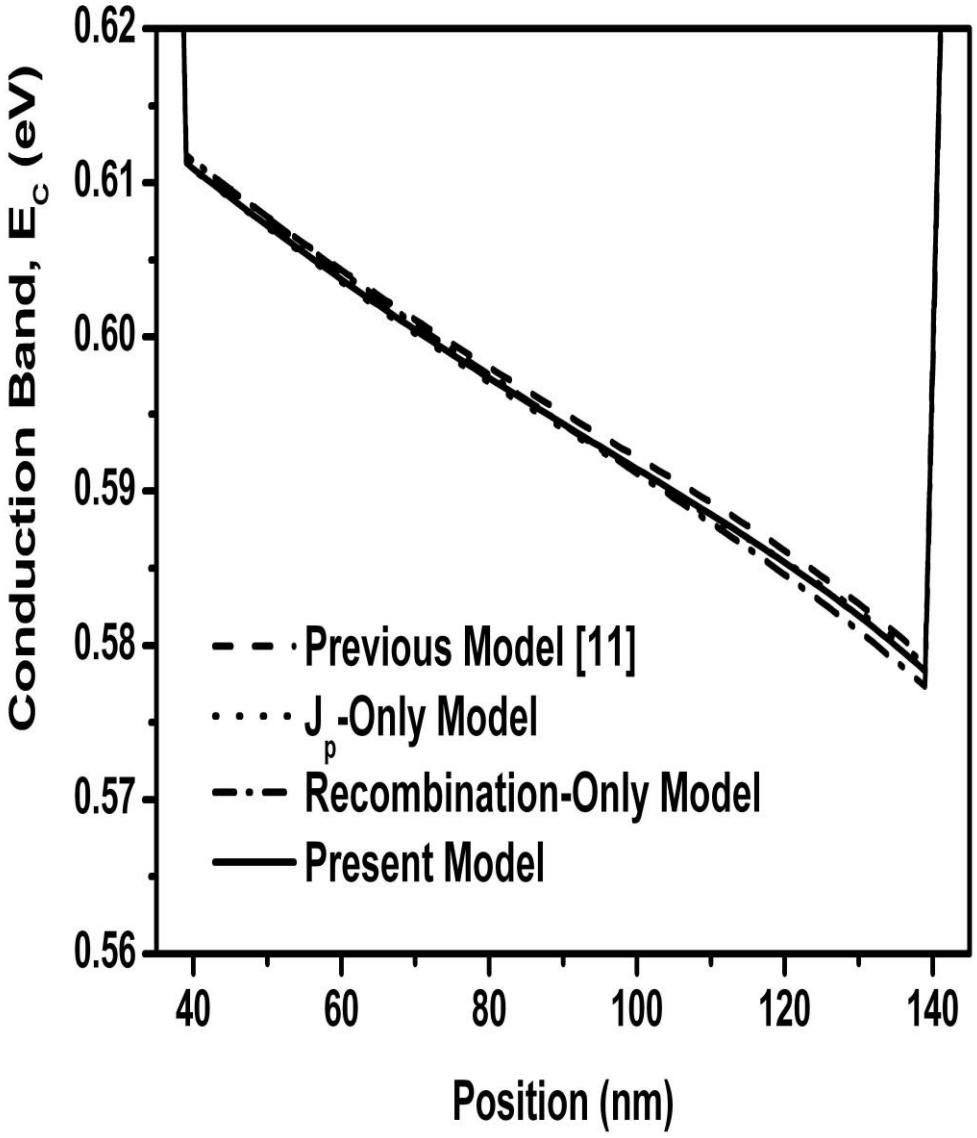

Figure 6.18: Comparison of energy band diagram for conduction band E_C in the base region for the present model, previous model [11], J_p-only model and recombination-only model. In this figure, $N_A(0) = 2\times10^{18}\ cm^{-3}$, $\eta = 3.69$ and $V_{BE} = 0.9V$. Uniform emitter doping profile is assumed.

Effects on the Emitter and Collector Currents

Emitter current I_E is the sum of the currents, J_n and J_p at $x = 0$. For a given doping level, this current increases when electric field at $x = 0$ i.e. $E_n(0)$ increases. Since, at $x = 0$, J_p is maximum and recombination is zero, E_n at this position is seen higher for J_p-only model and the present model, whereas, E_n is lower for recombination-only model and the previous model [Figure (6.16)]. Therefore, higher I_E is observed in Figure (6.19) for J_p-only model and the present model than the other models.

On the other hand, collector current I_C decreases due to recombination mechanism, since recombination is the highest at $x = W_B$. Due to recombination, a lower I_C is, therefore, observed in Figure (6.20) for the recombination-only model and the present model compared to the other models. Again, as one moves to the collector, a higher mobility is expected due to reduction of doping level. Lowering of electric field E_n at $x = W_B$ further increases the mobility. Therefore, increase in the mobility overwhelms the reduction of E_n and increases I_C. These facts justify the observed results shown in Figure (6.20).

Since, recombination mechanisms are neglected for the J_p-only model and the previous model, common-base current gain α is unity and hence, the common-emitter current gain $h_{fe}\ or\ \beta$ approaches infinity ($\beta = \frac{\alpha}{1-\alpha}$). Therefore, h_{fe} for these two models cannot be derived and hence, not be plotted in Figure (6.21). However, h_{fe} can be defined as the ratio of I_C and the base current, I_B. Due to lateral injection through the base, the divergence of majority hole current density is defined as [Equation (3.29)]

$$\frac{dJ_p}{dx} = -qR_x n + qgp(x) \tag{6.8}$$

where the second term of the right hand side represents the divergence due to the lateral injection through the base. Therefore, the total lateral injection current can be defined as the base current I_B and can be given as,

$$I_B = A_{base} \times -qg\int_0^{W_B} p(x)dx \tag{6.9}$$

According to this definition, the base current increases when either the generation rate 'g' or the stored base charge given by

$$Q_B = q\int_0^{W_B} n(x)dx \tag{6.10}$$

or both increases. When recombination mechanisms are considered, both 'g' and Q_B and henceforth, I_B decreases. The expected increase in $h_f e$ for the present model is, therefore, observed in the Figure (6.21). Since recombination mechanisms becomes significant as injection level increases, the increase of h_{fe} for the present model over the J_p-only model is observed under high-bias condition.

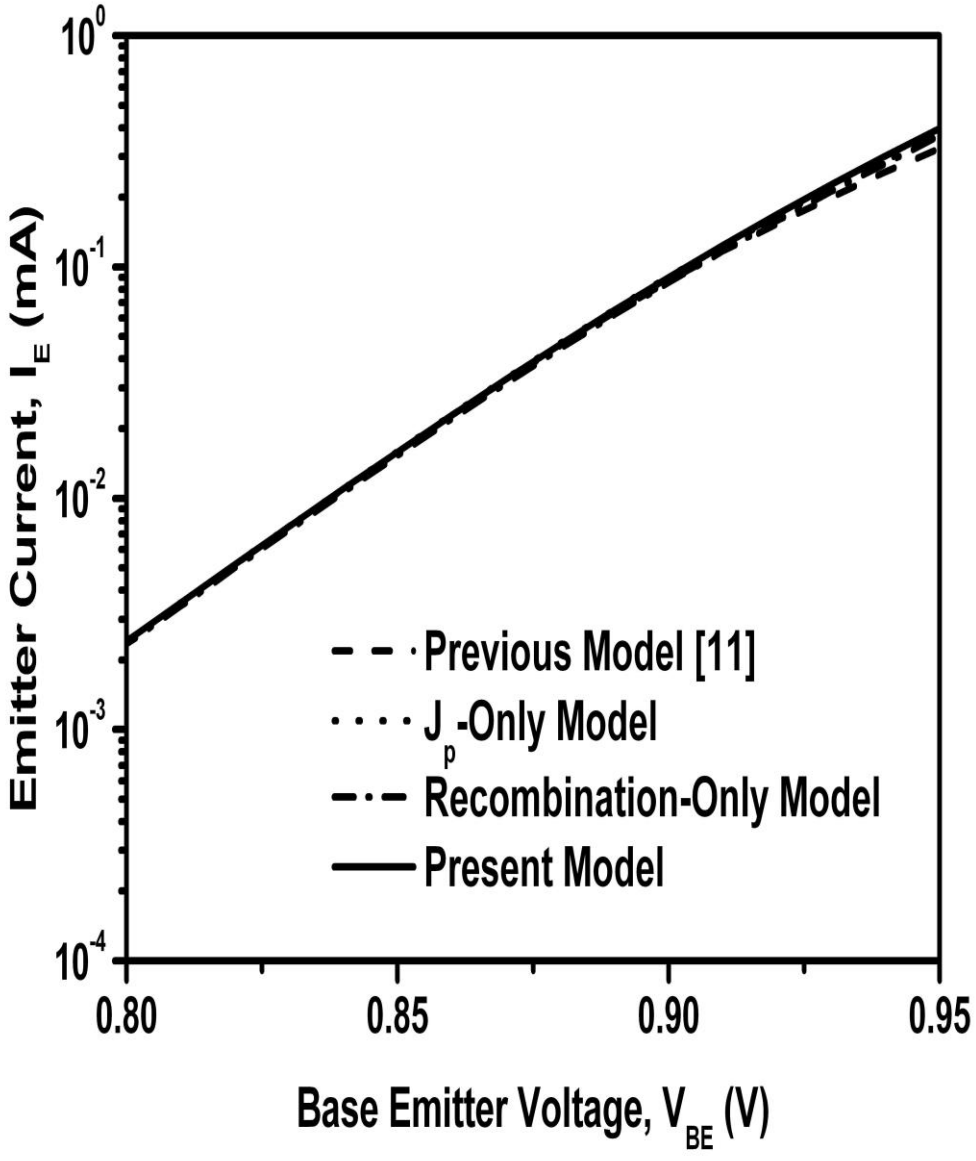

Figure 6.19: Comparison of emitter current I_E for the present model, previous model [11], J_p-only model and recombination-only model. In this figure, $N_A(0) = 2\times10^{18}\ cm^{-3}$, $\eta = 3.69$ and $V_{BE} = 0.9V$. Uniform emitter doping profile is assumed.

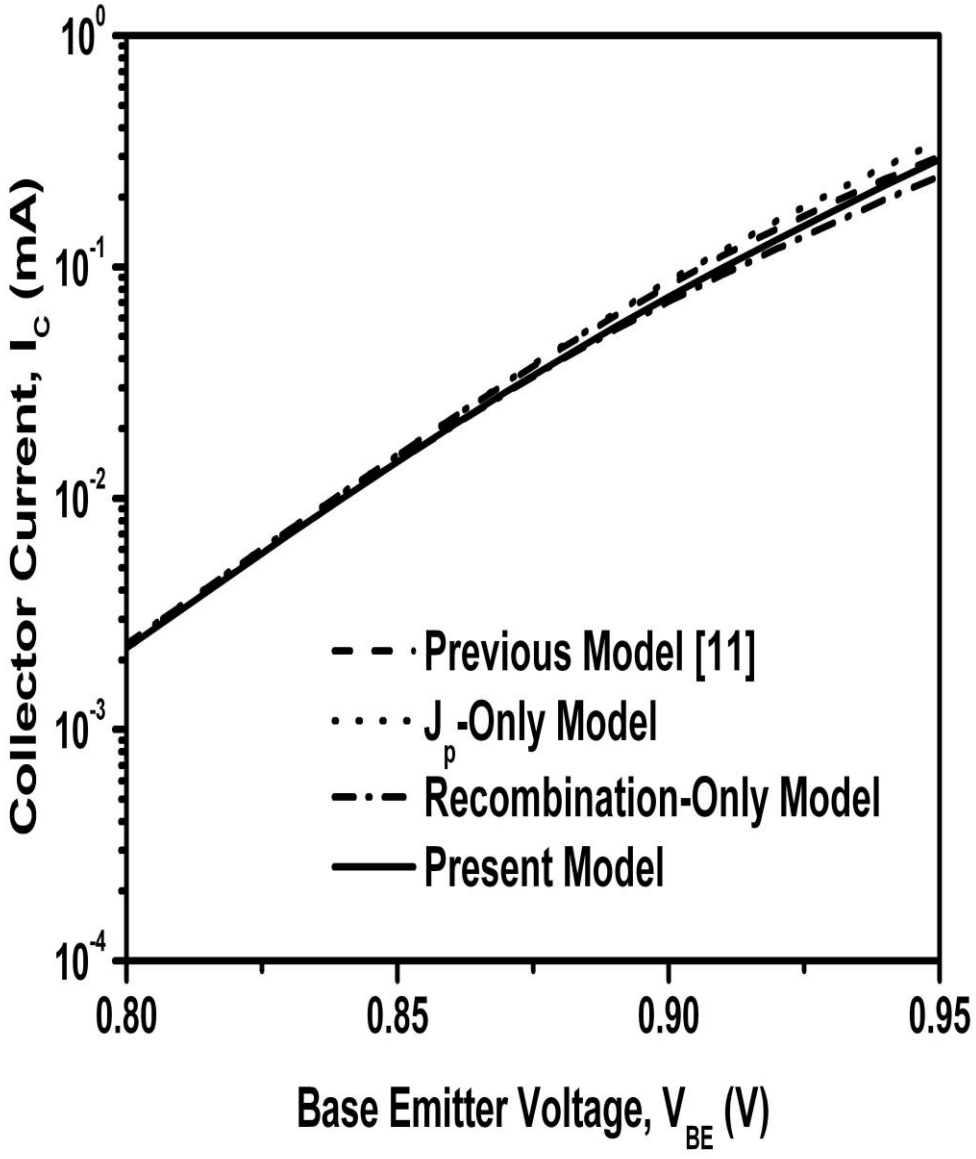

Figure 6.20: Comparison of collector current I_C for the present model, previous model [11], J_p-only model and recombination-only model. In this figure, $N_A(0) = 2\times10^{18}\ cm^{-3}$, $\eta = 3.69$ and $V_{BE} = 0.9V$. Uniform emitter doping profile is assumed.

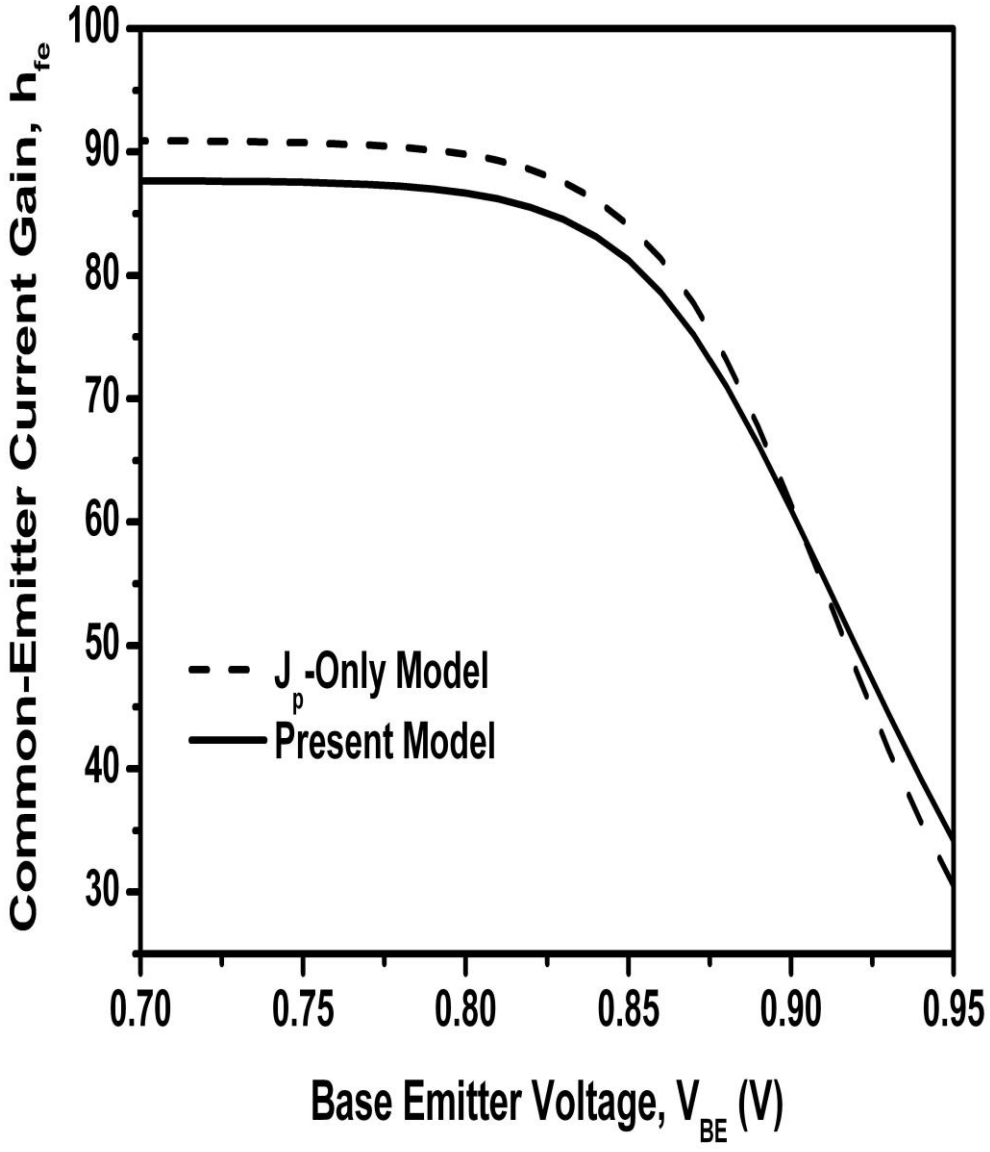

Figure 6.21: Comparison of common-emitter current gain h_{fe} for the present model and the J_p-only model. In this figure, $N_A(0) = 2\times10^{18}\ cm^{-3}$, $\eta = 3.69$ and $V_{BE} = 0.9V$. Uniform emitter doping profile is assumed.

Effects on the Transit Times

Base transit time τ_B increases when the electric field E_n decreases. Since E_n is the highest for the recombination-only model and lowest for the previous model [Figure (6.16)], the lowest and the highest τ_B are expected for these models, respectively. Figure (6.22) also supports this expectation.

Total transit time τ_{ec} mainly depends on the emitter transit time τ_E and the base transit time τ_B. τ_E is dominant under low-bias condition and increases with decreasing I_E, whereas, τ_B is prominent under high bias condition and increases with decreasing I_C. Since both I_E and I_C are lower for recombination-only model and the previous model than for the J_p-only model and the present model, tau_{ec} is found higher for the former models under all bias conditions. This fact is shown in Figure (6.23).

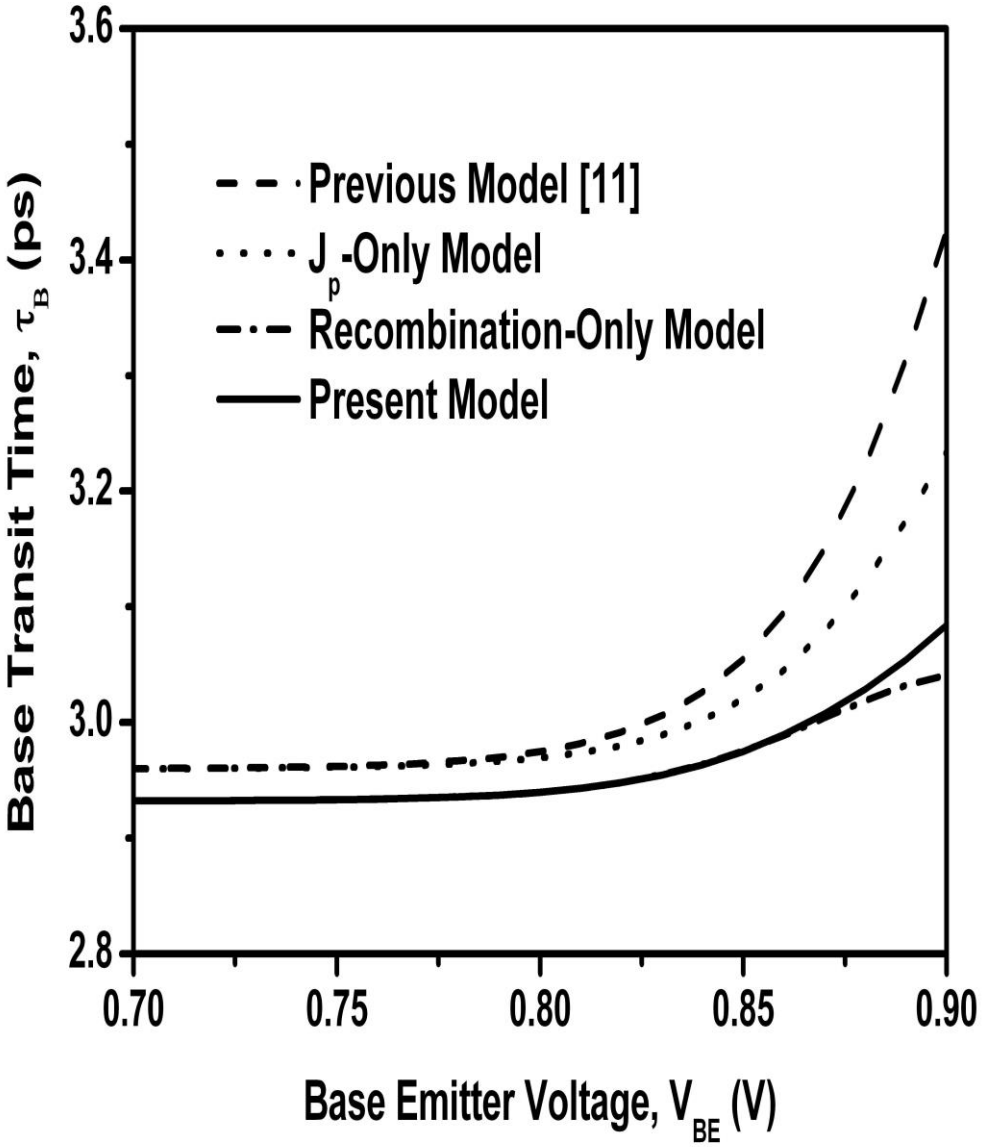

Figure 6.22: Comparison of base transit time τ_B for the present model, previous model [11], J_p-only model and recombination-only model. In this figure, $N_A(0) = 2\times10^{18}\ cm^{-3}$, $\eta = 3.69$ and $V_{BE} = 0.9V$. Uniform emitter doping profile is assumed.

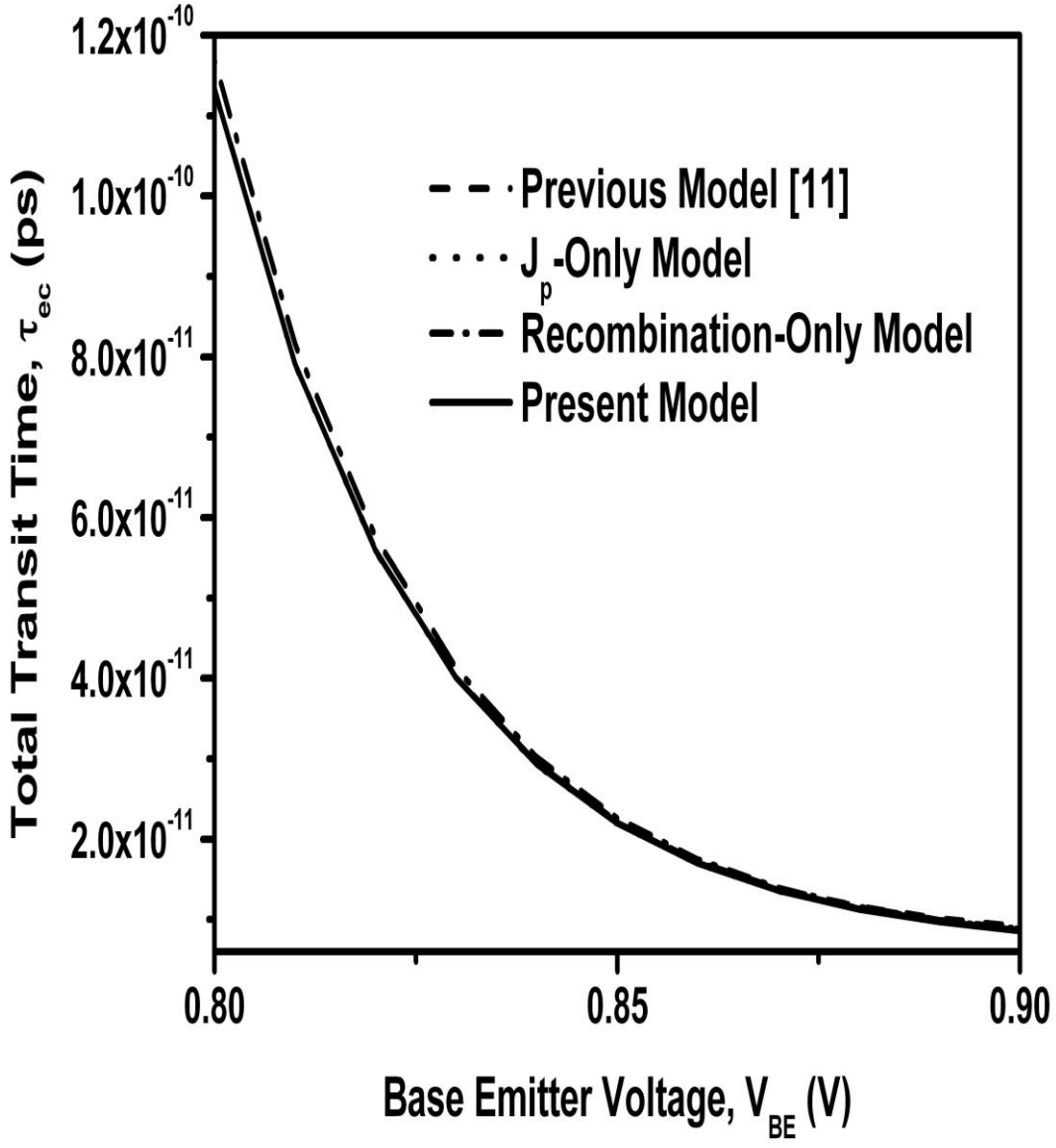

Figure 6.23: Comparison of emitter-to-collector transit time τ_{ec} for the present model, previous model [11], J_p-only model and recombination-only model. In this figure, $N_A(0) = 2\times10^{18}\ cm^{-3}$, $\eta = 3.69$ and $V_{BE} = 0.9V$. Uniform emitter doping profile is assumed.

Effects on High-Frequency Parameters

Unity-gain cutoff frequency f_T is inversely related to the total transit time τ_{ec}. A small change in τ_{ec} due to I_E or I_C is, therefore, reflected by this parameter. Due to the explanations described earlier in this section, Figure (6.24) shows higher f_T for the present model the J_p-only model than that for the other models.

The maximum frequency of operation f_max is defined in Equation (2 as

$$f_{max} \approx \frac{1}{2}\left(\frac{f_T}{2\pi R_B C_C}\right)^{\frac{1}{2}} \tag{6.11}$$

where the base resistance R_B can be defined as

$$R_B = \rho_B \frac{S}{LW_B} \tag{6.12}$$

where ρ_B is the average resistivity of the base layer. For the p-type base, this can be expressed as

$$\rho_B = \frac{1}{W_B}\int_0^{W_B}\left[\frac{1}{qn(x)\mu_n(x) + qp(x)\mu_p(x)}\right]dx \tag{6.13}$$

The above expression can be expressed in terms of diffusivity as

$$\rho_B = \frac{1}{W_B}\int_0^{W_B}\left[\frac{\frac{1}{qD_n}\times\frac{1}{qD_p}}{n(x)\left(\frac{1}{qD_n}+\frac{1}{qD_p}\right)+\frac{N_A}{qD_n}}\right] \tag{6.14}$$

The above expression for ρ_B shows that R_B depends not only on the dimensions of BJT, but also on the injection level, mobility and the doping level. For a given doping level ρ_B decreases as injection level increases and as mobility increases. Since injection level increases under high bias condition, ρ_B is expected to decrease under high bias condition.

This fact is observed in Figure (6.25) which shows the variation of R_B under various bias conditions. Again, electric field decreases the mobility and hence, increases the ρ_B under high bias conditions. Since the recombination-only model and the present model show higher electric field than the other models, these models, therefore, show the higher base resistance R_B than the other models under high bias conditions. Figure (6.25) also shows this fact.

It is evident from Equation (6.11) that maximum frequency of operation strongly depends on the base resistance R_B. Indeed, the dependence of f_{max} on f_T is strongly modulated by the small change in bias-dependent R_B. Therefore, the recombination-only model and the present model shows the lower value of f_{max} than the other models under high bias conditions. From the Figure (6.26), the same observation can be made.

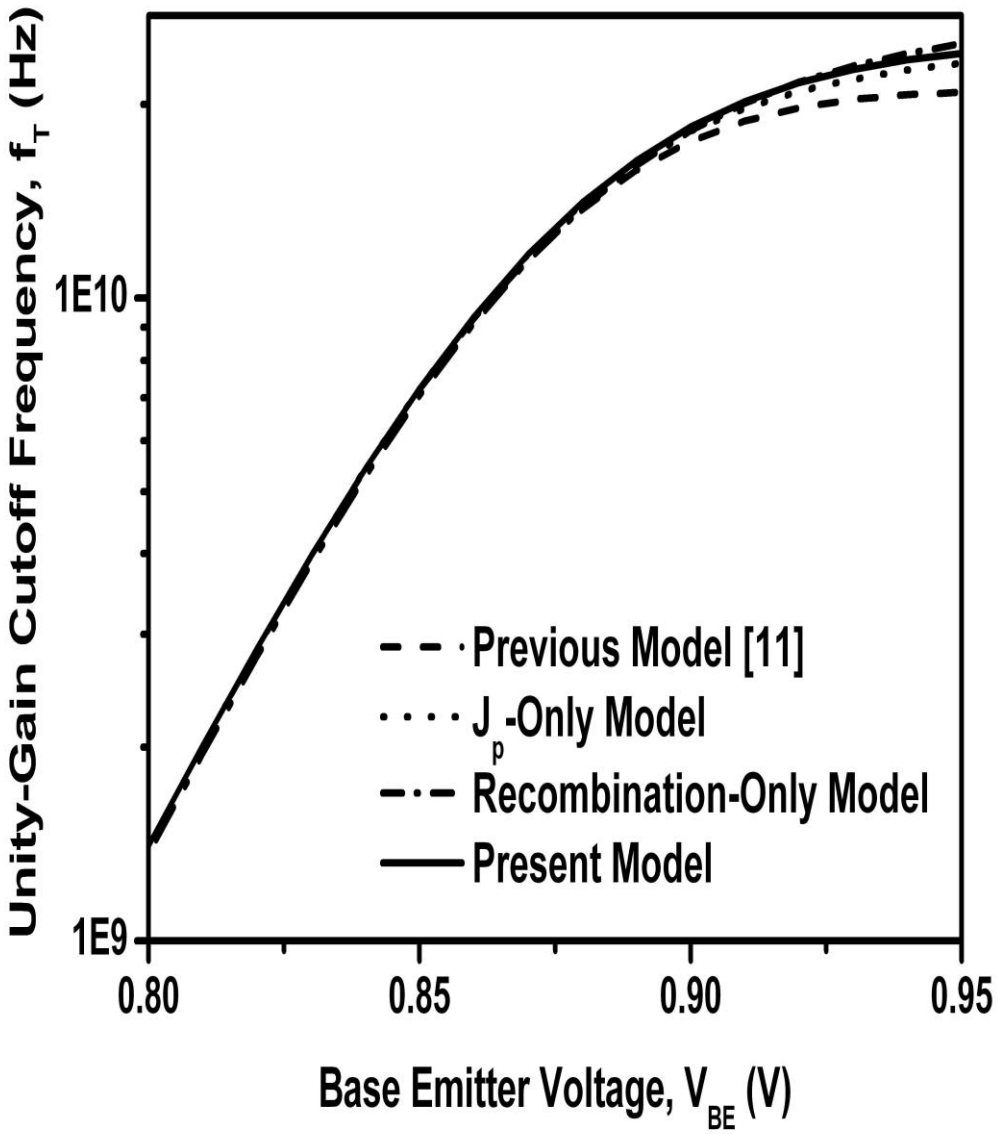

Figure 6.24: Comparison of unity-gain cutoff frequency f_T for the present model, previous model [11], J_p-only model and recombination-only model. In this figure, $N_A(0) = 2\times10^{18}\ cm^{-3}$, $\eta = 3.69$ and $V_{BE} = 0.9V$. Uniform emitter doping profile is assumed.

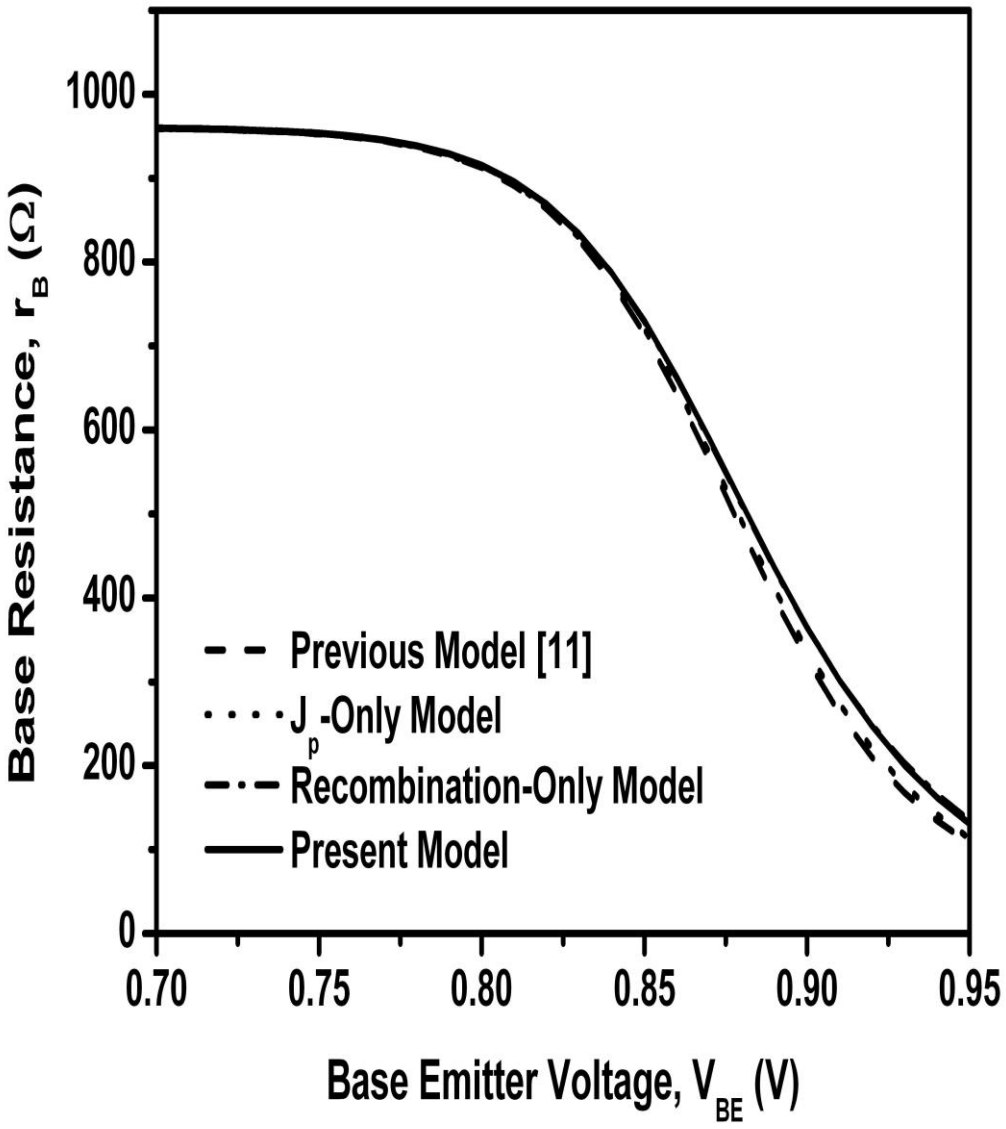

Figure 6.25: Comparison of base resistance R_B for the present model, previous model [11], J_p-only model and recombination-only model. In this figure, $N_A(0) = 2\times10^{18}\ cm^{-3}$, $\eta = 3.69$ and $V_{BE} = 0.9V$. Uniform emitter doping profile is assumed.

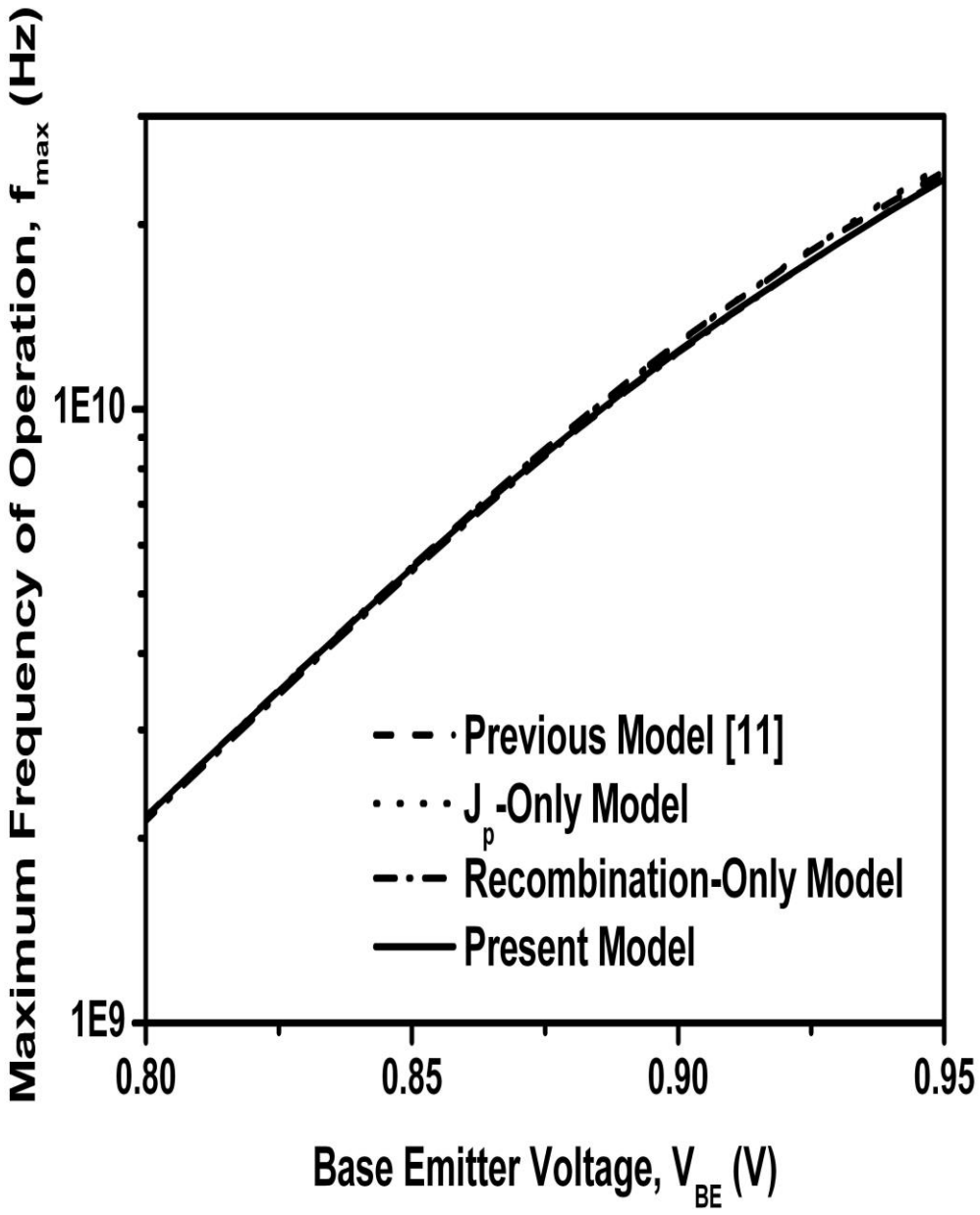

Figure 6.26: Comparison of maximum frequency of operation f_{max} for the present model, previous model [11], J_p-only model and recombination-only model. In this figure, $N_A(0) = 2\times10^{18}\ cm^{-3}$, $\eta = 3.69$ and $V_{BE} = 0.9V$. Uniform emitter doping profile is assumed.

6.2.4 Effects of Emitter Doping Profile

Earlier in this chapter it has been mentioned that majority carrier current $J_p(x)$ has dependency on the emitter region parameters such as emitter width, emitter doping level and emitter doping profile. In this section, the effects of emitter doping profile on the base transit time has been investigated. Three doping profiles are used: uniform, exponential and Gaussian.

Uniform doping profile offers zero electric field in the emitter region. Gaussian profile introduces a linearly decreasing field, whereas, exponential profile a constant field is developed throughout the emitter region. Since electric field enhances the carrier flow and hence, the current, exponential emitter doping profile causes the highest and the uniform doping causes the lowest current in the emitter region, where all the parameters are kept constant. Due to low-injection condition prevailed in the emitter region because of heavy doping level, recombination in the emitter is neglected. Therefore, the emitter current can be treated as the boundary value for the J_p in the base region.

From the above discussion, it is evident that for the exponential emitter doping profile the $J_p(x)$ in the base is expected to be higher in magnitude than that for the other two profiles. This is also verified by the Figure (6.27) which plots the majority carrier current density in the base for the uniform, exponential and Gaussian emitter doping profile.

Since, $J_p(x)$ has an aiding effect on the electron electric field E_n, a lower base transit time τ_B and a higher unity gain cutoff frequency f_T is expected for exponential emitter doping profile than for the other profiles. Figures (6.28) and (6.29) also verify this statement. From the Figure (6.28) it is seen that the lowest, the medium and the highest values for τ_B are obtained for the exponential, Gaussian and uniform emitter profile. The opposite case is seen for f_T from the Figure (6.29).

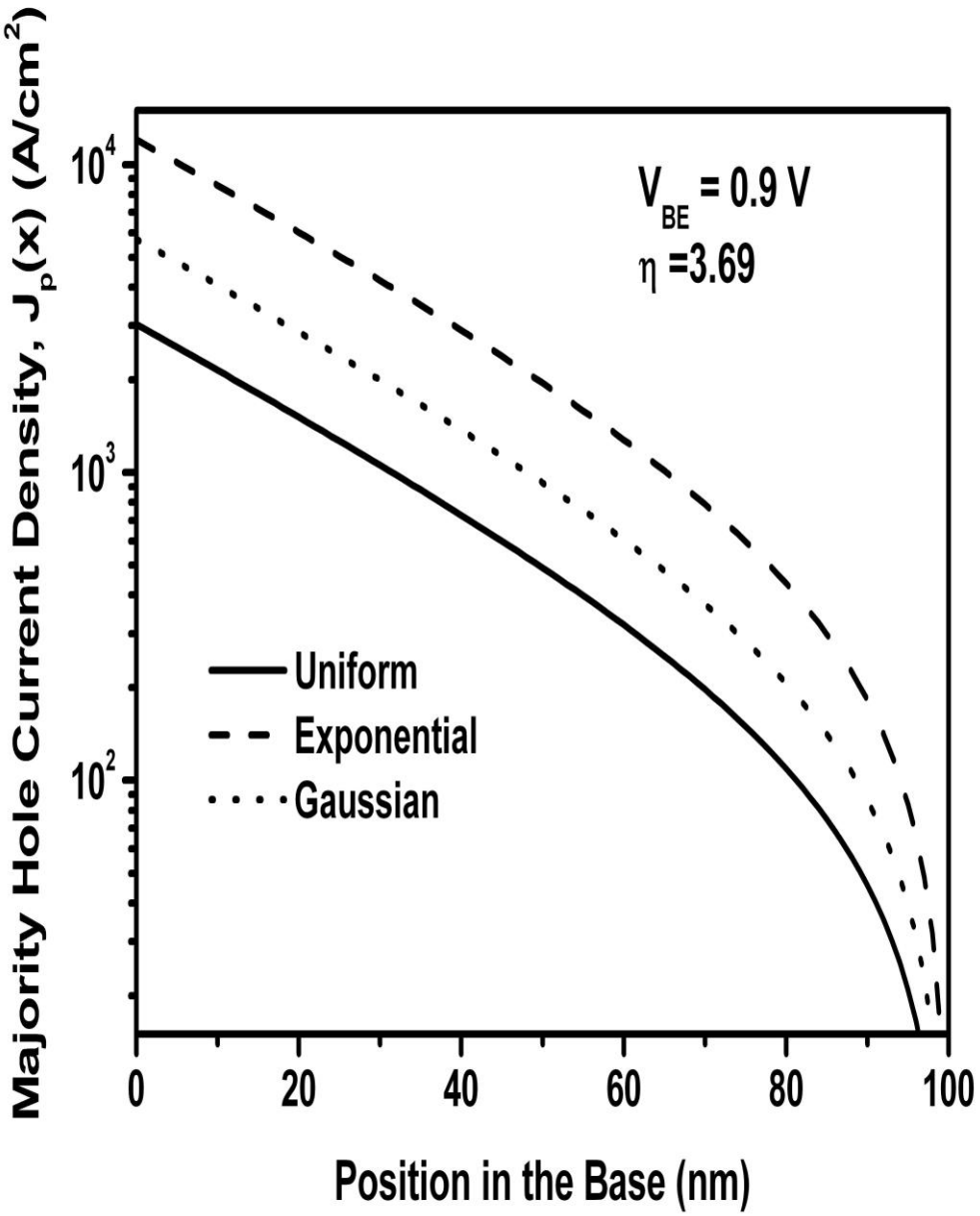

Figure 6.27: Effects on majority hole current density $J_p(x)$ for uniform, exponential and Gaussian emitter doping profile. In this figure, $N_A(0) = 2\times10^{18}\ cm^{-3}$, $\eta = 3.69$ and $V_{BE} = 0.9V$. Exponential base doping profile is assumed.

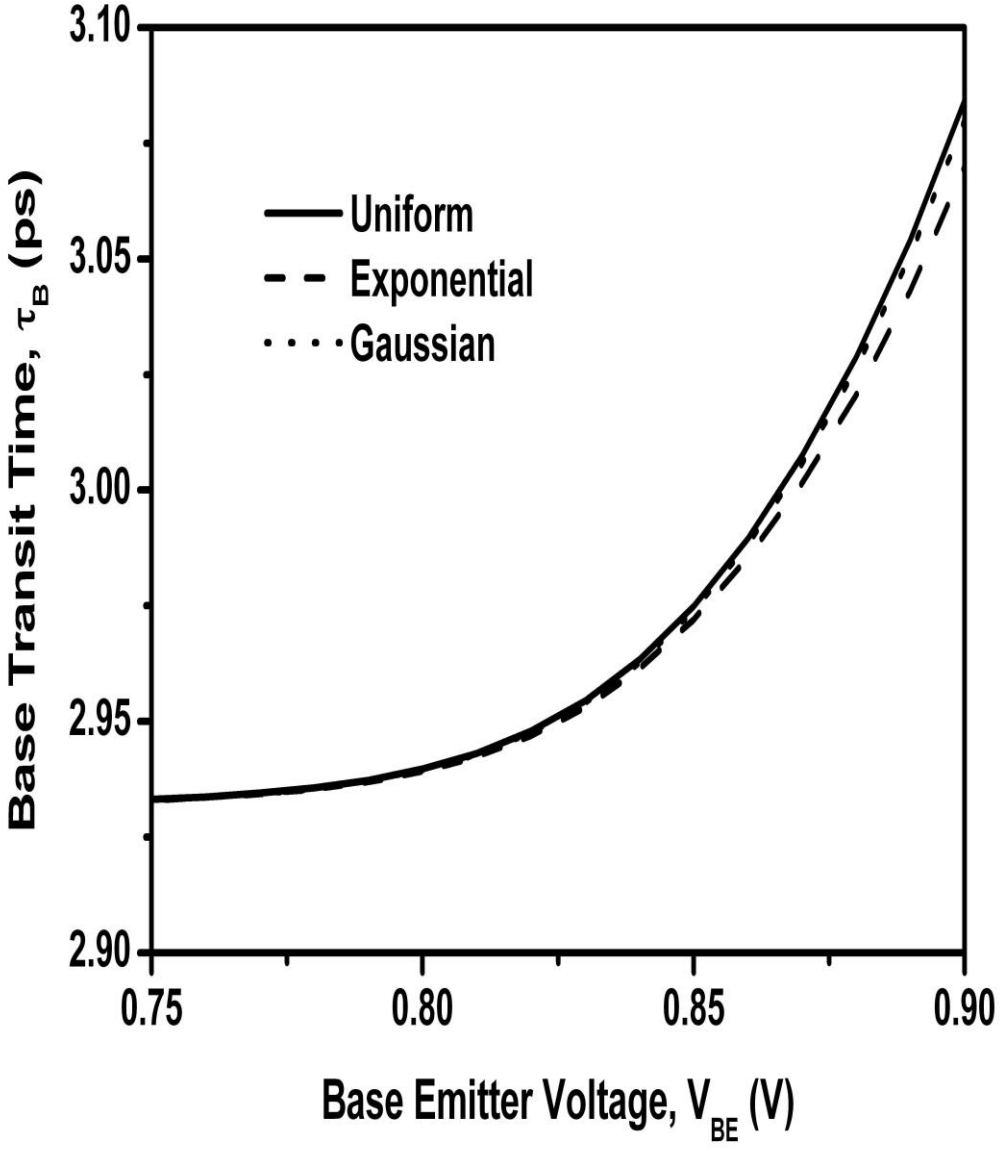

Figure 6.28: Effects on base transit time τ_B for uniform, exponential and Gaussian emitter doping profile. In this figure, $N_A(0) = 2\times10^{18}\ cm^{-3}$, $\eta = 3.69$ and $V_{BE} = 0.9V$. Exponential base doping profile is assumed.

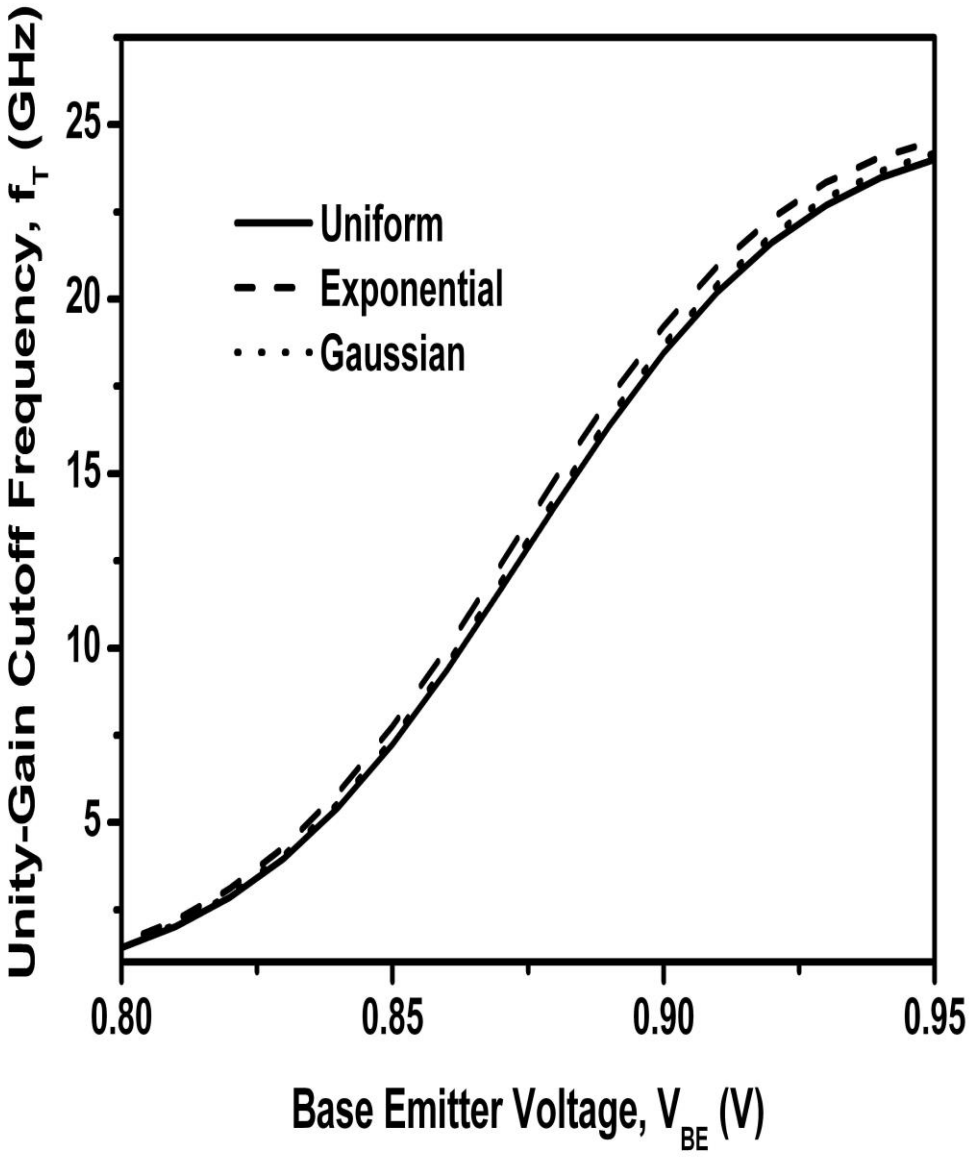

Figure 6.29: Effects on unity-gain cutoff frequency f_T for uniform, exponential and Gaussian emitter doping profile. In this figure, $N_A(0) = 2\times10^{18}\ cm^{-3}$, $\eta = 3.69$ and $V_{BE} = 0.9V$. Exponential base doping profile is assumed.

6.2.5 Effects of Base Doping Levels on Emitter and Collector Currents

In this section effects of base doping levels on the transistor currents are investigated. In doing so, the logarithmic slope of the profile η is kept constant. This results in negligible change in the electron electric field E_n in the base. However, increasing the peak doping concentration $N_A(0)$ keeping the slope η constant increases the doping level throughout the base region. As a result, the mobility throughout the base region decreases. The subsequent effect is, therefore, a decrease in the carrier currents in the base. This effect is seen in the Figure (6.30) for the emitter current I_E and in the Figure (6.31) for the collector current I_C.

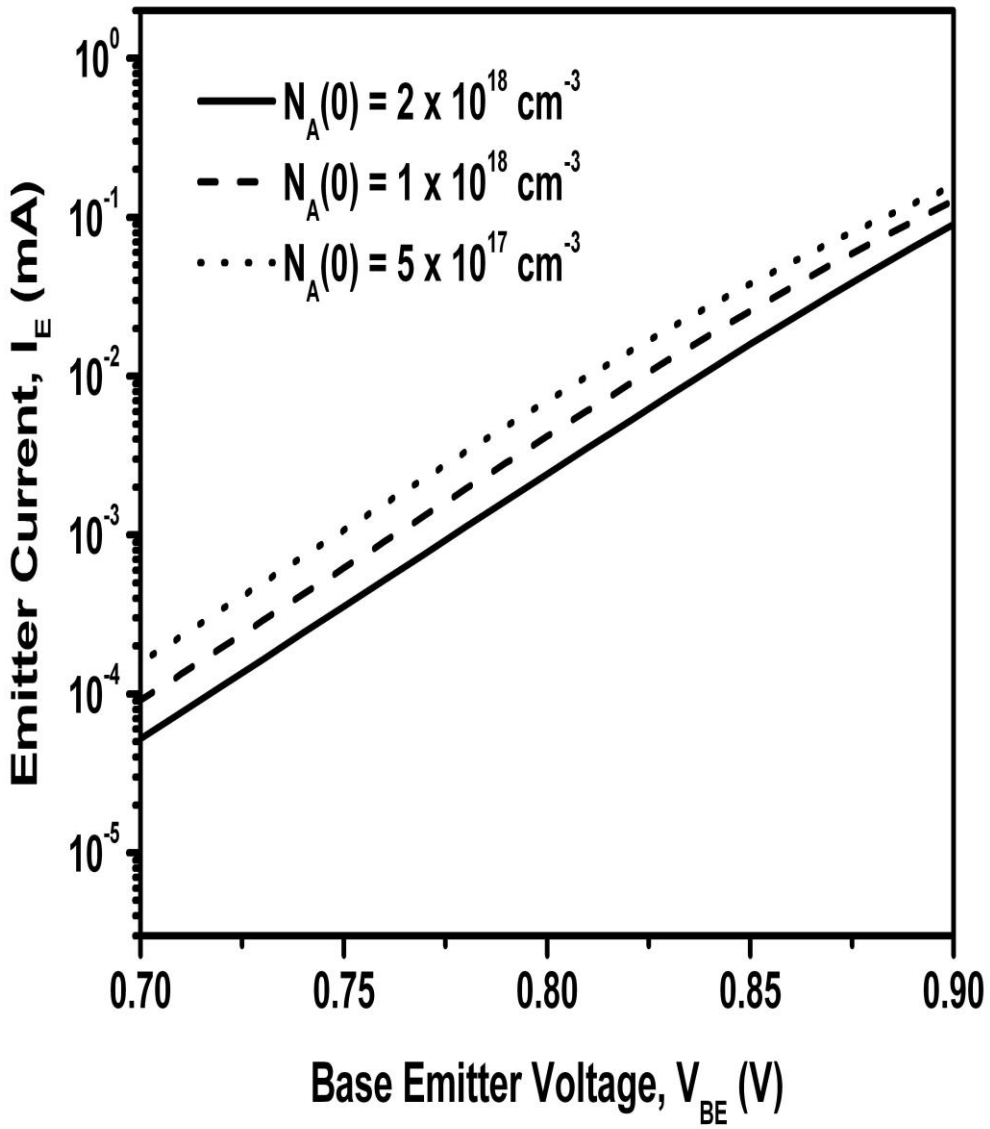

Figure 6.30: Effects on emitter current I_E for three peak base doping levels: $N_A(0) = 2 \times 10^{18}\ cm^{-3}$, $N_A(0) = 1 \times 10^{18}\ cm^{-3}$, $N_A(0) = 5 \times 10^{17}\ cm^{-3}$. In this figure, $\eta = 3.69$ and $V_{BE} = 0.9V$. Uniform emitter doping profile is assumed.

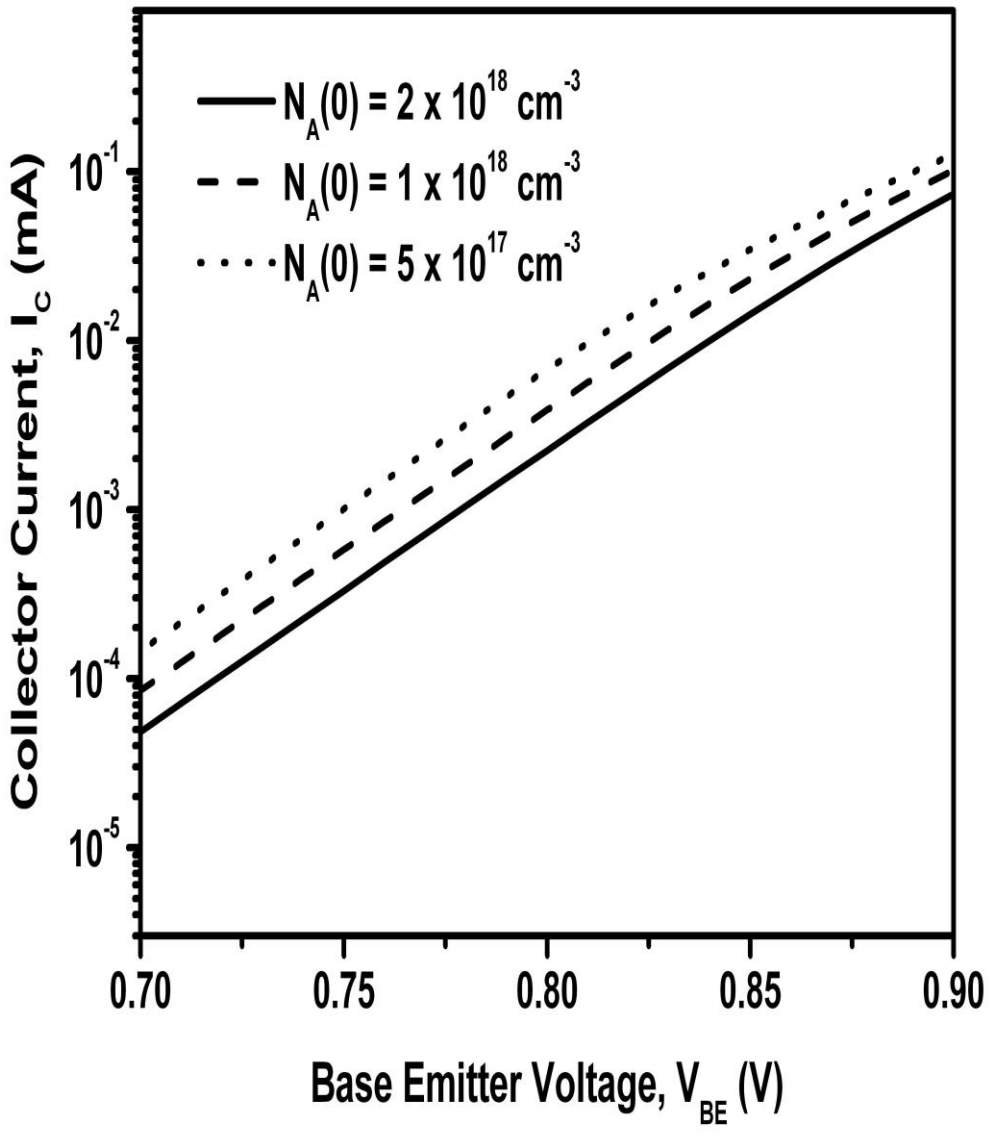

Figure 6.31: Effects on collector current I_C for three peak base doping levels: $N_A(0)=2\times10^{18}\ cm^{-3}$, $N_A(0)=1\times10^{18}\ cm^{-3}$, $N_A(0)=5\times10^{17}\ cm^{-3}$. In this figure, $\eta=3.69$ and $V_{BE}=0.9V$. Uniform emitter doping profile is assumed.

6.3 Conclusion

In this chapter, simulation results for the minority carrier profile, the minority and the majority carrier current densities, the collector current density and the base transit time are presented. The results establish that the consideration of both the J_p and the recombination mechanism has distinct and significant effects on the base transit time. The results show that both J_p and the recombination oppose the retarding field caused by an increase in injection level and hence, the base transit time at intermediate injection level becomes closer to its low-injection value. The numerical simulation results and the measurement data obtained from two experimental setups closely match with those of the proposed model. Therefore, the approximations used in this model are justified. These approximations are made to overcome the nonlinearity and the mathematical intractability. However, due to close matching of the proposed model data with the numerical and experimental data establishes the claim that majority carrier density along with the recombination mechanism has a significant effect on the base transit time and hence, must be included in the analytical model.

Chapter 7
Conclusion

In this work analytical expressions for the minority electron concentration profile, the minority electron current density, the majority hole current density and the base transit time have been developed by including the majority carrier density in the base of a bipolar junction transistor. The recombination mechanisms which include the SRH recombination and the Auger recombination as well as the lateral injection through the base are incorporated in the analytical modeling. The model also includes band-gap narrowing effects due to heavy doping, the Webster effect due to high injection level and considers velocity saturation, and doping and field dependance of the carrier mobility. The developed model is applicable to all levels of injection just before the onset of the Kirk effect. Therefore, the model can be characterized by its completeness and wide applicability.

This chapter gives a summary of the contributions of the current modeling effort. Suggestions are also given for future reference.

7.1 Contributions

A lot of challenges has to be overcome in developing the analytical model that does not ignore the majority carrier current through and the recombination in the base. These challenges include:

1. Inclusion of J_p that makes the estimation of E_p complicated.

2. Both electron and hole mobilities have to be incorporated to determine the electric

fields.

3. Unlike the models where only doping-dependency is considered the electron and hole carrier mobilities are not a simple exponential function of position, since both doping profile and electric field dependencies are considered in the present model.
4. For lifetime, inclusion of both SRH and Auger recombination leads to further complication.
5. Incorporation of all the effects results in a non-linear, non-homogeneous, variable-coefficient second order differential equation, the solution of which is analytically intractable.
6. For low injection, $n(x) << N_A(x)$ and for high injection, $n(x) >> N_A(x)$. However, for intermediate injection levels, n(x) is comparable to $N_A(x)$.
7. Mobility, electric field and J_p all are coupled and also depend on the minority carrier profile.
8. Conversion of a nonlinear, non-homogeneous and complicated-function variable-coefficient differential equation into a linear, homogeneous and simple-function variable coefficient one has to be made.
9. For analytical tractability, solution techniques have to be devised to solve the resulting differential equation.

To overcome these challenges, some innovative approaches are taken, which represents the major contributions of this work. These are listed as follows:

1. Different electric fields are considered for electrons and holes in the analytical modeling.
2. Both SRH and Auger recombination are simultaneously considered in the analytical modeling.

3. Exponential approximation technique is introduced for analytical modeling.
4. Lateral base injection is suitably incorporated.
5. An approximate analytical expression for majority hole current density is derived.
6. The electric field expression is approximately derived from which its dependance on the doping profile, the band-gap narrowing, the majority carrier current density and the injection-level is identified.
7. The governing differential equation for the minority electron carrier concentration is modified to include the intermediate-injection-level effect.
8. For the electron mobility, an approximate electric field is used to make the solution tractable.
9. A confluent hypergeometric function is utilized as a solution when only J_p is considered for low injection. A homogeneous Bessel equation is solved when recombination and injection-level dependency are incorporated. used.

7.2 Suggestions for Future Work

The analytical models developed in this work neglects the effects due to plasma-induced band-gap narrowing, which exists when injection level is high. Base push out is another effect to be considered, especially when bias levels approach 0.9 V or more. This mechanism leads to accurate modeling of two-dimensional effects such as emitter current-crowding and collector current-spreading. In this work, the velocity saturation is assumed to be occurred exactly at the $x = W_B$, which is not the case. Indeed, this saturation occurs in the base region near the collector side. These modifications could be incorporated in the model in the future.

7.3 Conclusion

The analytical model developed in this work include almost all the important effects investigated so far in the literature. However, the main achievement of this model is the inclusion of both the majority carrier current density and the recombination mechanism as well as the lateral injection into the base which were neglected by the analytical models reported in the literature. The proposed model is compared against numerical simulation results as well as experimental setups and was found to be in excellent agreement. It can be concluded, therefore, the developed model provides a better physical insight into the physics behind the base transit time.

Appendix

A.1 Derivation of Confluent Hypergeometric Function

Confluent hypergeometric function is defined as [57],

$$M(a;b;x) = \Sigma_{n=0}^{\infty} \frac{(a)_n}{(b)_n} \frac{x^n}{n} \tag{A.1}$$

where, $(a)_n, (b)_n$ are Pochhammer symbol defined as

$$(a)_n = a(a+1)(a+2).....(a+n-1) = \frac{(a+n-1)!}{(a-1)!}$$

$$(a)_0 = 1$$

Now, the integral term I obtained in Section (5.2) can be rearranged by substituting 'x' with the variable 'v' as,

$$I = -\frac{W_B}{\eta \beta_{0l}} (V_{0l})^{-\frac{\alpha}{\beta_{0l}}} \int_{V_{0l}}^{v_{l0}} v_{l0}^{\frac{\alpha}{\beta_{0l}}-1} e^{v_{l0}} dv_{l0} \tag{A.2}$$

Expanding the exponential term and then, integrating and rearranging results in,

$$I = -\frac{W_B}{\eta \alpha} I_0 \tag{A.3}$$

where

$$I_0 = \left[u^{\alpha} \left\{ 1 + \frac{\frac{\alpha}{\beta_{0l}}}{\frac{\alpha}{\beta_{0l}}+1} \frac{v_{0l}}{1!} + \frac{\frac{\alpha}{\beta_{0l}}(\frac{\alpha}{\beta_{0l}}+1)}{(\frac{\alpha}{\beta_{0l}}+1)(\frac{\alpha}{\beta_{0l}}+2)} \frac{v_{0l}^2}{2!} \right\} \right]_{V_{0l}}^{v_{l0}}$$

$$-\left[u^{\alpha}\left\{\frac{\frac{\alpha}{\beta_{0l}}(\frac{\alpha}{\beta_{0l}}+1)(\frac{\alpha}{\beta_{0l}}+2)}{(\frac{\alpha}{\beta_{0l}}+1)(\frac{\alpha}{\beta_{0l}}+2)(\frac{\alpha}{\beta_{0l}}+3)}\frac{v_{0l}^3}{3!}+....\infty\right\}\right]_{V_{0l}}^{v_{l0}}$$

$$=-\frac{W_B}{\eta\alpha}u^{\alpha}\Sigma_{n=0}^{\infty}\left[\frac{(\frac{\alpha}{\beta_{0l}})_n}{(\frac{\alpha}{\beta_{0l}}+1)_n}\frac{x^n}{n}\right]_{V_{0l}}^{v_{l0}}$$

$$=-\frac{W_B}{\eta\alpha}\left[u^{\alpha}M\left(\frac{\alpha}{\beta_{0l}};\frac{\alpha}{\beta_{0l}}+1;v_l\right)\right]_{V_{0l}}^{v_{l0}} \tag{A.4}$$

where the definition of confluent hypergeometric function given by Equation (A.1) is used.

A.2 Simulation Procedure

Three first order differential equations for n(x), $J_n(x)$ and $J_p(x)$ are solved numerically. The equations are:

$$\frac{dn}{dx}=-\frac{E_{n,eff}(x)}{V_T}n(x)+\frac{J_n(x)}{qD_{n,eff}(x)} \tag{A.5a}$$

$$\frac{dJ_n(x)}{dx}=qR_x(x)\left[n(x)-\frac{n_{ie}^2(x)}{n(x)+N_A(x)}\right] \tag{A.5b}$$

$$\frac{dJ_p(x)}{dx}=-qR_x(x)\left[n(x)-\frac{n_{ie}^2(x)}{n(x)+N_A(x)}\right]+qg\{n(x)+N_A(x)\} \tag{A.5c}$$

where,

$$\frac{E_{n,eff}(x)}{V_T}=\frac{1}{F_1(x)}\times\frac{\eta}{W_B}\frac{E_{n0}(x)}{V_T} \tag{A.6a}$$

$$\frac{1}{qD_{n,eff}(x)}=\frac{1}{F_1(x)}\left[F_e u^{\gamma_1}+G_e\left|\frac{E_{n0}(x)}{V_T}+\frac{\frac{dn}{dx}}{\frac{\eta}{W_B}\{n(x)+N_A(x)\}+J_p(x)G_h}\right|\right] \tag{A.6b}$$

$$R_x(x)=\left[\frac{\frac{N_A(x)+N_{0,ref}}{\tau_{n0}N_{0,ref}}}{(1+r_s)n(x)+N_A(x)}+C_{Ap}\{(1+r_a)n(x)+N_A(x)\}\right]\times\{n(x)+N_A(x)\} \tag{A.6c}$$

where,

$$F_1(x) = \frac{\frac{\eta}{W_B}\{2n(x) + N_A(x)\} + J_p(x)G_h}{\frac{\eta}{W_B}\{n(x) + N_A(x)\} + J_p(x)G_h} \tag{A.7a}$$

$$\frac{E_{n0}(x)}{V_T} = -\left[1 - \gamma_2 - \frac{\frac{\eta}{W_B}n(x) + J_p(x)(F_h u^{\gamma_3} + G_h)}{\frac{\eta}{W_B}\{n(x) + N_A(x)\} + J_p(x)G_h}\right] \tag{A.7b}$$

$$g = \frac{J_p(0) - J_p(W_B) + q\frac{W_B}{\eta}\int_{x=0}^{W_B} R_x(x)\left[n(x) - \frac{n_{ie}^2(x)}{n(x) + N_A(x)}\right]}{\frac{q}{W_B}\int_{x=0}^{W_B}\{n(x) + N_A(x)\}} \tag{A.7c}$$

Following four boundary conditions are needed to solve the the Equations (A.5)(one additional boundary condition is needed to determine *g*):

$$n(0) = \frac{\frac{n_{ie}^2(0)}{N_A(0)}e^{\frac{V_{BE}}{V_T}}}{\frac{1}{2} + \sqrt{\frac{1}{4} + \left[\frac{n_{ie}(0)}{N_A(0)}\right]^2 e^{\frac{V_{BE}}{V_T}}}} \tag{A.8a}$$

$$J_n(W_B) = qv_{sn}n(W_B) \tag{A.8b}$$

$$J_p(0) = -\frac{qD_{pE}(0)}{W_E}\frac{n_{ieE}^2}{N_E}e^{\frac{qV_{BE}}{kT}} \tag{A.8c}$$

$$J_p(W_B) = -\frac{qD_{pC}(0)}{W_C}\frac{n_{ieC}^2}{N_C} \approx 0 \tag{A.8d}$$

Equations (A.5b) and (A.5c) offer boundary problem, whereas, Equation (A.5a) offer initial value problem. Therefore, two iterative procedures are required: one for J_p and the other for J_n. Matlab routines are used to perform the iteration process. The iteration procedure is outlined below:

1. First, an initial guess of $J_n(0)$ is chosen. J_n obtained using the model (Ref. [11]) is used for this guess.
2. Second, an initial guess for the generation rate *g* is required. For this, the Equation (A.7c) is used by letting $n(x) = 0$.
3. The Equations (A.5) are then solved.

4. Using the new $J_p(W_B)$ and n(x) obtained in the preceding step, the new value of *g* is calculated from the Equation (A.7c).
5. Since $J_n(W_B)$ and $J_p(W_B)$ thus obtained do not satisfy the boundary conditions given by the Equations (A.8b) and (A.8d), an iterative procedure is required.
6. The Equations (A.5) are again solved using the new values.
7. A new value of $J_p(W_B)$ is obtained, which may be higher or lower than the previous value. Since $J_p(W_B) \approx 0$, this value should be lowered down. When the new value is higher than the previous value, this lowering can be achieved by continually dividing it by a number (i.e 10) until it lowers down from the previous value; otherwise, the new value is preserved.
8. A new '*g'* is calculated and the Equations (A.5) are again solved.
9. This iteration process is continued until the value of $J_p(W_B)$ is reached very close to zero. This satisfies the boundary condition given by the Equation (A.8b).
10. A second iteration is required to satisfy the other boundary condition given by the Equation (A.8b).
11. The value of $J_n(0)$ is then increased by a very small factor (0.01%) if $J_n(W_B) < qv_{sn}n(W_B)$ and it is decreased by the same factor if $J_n(W_B) > qv_{sn}n(W_B)$.
12. The steps (6) to (9) are repeated for this new value of $J_n(0)$.
13. The iteration is continued until the percentage error $\left|\frac{J_n(W_B) - qv_{sn}n(W_B)}{J_n(W_B)}\right| \times 100$ is reached within a prescribed limit (i.e. within the 0.01%).
14. The base transit time is then calculated using the numerically solved n(x) and $J_n(x)$.

Bibliography

[1] S. M. Sze, *Physics of Semiconductor Devices*, 2nd ed., New York: Wiley, 1981.

[2] J. J. H. van der Beisen, "A simple regional analysis of transit times in bipolar transistors", *Solid State Electron.*, vol. 29, no. 5, pp. 529-534, May 1986.

[3] M. M. Shahidul Hassan and A. H. Khandoker, "A new expression for base transit time in a bipolar junction transistor for all level of injection", *Microelectronics Reliability*, vol. 41, no. 1, pp. 137-140, Jan. 2001.

[4] H. Kroemer, "Two integral relationship pertaining to the electron transport through a bipolar transistor with nonuniform energy gap in the base region", *Solid State Electron.*, vol. 28, no. 11, pp. 1101-1103, 1985.

[5] J. S. Yuan, "Effect of base profile on the base transit time of bipolar transistors for all levels of injection", *IEEE Trans. Electron Devices*, vol. 41, no. 2, pp. 212-216, Feb. 1994.

[6] K. Suzuki, "Analytical base transit time model of uniformly-doped-base bipolar transistors for high-injection regions", *Solid-Stae Electron.*, vol. 36, No.1, pp. 109-110, 1993.

[7] K. Suzuki, "Analytical base transit time model for high-injection regions", *Solid State Electron.*, vol. 37, no. 3, pp. 487-493, Mar. 1994.

[8] M. Pingxi, L. Zhang, and Y. Wang, "Analytical model of collector current density and base transit time based on iteration method", *Solid State*

Electron., vol. 39, no. 11, pp. 1683-1686, Nov. 1996.

[9] M. Pingxi, L. Zhang, and M. Ostling,, "A new set of initial conditions for fast and accurate calculation of base transit time and collector current density in bipolar transistors", *Solid State Electron.*, vol. 41, no. 11, pp. 2023-2026, Nov. 1998.

[10] M. Z. R. Khan, M. M. Shahidul Hassan, T. Rahman and A. K. M. Ahsan, "Expression for base transit time in bipolar transistors", *Int. J. Electron.*, vol. 92, no. 4, pp. 215-229, Apr. 2005.

[11] M. M. Shahidul Hassan and Md. Waliullah Khan Nomani, "Base-transit-time model considering field dependent mobility for BJTs operating at high-level injection", *IEEE Trans. Electron Devices*, vol. 53, no. 10, pp. 2532-2539, Oct. 2006.

[12] J. Weng, "A physical model of the transit time in bipolar transistors", *Solid State Electron.*, vol. 36, no. 9, pp. 1197-1201, Aug. 1993.

[13] J. J. Liou and Y. Yue, "High-level free-carrier injection in advance bipolar junction transistors (invited)", *IEEE Trans. Electron Devices*, vol. 29, no. 5, pp. 174-182, May 1994.

[14] Y. Yue, J. J. Liou, A. Ortiz-Conde and F. Garcia Sanchez, "Effects of high-level free-carrier injection on the base transit time of bipolar junction transistors", *Solid State Electron.*, vol. 39, no. 1, pp. 27-31, January 1996.

[15] Md. Iqbal Bahar Chowdhury and M. M. Shahidul Hassan, "Base Transit Time of a Bipolar Junction Transistor Considering Majority-carrier Current", *Proceedings of the 5th Intrenational Conference on Electrical and Computer Engineering, ICECE 2008, Dhaka, Bangladesh* , vol. 1, pp. 133-138, December 2008.

[16] Md. Iqbal Bahar Chowdhury and M. M. Shahidul Hassan, "Analytical Modeling of Base Transit Time for Bipolar Junction Transistors Considering Majority-Carrier Current", *Journal of Electrical Engineering, The Institute of Engineers, Bangladesh*, vol. EE 36, No. 1, pp. 30-36, June 2009.

[17] M M Shahidul Hassan and Md. Iqbal Bahar Chowdhury, "Effect of Majority Carrier Current on the BaseTransit Time of a BJT", *IEEE International Conference of Electron Devices and Solid-State Circuits, EDSSC 2010, Hong Kong*, pp. 1-4, 15-17 Dec, 2010.

[18] Md. Iqbal Bahar Chowdhury and M. M. Shahidul Hassan, "Analysis of Base Transit Time for a Bipolar Junction Transistor Considering Base Current", *Proceedings of the 6th Intrenational Conference on Electrical and Computer Engineering, ICECE 2010, Dhaka, Bangladesh*, vol. 1, pp. 20-24, Dec 19-21, 2010.

[19] Md. Iqbal Bahar Chowdhury and M. M. Shahidul Hassan, "Analytical Modeling of Base Transit Time Considering Recombination in the Non-uniformly Doped Base", *International Symposium on Humanities, Science and Engineering Research, SHUSER 2011, Kuala Lumpur, Malaysia*, Presented, 5-7 June, 2011.

[20] W. L. Engl, *Process and Device Modeling*, Amsterdam, The Netherlands: Elsevier, 1986.

[21] R. P. Mertens, R. J. van Overstraeten and H. J. Deman, "Heavy doping effects in silicon", *Advanced in Electronics and Electron Physics*, L. Marton, C. Marton, Eds. New York: Academic Press, 1981, vol. 55.

[22] T. N. Morgan, "Broadening of impurity bands in heavily-doped semiconductors", *Phys. Rev. A*, vol 139, pp. 343-348, 1965.

[23] E. O. Kane, "Thomas-Fermi approach to impure semiconductor band structure", *Phys. Rev.*, vol 131, pp. 79-88, 1963.

[24] J. W. Slotboom and H. C. de Graaff, "Measurements of bandgap narrowing in Si-bipolar transistors", *Solid State Electron.*, vol. 19, pp. 857-862, 1976.

[25] J. W. Slotboom and H. C. de Graaff, "Bandgap narrowing in Silicon bipolar transistors", *IEEE Trans. Electron Devices*, vol. ED-24, no. 8, pp. 1123-1125, 1977.

[26] J. W. Slotboom, "The pn-product in Silicon", *Solid State Electron.*, vol. 20, pp. 279-283, 1977.

[27] D. B. M. Klaassen, J. W. Slotboom and H. C. de Graaff, "Unified apparent bandgap narrowing in n- and p-type Silicon", *Solid State Electron.*, vol. 35, no. 2, pp. 125-129, 1992.

[28] K. Suzuki, "Optimum base-doping profile for minimum base transit time considering velocity saturation at base-collector junction and dependence of mobility and bandgap narrowing on doping concentration", *IEEE Trans. Electron Devices*, vol. 48, no. 9, pp. 2102-2107, September 2001.

[29] S. Selberherr, *Analysis and Simulation of Semiconductor Devices*, Wein: Springer-Verlag, 1984.

[30] D. M. Caughey and R. E. Thomas, "Carrier mobilities in silicon empirically related to doping and field", *Proc. IEEE*, vol. 52, pp. 2192-2193, 1967.

[31] G. Baccarani and P. Ostoja, "Electron mobility empirically related to the phosphorus concentration in silicon", *Solid-State Electron*, vol. 18, pp. 579-580, 1975.

[32] N. D. Arora, J. R. Houser and D. J. Roulston, "Elctron and hole mobilities as a function of concentration and temperature", *IEEE Trans. Electron*

Devices, vol. ED-29, pp. 292-295, 1982.

[33] Lendert A. Verhoff and Wim C. Sinke, "Minority-carrier transport in nonuniformly doped silicon-an analytical approach", *IEEE Trans. Electron Devices*, vol. 37, no. 1, pp. 210-221, January 1990.

[34] Tao-Cheng Lu and James B. Kuo, "A closed-form analytical forward transit time model considering specific models for bandgap narrowing effects and concentration-dependent diffusion coefficients for BJT devoces operating at 77 K ", *IEEE Trans. Electron Devices*, vol. 40, no. 4, pp. 766-772, April 1993.

[35] K. K. Thornber, "Relation of drift velocity to low-field mobility and high-field saturation velocity", *J. Appl. Phys.*, vol. 52, pp. 279-290, 1981.

[36] G. M. Kull, W. Nagel, S. W. Lee, P. Lloyd, E. J. Prendergast and H. Dirks, "A unified circuit model for bipolar transistors including quasi-saturation effect", *IEEE Trans. Electron Devices*, vol. ED-32, no. 6, pp. 1103-1113, June 1985.

[37] B. Y. Chen and J. B. Kuo, "An accurate knee current model considering quasi-saturation for BJTs operating at high current density", *Solid State Electron*, vol. 38, no. 6, pp. 1282-1284, June 1995.

[38] W. Shockley and W. T. Read, "Statistics of the recombination of holes and electrons", *Phys. Rev.*, vol. 87, pp. 835-842, 1952.

[39] R. N. Hall, "Electron-hole recombination in germanium", *Phys. Rev.*, vol. 87, pp. 387, 1952.

[40] J. G. Fossum and D. S. Lee, "A physical model for the dependence of carrier lifetime on doping density in nondegenrate silicon", *Solid-State Electron.*, vol. 25, no. 8, pp. 741-747, 1982.

[41] J. G. Fossum, "Computer-aided numerical analysis of silicon solar cells", *Solid-State Electron.*, vol. 19, pp. 269-277, 1976.

[42] W. Anheier and W. Engl, "Numerical analysis of gate triggered SCR turn-on transients", *IEDM Tech. Digest*, pp. 303a-303d, December 1977.

[43] W. Engl and H. K. Driks, "Models of physical parameters", in *An Introduction to the Numerical Analysis of Semiconductor Devices and Integrated Circuits*, J. J. H. Miller, Ed. Dublin: Boole Press, 1981.

[44] J. G. Fossum, R. P. Martens, D. S. Lee and J. F. Nijs "Carrier recombination and lifetime in highly doped silicon", *Solid-State Electron.*, vol. 26, no. 6, pp. 569-576, 1983.

[45] J. Dziewior and W. Schmid, "Auger coefficient for highly doped and highly excited silicon", *Appl. Phys. Lett.*, vol. 31, pp. 346-348, 1977.

[46] R. J. van Overstraeten, H. J. Deman and R. P. Mertens, "Transport equations in heavy doped silicon", *IEEE Trans. Electron Devices*, vol. ED-20, no. 3, pp. 290-298, March 1973.

[47] D. J. Roulston, "Early voltage in very-narrow-base bipolar transistors", *IEEE Electron Device Lett.*, vol. EDL-11, no. 2, pp. 88-89, February 1990.

[48] W. M. Webster, "On the variation of junction-transistor current-amplifier factor with emitter current", *Proc. IRE*, vol. 42, pp. 914-921, 1954.

[49] R. S. Muller and T. I. Kamins, *Device Electronics for Integrated Circuits*, 2nd ed., New York: Wiley, 1986.

[50] C. T. Kirk, "A theory of transistor cutoff frequency (f_T)falloff at high current densities", *IRE Trans. Electron Devices*, vol. ED-9, pp. 164-174, 1962.

[51] G. T. Wright and P. P. Frangos, "Simple analytical one-dimensional model

for saturation operation of the high-voltage bipolar power transistor", *Solid-State and Electron Devices, IEE Proceedings I*, vol. 131, issue. 6, pp. 207-212, December 1984.

[52] B. V. Gokhale, "Numerical Solutions for a One-dimensional Silicon n-p-n Transistor", *IEEE Trans. Electron Devices*, vol. ED-17, no. 8, pp. 594-602, August 1970.

[53] S. E. Swirhun, J. A. Del Alamo and R. M. Swanson, "Measurement of hole mobility in heavily doped n-type silicon", *Electron Device Lett.*, vol. EDL-7, pp. 168-171, Mar. 1986.

[54] M. Jagadesh Kumar and K. N. Bhat, "The effects of emitter region recombination and bandgap narrowing on the current gain and the collector lifetime of high-voltage bipolar transistors", *IEEE Trans. Electron Devices*, vol. 36, no. 9, pp. 1803-1810, Sep. 1989.

[55] Guoxin Li, Arnost Neugroschel, C. T. Sah, Don Hemmenway, Tony Rivoli and Jay Maddux, "Analysis of bipolar junction transistors with a Gaussian base-dopant impurity-concentration profile", *IEEE Trans. Electron Devices*, vol. 48, no. 12, pp. 2945-2947, December 2001.

[56] M. D. Raisinghania, *Avanced Differntial Equations*, 8th ed., Ram Nagar, New Delhi: S. Chand & Company Ltd., 2001.

[57] George B. Arfken and Hans J. Weber, *Mathematical Methods for Physicists*, 4th ed., San Diego: Academic Press, Inc., 1995

[58] Hartmut Stubing and Hans-Martin Rein, "A Compact Physical Large-Signal Model for High- Speed Bipolar Transistors at High Current Densities- Part I: One- Dimen- sional Model", *IEEE Trans. Electron Devices*, vol. ED-34, No. 8, pp. 1741- 1751, August 1987.

[59] Hans-Martin Rein and Michael Schroter, "A Compact Physical Lar e-Signal Model for High- Speed Bipolar Transistors at High Current Densities- Part II: Two- Dimensional Model and Experimental Results", *IEEE Trans. Electron Devices*, vol. ED-34, No. 8, pp. 1752- 1761, August 1987.

[60] Tsuneaki Fuse, Toshihiko Hamasaki, Kazuya Matsuzawa, and Shigeyoshi Watanabe, "A Physically Based Base Pushout Model for Submicrometer BJT's in the Presence of Velocity Overshoot", *IEEE Trans. Electron Devices*, vol. 39, No. 2, pp. 396- 403, February 1992.

[61] J. J. Liou and C. S. Ho, "A Pjysical Model for the Base Transit Time of Advanced Bipolar Transistor", *Solid-State Electron.*, vol. 38, no. 1, pp. 143-147, 1995.